NORTHWESTERN UNIVERSITY

Nicotinamide Enhances Primary Human Megakaryocytic Differentiation from Hematopoietic Stem Cells: Phenotypic Characterization and Mechanism of Action

A DISSERTATION

SUBMITTED TO THE GRADUATE SCHOOL IN PARTIAL FULFILLMENT OF THE REQUIREMENTS

for the degree

DOCTOR OF PHILOSOPHY

Field of Chemical Engineering

By

Lisa M. Giammona

EVANSTON, ILLINOIS

DECEMBER 2007

Abstract

Nicotinamide Enhances Primary Human Megakaryocytic Differentiation from Hematopoietic Stem Cells: Phenotypic Characterization and Mechanism of Action

Lisa M. Giammona

Megakaryocytic cells (Mks) are derived from hematopoietic stem cells (HSCs) and give rise to platelets. *Ex vivo* culture of HSCs under conditions that promote Mk differentiation has been proposed as a method for producing Mks and platelets for cell therapies. Mk maturation involves the development of polyploid cells via endomitosis, and the number of platelets produced increases with Mk DNA content. However, ploidy levels in cultured human Mks are much lower than those observed *in vivo.* We have found that adding the water-soluble vitamin nicotinamide (NIC) to mobilized peripheral blood $CD34^+$ cells cultured with thrombopoietin (Tpo) more than doubles the percentage of high-ploidy (≥8N) Mks. This was observed regardless of donor-dependent differences in Mk differentiation. Furthermore, Mks in cultures with NIC are larger, have more highly lobated nuclei, reach a maximum DNA content of 64N (vs. 16N with Tpo only), and exhibit more frequent and more elaborate cytoplasmic extensions – an indication of greater platelet producing capacity. However, NIC does not alter Mk commitment, apoptosis, or the time at which endomitosis is initiated. Despite the dramatic phenotypic differences observed with NIC addition, gene expression microarray analysis revealed similar overall transcriptional patterns in primary human Mk cultures with or without NIC, indicating that NIC does not disrupt the normal Mk transcriptional program. As a result, we investigated the hypothesis that changes in post-translational modifications, as well as cellular programs such as metabolic regulation, were largely responsible for the observed effects of NIC on Mks. NIC was

found to increase Tpo-mediated ERK activation and activation of the downstream ERK target RSK1. NIC was also found to increase the levels of intracellular NAD(H) in a dose-dependent manner.

This work demonstrates that NIC is useful as a supplement to increase the productivity of *ex vivo* Mk cultures. Moreover, NIC-treated Mks could serve as a novel model for studying Mk polyploidization where cells reach ploidy levels closer to that observed *in vivo*. Further elucidation of the mechanisms by which NIC increases Mk maturation could lead to a greater understanding of Mk differentiation and may lead to advances in the treatment of Mk and platelet disorders.

Table of Contents

List of Figures

CHAPTER 1 – Introduction, Significance and Background

CHAPTER 2 – Phenotypic characterization of the effects of NIC on Mk differentiation

CHAPTER 3 – Characterization of the mechanism(s) underlying the effects of NIC on Mk differentiation

CHAPTER 4 – Effects of NIC on hematopoietic stem cell differentiation towards other lineages (erythrocytic and granulocytic)

CHAPTER 5 – Conclusions and Recommendations

CHAPTER 6 – Appendix

1. CHAPTER 1

1.1. Introduction and significance

Megakaryocytes (Mks) are derived from hematopoietic stem cells (HSCs) via bi-potent erythro-megakaryocytic progenitors.[2,3] Mks are distinguished by their very large size and rarity (less than 1% of marrow cells) in the bone marrow. As the immediate precursors to platelets, Mks are central to blood coagulation and hemostasis. The sequence of Mk differentiation is well understood, including progression through several rounds of endomitosis to become polyploid cells with multilobated nuclei, the development of a demarcation membrane system, and the production of cytoplasmic extensions called proplatelets, from which platelets are released. However, Mk commitment and the molecular and cellular mechanisms through which Mks differentiate and mature remain poorly understood, due in large part to their scarcity *in vivo* and the difficulties encountered in culturing human Mks *in vitro*. Elucidating these mechanisms is important to understanding megakaryopoiesis under physiological and pathophysiological conditions and could provide the basis for clinical advances for the treatment of Mk and platelet disorders, such as thrombocytopenia, refractory thrombocytopenia in myelodysplastic syndrome, megakaryoblastic leukemia, and essential thrombocythemia.[4-6] Furthermore, *ex vivo* culture of HSCs under conditions that promote Mk commitment, expansion, and differentiation would enable the production of Mk post-progenitor cells and mature Mks for transplantation therapies to offset thrombocytopenia associated with HSC transplants following high-dose chemotherapy.[7,8] In the longer term, the ability to control these processes may allow for the production of large numbers of platelets *in vitro* for use in platelet transfusions.

Thrombopoietin (Tpo) is the major cytokine controlling Mk commitment, maturation, and platelet production.[9,10] *Ex vivo* culture of hematopoietic stem and progenitor ($CD34^+$) cells with Tpo alone yields a high purity of $CD41^+$ Mks.[11-13] However, the size and ploidy of human Mks produced in culture with Tpo alone are much smaller than those observed *in vivo*. Increasing the number of high-ploidy cells and/or the degree of polyploidization is important because there is a direct correlation between Mk DNA content and the number of platelets produced per Mk.[14]

We have discovered that nicotinamide (NIC), one of the two principle forms of niacin (vitamin B3), greatly increases Mk ploidy and proplatelet production – without affecting Mk commitment – in Tpo-stimulated cultures of mobilized peripheral blood $CD34^+$ cells. Studies to thoroughly characterize the effects of NIC on Mk maturation are presented in Chapter 2 and demonstrate that NIC can be used directly to increase the productivity of *ex vivo* Mk cultures. Furthermore, NIC-treated cells could also serve as a novel model for studying Mk polyploidization where cells reach ploidy levels closer to those observed *in vivo*. However, it was also important to determine the underlying mechanisms of NIC. Doing so would lead to a greater understanding of Mk differentiation and may allow for further modulation of Mk maturation. Chapter 3 outlines the studies performed to address several hypotheses as to how NIC may be enhancing Mk maturation. Lastly, since it is possible that NIC may also increase Mk maturation and platelet production *in vivo*, it was important to understand how NIC may affect the differentiation of cells towards other hematopoietic lineages. Therefore, erythrocytic and granulocytic differentiation was examined in cultures with NIC (Chapter 4).

1.2. Background

1.2.1. Megakaryopoiesis

Megakaryocytes (Mks) are distinguished by their prominent large size and rarity (less than 1% of marrow cells) in bone marrow. Consecutive yet distinct developmental stages and respective stage-specific markers of megakaryopoiesis have been well established. Mks are derived from bi-potent erythro-Mk progenitors (Fig 1.1).[2,3] Once committed, Mks undergo a complex process of differentiation to form platelets (Fig 1.2). Megakaryocyte maturation involves the development of polyploid cells via endomitosis, a modified cell cycle in which several rounds of DNA replication occur without cytokinesis. Endomitosis results in cells accumulating DNA content as great as 128N *in vivo* (media DNA content 16N). At this stage, Mks undergo identifiable morphological changes including the development of a demarcation membrane system and a large increase in cell size. Mk terminal differentiation is also characterized by a constitutive program of apoptosis. Once apoptosis is initiated, cytoplasmic extensions, called proplatelets, protrude from Mks; platelets are then packaged and released at the proplatelet tips.[15]

In vitro megakaryopoiesis varies with the culture conditions. Thrombopoietin (Tpo) is the major cytokine controlling Mk commitment, maturation, and platelet production[9,10] and *ex vivo* culture with Tpo alone leads to a high purity of $CD41^+$ Mks.[12,16,17] Stimulation with additional cytokines can lead to improved Mk expansion, but typically at the cost of lower purity.[10,18-20] Flt-3 ligand promotes the expansion of total $CD41^+$ cells, likely via expansion of uncommitted early progenitors.[19] IL-3 promotes Mk progenitor expansion, but not maturation.[19] Stem cell factor (SCF) together with Tpo promotes Mk maturation and down-regulates apoptosis

in vitro.[21] Stromal cell-derived (SDF)-1α enhances Mk polyploidization.[22] In addition to cytokines, numerous other factors have been found to influence Mk culture outcomes; these include pH,[23] pO_2,[18] temperature,[24] and signaling pathway inhibitors.[25] Also, the extracellular matrix components fibronectin[26-29] and fibrinogen[30] have been shown to enhance Mk growth and to promote Mk adhesion.

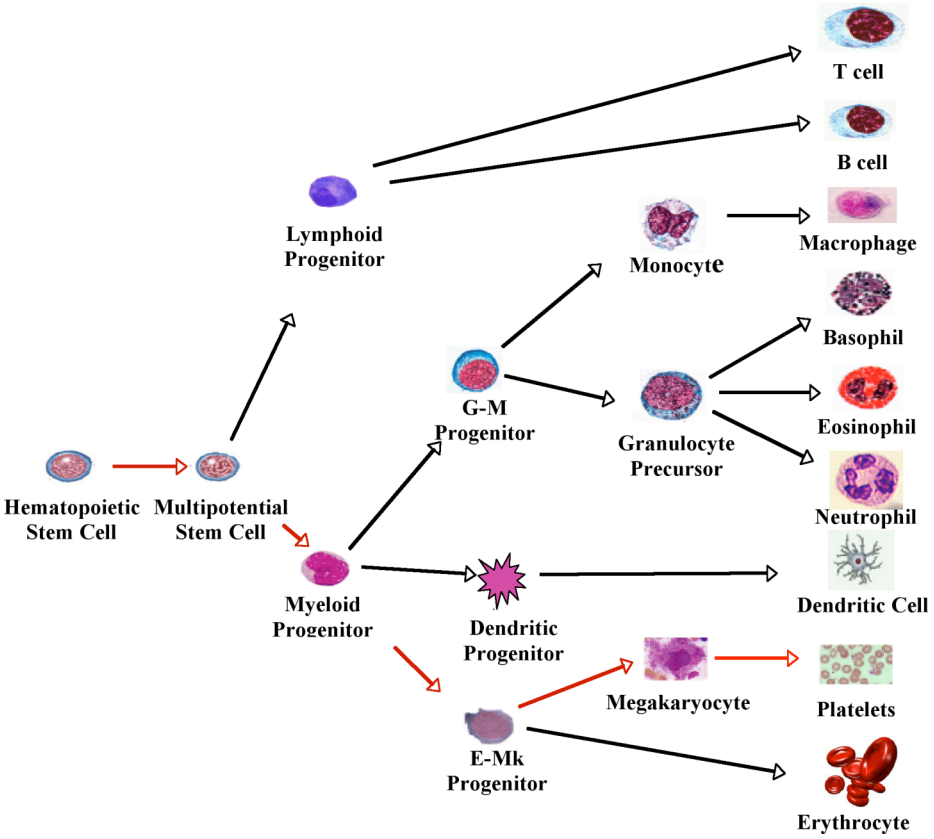

Figure 1.1. Hematopoietic hierarchy.

Megakaryocytes are mature blood cells responsible for the production of platelets, which are necessary for the formation of blood clots. Similar to all mature blood cells, Mks arise from a lineage restricted progenitor cell which is generated from a hematopoietic stem cell. Once committed, Mks undergo a complex process of maturation.

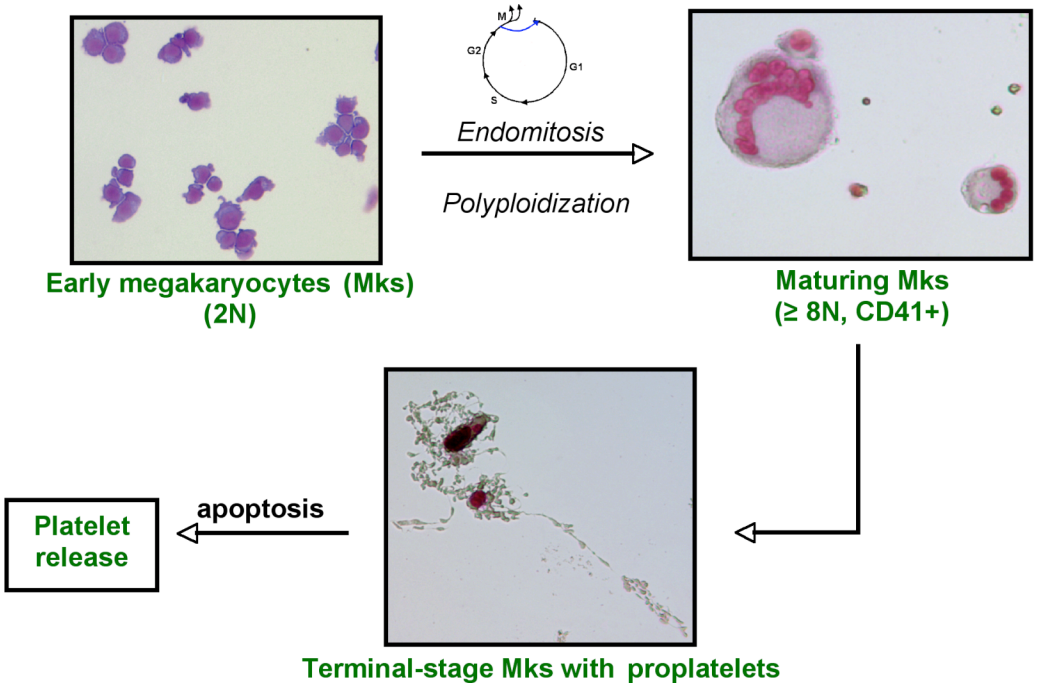

Figure 1.2. Mk maturation.

Early Mks are small in size and are diploid having a DNA content of 2N. During normal development, the cells undergo endomitosis that results in the formation of large polyploid cells with a DNA content of 8N and greater. Further maturation involves the formation of long cytoplasmic extensions termed proplatelets and maturation concludes with the shedding of platelets. The DNA content of cells is directly proportional to the number of platelets released per Mk. The process is also characterized by a constitutive program of apoptosis, which is thought to be linked to platelet release.

1.2.2. Nicotinamide

Nicotinamide (NIC) is one form of niacin (vitamin B3); the other major form is nicotinic acid (NA) (Fig 1.3). Both compounds are precursors to nicotinamide adenine dinucleotide (NAD^+), which is necessary for cellular function and metabolism (Fig 1.4); however, they possess different pharmacological activities.[31,32]

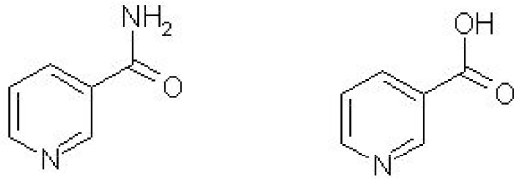

Nicotinamide (NIC) Nicotinic acid (NA)

Figure 1.3. Chemical structures of the two forms of niacin – nicotinamide (NIC) and nicotinic acid (NA).

Nicotinamide has a variety of known functions including its ability to inhibit the activity of two NAD^+-dependent enzymes, poly (ADP-ribose) polymerase (PARP) and Sir2 (Class III HDAC inhibitor). DNA damage leads to PARP activation that then catalyzes the sequential transfer of ADP-ribose monomers onto a variety of nuclear protein acceptors using NAD^+ as substrate. NIC acts as an inhibitor of PARP by blocking NAD^+ binding to the catalytic domain of the enzyme. Inhibition of PARP preserves NAD^+ stores and thereby allows cells to either function normally or die by apoptosis as opposed to necrosis. Evidence has also shown a role for PARP in DNA replication.[33] PARP-1 has been shown to interact with many cell cycle regulators such as p21,[34] proliferating cell nuclear antigen (PCNA),[34] and p53.[35] Additionally, $PARP1^{-/-}$ fibroblasts show abnormal cell ploidy with cells having 1N, 3N, and 8N DNA content compared to wild type 2N and 4N.[36] Taken together, this suggests that inactivation of PARP may lead to a disruption in the control of normal cell ploidy.

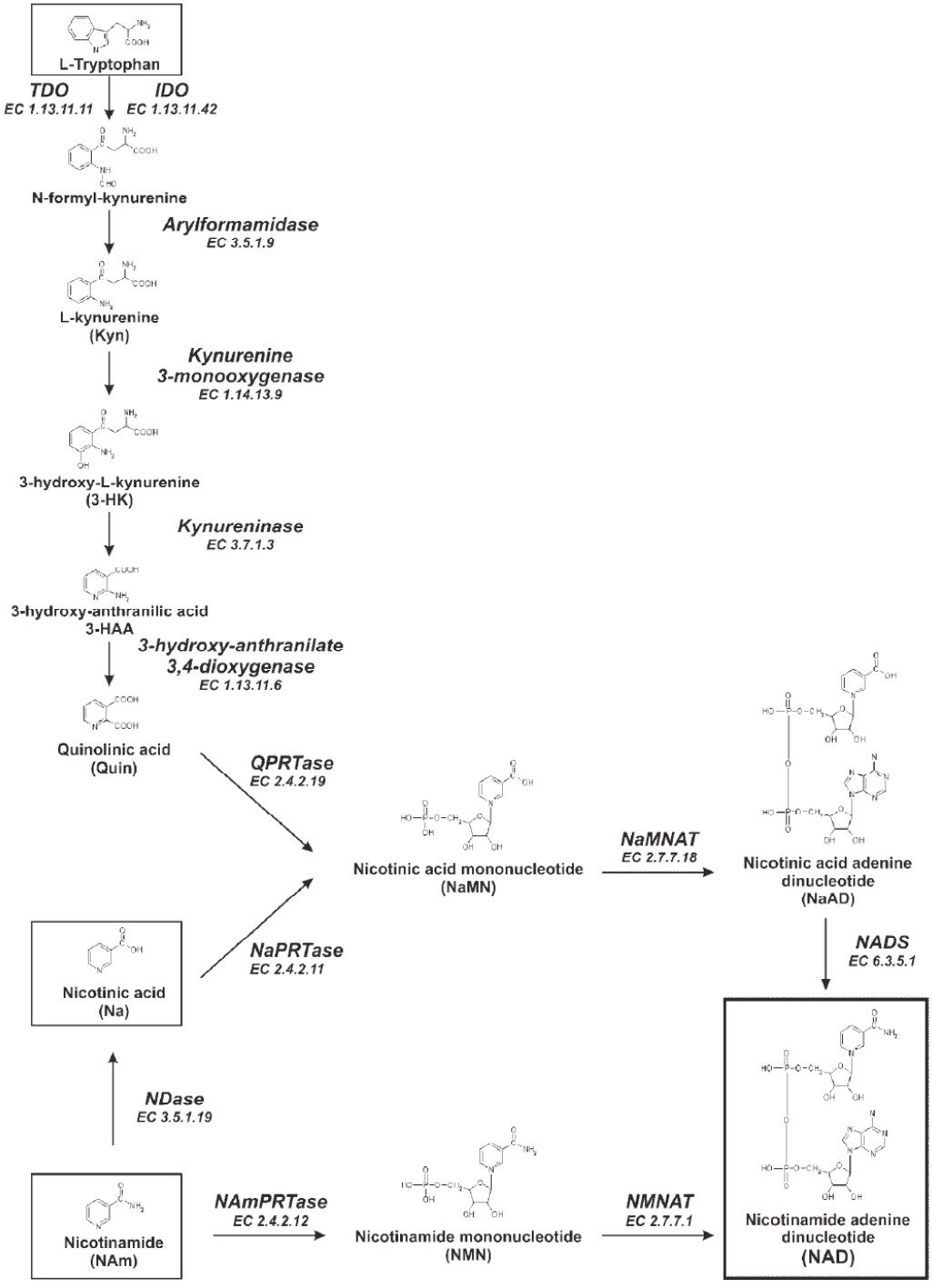

Figure 1.4. NAD metabolism in humans.

Figure from Rongvaux *et al*. BioEssays, 2003.[1]

NIC also inhibits the activity of several members of the silent information regulator 2 (Sir2) family of proteins, a class of NAD^+-dependent histone deacetylases. Sirtuins catalyze a unique NAD^+-dependent reaction and are required for a wide variety of biological processes including transcriptional silencing, regulation of apoptosis, and lifespan regulation.[37,38] NIC inhibits the ability of SIRT1 to deacetylate p53.[39] In general, post-translational modifications such as acetylation promote p53 stability.[40] NIC also inhibits SIRT2, which acts as an α-tubulin deacetylase. α-tubulin has an important role in the regulation of cell shape, cell division, and intracellular transport.[41] More specifically, acetylated α-tubulin plays a role in stabilization of microtubules.[42] While βı-tubulin is the major isoform present in proplatelet and platelet microtubules, α-tubulin can be visualized in Mks.[43,44]

NIC has also been shown to exert a protective effect against apoptosis through activation of Akt1 and Bad phosphorylation.[45,46] In addition to its role in apoptosis, Akt is a broad acting molecule affecting modulators of cytoskeleton organization such as Gsk3 (glycogen synthase kinase 3). Akt phosphorylates and inactivates Gsk3 which has a role in microtubule dynamics and is also expressed in human platelets.[47] Various cell-cycle regulators with an established role in Mk maturation including p21, cyclinD1 and cyclinD3 are also present downstream from Akt.[48-51]

More generally, nicotinamide (and nicotinic acid) serve as precursors for NAD^+. NIC supplementation increases levels of intracellular NAD^+ in cultured cells by as much as 40% after 3 hours and up to 3-fold after 48 hours.[52-54] *In vivo* administration of NIC also leads to increased NAD^+ levels in the blood, liver[55] and brain.[56] Alternatively, cells may synthesize NAD^+ from nicotinic acid (NA). NA supplementation increases intracellular NAD levels in various types of

cultured cells,[57,58] and dietary supplementation of NA leads to elevated levels of NAD^+ in the kidney, liver, blood and heart.[55] NAD can also be synthesized from tryptophan via its metabolite quinolinic acid (QA) (*de novo* pathway). Direct supplementation of QA has been shown to increase intracellular NAD^+ levels in cultured glial cells.[57] Importantly, the efficacy of NAD^+ synthesis from QA, NIC or NA appears to vary among different cell and tissue types.

NAD^+ regulates a range of intracellular activities. Most widely known for its role as an essential cofactor for energy metabolism, NAD^+ is used extensively in glycolysis and the citric acid cycle of cellular respiration and also acts as an electron acceptor in the electron transport chain. NAD^+ also has non-redox functions, serving as a substrate for reactions involved in protein modifications including the previously mentioned poly (ADP-ribose) polymerases and Sir2 family of histone deacetylases. Additionally, increased levels of intracellular NAD^+ have been shown to alter DNA binding specificity of p53, leading to reduced radiation-induced expression of p53 targets (hdm2 and PIG3) and increased frequency of aneuploid cells.[52] Since p53 is responsible for the prevention of aneuploidy and rereplication,[59] this suggests that NAD^+ levels may modulate cellular DNA content via p53.

1.2.3. Clinical applications of nicotinamide

NIC has been administered safely at pharmacological doses for a variety of therapeutic applications, dating back to the late 1950s for treatment of psychiatric conditions such as schizophrenia. More recently, NIC has undergone clinical testing for use as a preventative agent for Type I diabetes.[60-62] Daily administration of large doses of NIC (500 mg/kg) for 2-5 weeks has been shown to prevent or delay the development of diabetes in animal models.[63-65] However,

results from human trials have been inconsistent. Early clinical trials were promising,[60] but additional studies have shown that NIC is not effective for the prevention of Type I diabetes at oral doses of 1-3 g/day for 5 years. Significantly, however, no major adverse effects were reported.[61,62] The safety of high-dose NIC has been recently reviewed.[31] Doses up to 3 g/day have been generally well tolerated. Overall, few side effects are reported following NIC administration, with the most common being nausea, vomiting, and headache. Large doses of NIC (9-10 g/day) may be hepatotoxic[66] and cause severe nausea and vomiting[67] in some patients. However, 60-80 mg/kg doses of NIC (up to a total of 6 g/day) are commonly used in clinical studies in combination with accelerated radiotherapy and carbogen to enhance radiation damage in tumors.[68-70] NIC administration at 6 g/day to humans produces the millimolar plasma concentrations necessary to obtain a radiosensitizing effect.[71,72]

2. CHAPTER 2: Phenotypic characterization of the effects of nicotinamide on megakaryopoiesis

2.1. Introduction

As the immediate precursors to platelets, megakaryocytic cells (Mks) are central to blood coagulation and hemostasis. Megakaryocytic differentiation from hematopoietic stem cells (HSCs) involves the development of polyploid cells via endomitosis – a modified cell cycle in which several rounds of DNA replication occur without cytokinesis.[73,74] The increase in DNA content is associated with the development of multilobated nuclei and increases in cytoplasmic volume and cell surface area. This is followed by the extension of proplatelets (long branched cytoplasmic protrusions) from which platelets are released.[43,75] Mk maturation is further characterized by the induction of apoptosis,[16,76] which is thought to be correlated to and occur concurrently with platelet formation.[17] Thrombopoietin (Tpo) is the primary regulator of megakaryopoiesis, inducing both recruitment of progenitor cells into the Mk lineage and polyploidization.[77-79]

Mk commitment and the molecular and cellular mechanisms through which Mks differentiate and mature remain poorly characterized, due in large part to the rarity of Mks *in vivo*. Elucidating these mechanisms is key to understanding megakaryopoiesis under physiological and pathophysiological conditions and could provide the basis for clinical advances for the treatment of Mk and platelet disorders, such as thrombocytopenia, refractory thrombocytopenia in myelodysplastic syndromes, megakaryoblastic leukemia, and essential thrombocythemia. Furthermore, *ex vivo* culture of HSCs under conditions that promote Mk commitment, expansion, and differentiation would enable the production of immature and

mature Mks for transplantation therapies and may also allow for the production of platelets *in vitro* for use in platelet transfusions.[80]

In vitro models have proven useful for studying the molecular events governing megakaryopoiesis. However, it is not yet possible to achieve ploidy levels in cultured human cells that are as high as those observed *in vivo*. Human bone marrow Mks reach a maximum DNA content of 128N, with a modal ploidy of 16N.[81] In contrast, cultured human Mks typically reach a maximum DNA content of 16N,[22,25,82,83] with only a few reports of cultures containing a low frequency of cells with a ploidy of 32N or 64N.[14,84] Culture conditions that yield high Mk ploidy are desirable because there is a direct correlation between Mk DNA content and platelet production.[14] Some progress has been made to increase Mk ploidy using genetic modification or chemical modulation of signaling pathways. However, most studies have been conducted using megakaryocytic cell line models and murine Mks, with only a limited number of studies performed using primary human Mks.[22,25,51,83]

We have used gene expression microarrays to characterize the changes in gene transcription that accompany Mk differentiation (C. Chen, P. Fuhrken, W. Miller and E.T. Papoutsakis, manuscript submitted April 2007). These studies revealed the up-regulation of several members of the silent information regulator 2 (Sir2) family of histone/protein deacetylases with Mk differentiation. Nicotinamide (NIC), also known as water-soluble vitamin B3, is a known Sir2 inhibitor. In the present study, we characterize the effects of NIC on primary human Mk maturation *in vitro*. We demonstrate that NIC greatly enhances Mk endomitosis and proplatelet formation, irrespective of donor-dependent variations in Mk maturation. In doing so, we also provide a novel experimental model to explore the complex process of Mk

differentiation in which cells achieve a maximal ploidy of 64N, which is close to that reached *in vivo*.

2.2. Materials and methods

2.2.1. Human Mk culture

Unless otherwise noted, all reagents were obtained from Sigma-Aldrich (St. Louis, MO). Cultures were initiated with previously frozen human mobilized peripheral blood $CD34^+$ cells (AllCells; Berkeley, CA). Cells were cultured in T-flasks and maintained at a density of 100,000–200,000 cells/mL with a constant liquid depth of 0.33 cm. All cultures were performed using X-VIVO 20 (BioWhittaker; Walkersville, MD) supplemented with 100 ng/mL Tpo (generously provided by Genentech; South San Francisco, CA). Beginning at various time points (days 0, 3, 5, 7), cells were continuously treated with nicotinamide. Every other day, half-media exchanges were performed using fresh medium containing 100 ng/mL Tpo and either 3 or 6.25 mM NIC. Cells receiving no NIC were used as a control. Cells were incubated at 37^oC in a fully humidified atmosphere of 5% CO_2 and 95% air.

2.2.2. Murine Mk culture

Bone marrow cells were isolated from normal male CD-1 mice (Charles River; Wilmington, MA) with approval from the Northwestern University Animal Care and Use Committee. Mice were sacrificed using CO_2 and cervical dislocation and the femurs were dissected. Cells from the bone marrow were collected by flushing the bones with Hank's Balanced Salt Solution (HBSS) containing 1% penicillin/streptomycin using a syringe and a 21-gauge needle until the bones appeared white. Bone marrow cells were washed with PBS and resuspended in ACK buffer (0.15 M NH_4Cl, 1.0 mM $KHCO_3$, 0.1 mM Na_2EDTA, pH 7.2-7.4)

for red cell lysis. Cells were plated in 6-well plates at a concentration of 1 x 10^6 cells/mL in Dubelcco's modified Eagle's medium (DMEM) supplemented with 10% fetal bovine serum (FBS; HyClone, Logan, UT), 1% penicillin/streptomycin and 100 ng/mL human Tpo (Genentech). Cultured murine Mks mature more rapidly than human Mks; therefore, NIC was added on day 1 after seeding and DNA content was assessed using flow cytometry on day 4.

2.2.3. Human megakaryoblastic cell line culture

The human megakaryoblastic CHRF-288-11 (CHRF) cell line[85,86] was generously provided by Dr. R. Smith (NIH; Bethesda, MD). CHRF cells were cultured in Iscove's modified Dubelcco's medium (IMDM) supplemented with 10% FBS (HyClone). Cells were treated with 10 ng/mL phorbol 12-myristate 13-acetate to induce megakaryocytic differentiation, as characterized by morphological changes including adherence, increased cell size, and the formation of long cytoplasmic extensions. NIC was added beginning at the time of PMA addition.

2.2.4. Mk culture with Sir2/PARP inhibitors

Synthetic inhibitors of Sir2 or poly (ADP-ribose) polymerase (PARP) were dissolved in DMSO and added to human Mk cultures beginning on day 5. Half-media exchanges were performed every other day for inhibitor replacement. Sir2 inhibitors were tested in the following concentration ranges: sirtinol (Calbiochem; San Diego, CA) (1–50 μM) and splitomicin (1–100 μM). PARP inhibitors were tested in the following concentration ranges: 3-aminobenzamide and

benzamide (0.1–6.25 mM), 5-iodo-6-amino-1,2 benzopyrone (INH_2BP, Calbiochem) (1–100 μM). Cells treated with an equal volume of DMSO were included as a control.

2.2.5. Mk characterization

2.2.5.1. Flow cytometric detection of CD41 expression

Cells were washed with phosphate-buffered saline (PBS) containing 2 mM EDTA (to reduce platelet adhesion) and 0.5% bovine serum albumin (BSA) [PEB], incubated with fluorescein (FITC)-labeled anti-CD41 antibody (Becton Dickinson; San Jose, CA) for 30 minutes at room temperature, and then analyzed on a Becton Dickinson LSRII flow cytometer using FACSDiva software (Becton Dickinson). 7-amino-actinomycin D (7-AAD; 2 μg/mL) was added to samples shortly prior to acquisition to exclude dead cells.

2.2.5.2. Flow cytometric analysis for Mk apoptosis

Simultaneous staining for CD41, Annexin V, and 7-AAD was used to detect viable Mks undergoing apoptosis ($CD41^+$, Annexin V^+, $7AAD^-$). Briefly, cells were washed with PEB and incubated with PE-conjugated anti-CD41 antibody (Becton Dickinson; San Jose, CA). After washing, cells were resuspended in Annexin V binding buffer (10 mM HEPES, 140 mM NaCl, 2.5 mM $CaCl_2$, pH 7.4) containing FITC-conjugated Annexin V and 7-AAD, and analyzed by flow cytometry. The ratio of the number of apoptotic Mks to the total number of $7AAD^-$ Mks was used to calculate the percentage of apoptotic Mks.

2.2.5.3. Flow cytometric analysis for Mk ploidy

Cells were labeled with FITC-conjugated anti-CD41 antibody (Becton Dickinson; San Jose, CA) and fixed with 0.5% paraformaldehyde (15 minutes at room temperature), followed by permeabilization with cold 70% methanol (1 hour at 4^{o}C). Cells were treated with RNAse followed by 50 μg/mL propidium iodide to stain DNA, and analyzed by flow cytometry. The percentage of high-ploidy Mks was determined from the ratio of the number of $CD41^{+}$ Mks with 8N or higher DNA ploidy to the total number of $CD41^{+}$ Mks. The geometric mean (GM) ploidy was determined as described by Iancu-Rubin *et al.*[87]

2.2.5.4. Morphological analysis

2.2.5.4.1. Giemsa staining

Cells collected at different days of culture were cytocentrifuged (Shandon Cytospin3, Thermo Electron; Waltham, MA) onto glass slides, stained with Wright-Giemsa (Quik Stain II, Camco; Ft. Lauderdale, FL) and observed by light microscopy. To obtain images of proplatelet-forming Mks, cells were fixed *in situ* with 2% paraformaldehyde prior to cytocentrifugation. Cells were observed with a Leica DM IL inverted contrasting microscope (Heidenheim, Germany) fitted with a SPOT Insight 2MP Firewire Color Mosaic camera (Diagnostic Instruments; Sterling Heights, MI). Images were captured using SPOT software (Diagnostic Instruments). Cells displaying 1 or more cytoplasmic extensions were counted in 5 fields of view at 300x magnification.

2.2.5.4.2. Electron microscopy

Cells from Tpo only and Tpo + NIC cultures were removed from culture on day 8 and transferred to fibronectin-coated 35-mm petri dishes (BD Biosciences) to induce cell adherence. After 48 hours, media was removed and cells were fixed for 4 hours (2.5% glutaraldehyde/2.5% paraformaldehyde in 0.1 M cacodylate buffer, pH 7.4). Cells were then processed for EM by the Northwestern University Cell Imaging Facility. Briefly, after embedding the cells in Epoxy resin in an inverted capsular mold, ultra thin sections were cut, stained with uranyl acetate and lead citrate, and examined with a JEOL-1220 transmission electron microscope at an accelerating voltage of 60kV.

2.2.5.4.3. Immunofluorescence detection of β-tubulin expression

Cells were prepared as previously described[88] and stained with an anti-human β-tubulin antibody (BD Biosciences) followed by a FITC-conjugated goat anti-mouse IgM antibody (Jackson ImmunoResearch). Cells were then mounted using Prolong Gold anti-fade reagent with DAPI (Invitrogen; Carlsbad, CA) and imaged using a DMIRE2 inverted microscope (Wetzlar, Germany) at 40x magnification.

2.2.6. PARP activity assay

The Universal Colorimetric PARP Assay Kit (Trevigen; Gaithersburg, MD) was used following the manufacturer's instructions to measure the incorporation of biotinylated poly (ADP-ribose) onto histone-coated plates by PARP present in cell lysates. The incorporated biotin

is detected using horseradish peroxidase (HRP)-conjugated streptavidin and a colorimetric HRP substrate. Cell extracts were prepared on days 5 (2 hrs after NIC treatment), 7, and 9 from cells cultured with Tpo only and with Tpo + 6.25 mM NIC.

2.2.7. Microarray analysis of gene expression

Primary human Mk cultures were performed as described above. 6.25 mM NIC was supplemented to cultures beginning on day 5. Cells were sampled on days 5 (before NIC addition), 6, 8, and 10 from both the Tpo only and Tpo + NIC conditions and frozen for later analysis.

Detailed protocols for microarray sample preparation, hybridization, and data analysis are provided below (2.2.7.1-2.2.7.2). Briefly, RNA was isolated, linearly amplified, and hybridized to Human 1A(v2) 60-mer oligonucleotide microarrays following the manufacturer's protocols (Agilent Technologies; Wilmington, DE). Hybridizations were performed in a reference design with each biological sample, labeled with cyanine 3 (Cy3), co-hybridized with amplified Universal Reference RNA (Stratagene; LaJolla, CA) labeled with Cy5. All hybridizations were performed in duplicate or triplicate. Raw and normalized data were deposited in the Gene Expression Omnibus (GSE4974; http://www.ncbi.nlm.nih.gov/geo/).

2.2.7.1. Microarray sample preparation, hybridization, and scanning

All materials and methods for microarray analysis were from Agilent Technologies (Wilmington, DE) unless otherwise noted. Total RNA was isolated from frozen cell samples using the RNA Isolation Mini-kit and then linearly amplified and labeled with cyanine 3 (Cy3)

using the Low RNA Input Fluorescent Linear Amplification Kit. Similarly, Universal Reference RNA (Stratagene; La Jolla, CA) was amplified and labeled with Cy5. Samples were hybridized in a reference design configuration to permit flexible data analysis between experiments and across time courses. A Cy3-labeled sample and Cy5-labeled Reference RNA were co-hybridized to Agilent Human 1A(v2) 60-mer oligonucleotide microarrays, washed with buffers containing saline sodium citrate and Triton X-102, dried using compressed nitrogen, and scanned on an Agilent Microarray Scanner (G2565BA), all per the manufacturer's instructions.

2.2.7.2. Microarray data analysis

Agilent's Feature Extraction software (G2567AA, version 7.2) was used to assess spot quality and extract feature intensity statistics; then, duplicate spots were averaged and data were normalized.[89] Normalized log ratios from replicate hybridizations (at least two per sample) were averaged.

Two-way ANOVA was performed using the MultiExperiment Viewer 3.1 (MeV; Institute for Genomic Research, Rockville, MD; http://www.tm4.org/mev.html)[90] with a statistical cut-off of $p<0.001$. Genes with significant treatment effects or treatment-time interaction effects were considered to be affected by NIC. Because of substantial differences in the kinetics of maturation observed in the two cultures, ANOVA was performed separately on each experiment and only genes found to be affected by NIC in both experiments were included in the final set of differentially expressed genes.

The Mk-core gene set of Balduini *et al*.,[91] which is presented in Fig 2.11A , was mapped from the Affymetrix probe set ID to the Agilent probe_ID using Ensembl v38

(www.emsembl.org). The original set of 70 genes mapped to a total of 59 probes for which valid data was available on the Agilent Human 1A(v2) microarray.

Heirarchical clustering was performed using the Euclidian distance metric as implemented in MeV.

2.2.8. Quantitative (Q)-RT-PCR

Quantitative (Q) reverse transcription (RT) polymerase chain reaction (PCR) was performed using the High-Capacity cDNA Archive Kit and Assays-on-Demand Taqman Kit with the accompanying protocols (Applied Biosystems; Foster City, CA). The following primer codes were used: c-Myb, Hs00193527_m1; GUS-β, Hs99999908_m1; RPLP0, Hs99999902_m1; 18s, Hs99999901_s1. PCR reactions were scaled-down to 25 μL and performed on a Bio-Rad iCycler (BioRad; Hercules, CA). A standard curve using serial dilutions of the reference RNA (Stratagene) was used to verify linearity, and samples were diluted to ensure they remained within the linear range for the assay. The amount of mRNA for each sample was normalized using the average of three housekeeping genes (glucuronidase-β, large ribosomal protein P0, and 18s ribosomal RNA), as recommended by Applied Biosystems.

2.2.9. Statistical analysis

Statistical comparisons between cultures with Tpo only and those with Tpo + NIC were performed using a paired Student's t-test. p values < 0.05 are considered significant.

2.3. Results

2.3.1. NIC increases Mk ploidy and proplatelet formation in a dose-dependent manner

We first examined the effects of different amounts of NIC on primary human Mk maturation in the presence of Tpo (100 ng/mL). Replicate cultures with mPB $CD34^+$ cells from the same donor were performed in which 3, 6.25, 12.5, or 25 mM NIC was added beginning on day 5. NIC inhibited cell growth in a dose-dependent manner (Fig 2.1). 12.5 mM NIC completely inhibited growth and 25 mM was cytotoxic. Therefore, NIC doses $\geq$ 12.5 mM were not analyzed further. Cell growth with 3 mM NIC was only slightly lower than that with Tpo only and 6.25 mM NIC had an intermediate effect. Morphological analysis of cells cultured with 3 mM or 6.25 mM NIC revealed the presence of more highly-lobated nuclei and a dose-dependent increase in cell size (Fig 2.2A). DNA histograms show that NIC addition also

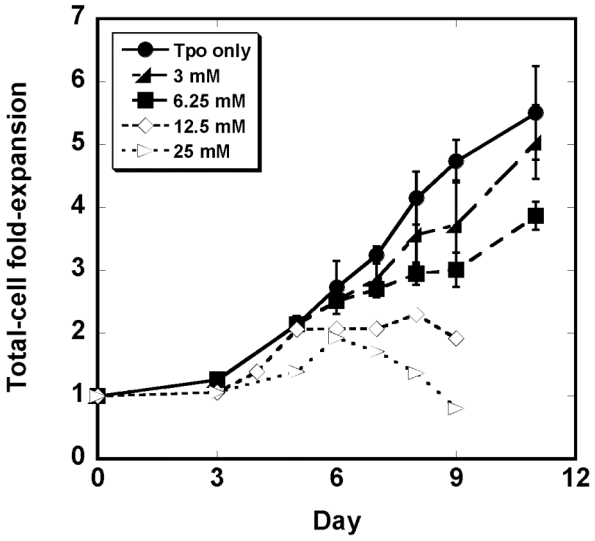

Figure 2.1. Dose-dependent growth inhibition by NIC. mPB $CD34^+$ cells were cultured with Tpo only, and either 0, 3, 6.25, 12.5, or 25 mM NIC was added on day 5. The average total-cell fold-expansion is shown for 0, 3, and 6.25 mM NIC for two replicate cultures performed with cells from the same donor. 12.5 mM NIC completely inhibited growth and 25 mM was cytotoxic; therefore only 1 culture was performed with these concentrations.

yielded much greater DNA content (Fig 2.2B). Mks reached a maximum ploidy of 64N for 6.25 mM NIC and 32N for 3 mM NIC compared to 16N for cells cultured with Tpo only. NIC also increased the percentage of high-ploidy ($\geq$ 8N) Mks. On day 13, the percentages of high-ploidy Mks for the Tpo only, Tpo + 3 mM NIC, and Tpo + 6.25 mM NIC conditions were 23.6 $\pm$ 0.3, 48.1 $\pm$ 2.7, and 62.2 $\pm$ 0.1, respectively. Addition of NIC also increased the number of proplatelet-bearing Mks, as well as the size and complexity of their cytoplasmic extensions (Fig 2.2C). β-tubulin staining also illustrates the more elaborate proplatelets formed with the addition of NIC (Fig 2.2D).

Figure 2.2. NIC increases primary human Mk size, DNA content and proplatelet formation.

(A) Morphology of Mks examined by staining cytocentrifuged cells with Wright-Giemsa. mPB $CD34^+$ cells were cultured with 100 ng/mL Tpo, Tpo + 3 mM NIC, or Tpo + 6.25 mM NIC. Images are shown for cells on day 11. A dramatic dose-dependent increase in cell size, along with more highly-lobated nuclei, is observed with NIC treatment (magnification 20x; scale bar 50 μm). (B) DNA content was evaluated by propidium iodide staining of permeabilized Mks. DNA histograms are shown for $CD41^+$ Mks cultured with Tpo only (left), Tpo + 3 mM NIC (middle), or Tpo + 6.25 mM NIC (right). Gate shows high-ploidy $CD41^+$ Mks with DNA content greater than or equal to 8N. (C) Proplatelet-bearing Mks (arrow heads) from cultures with Tpo only or Tpo + 6.25 mM NIC were examined by *in situ* fixation followed by cytocentrifugation and staining with Wright-Giemsa (D) $CD34^+$ cells cultured with either Tpo only or Tpo + NIC were transferred to well-plates coated with fibronectin to induce proplatelet formation. β-tubulin expression (green) was detected using immunofluorescence microscopy. DAPI (blue) was used to stain the nucleus. More elaborate proplatelet extensions are observed with NIC. For images in C-D: day 11; magnification 40x; scale bar 50 μm.

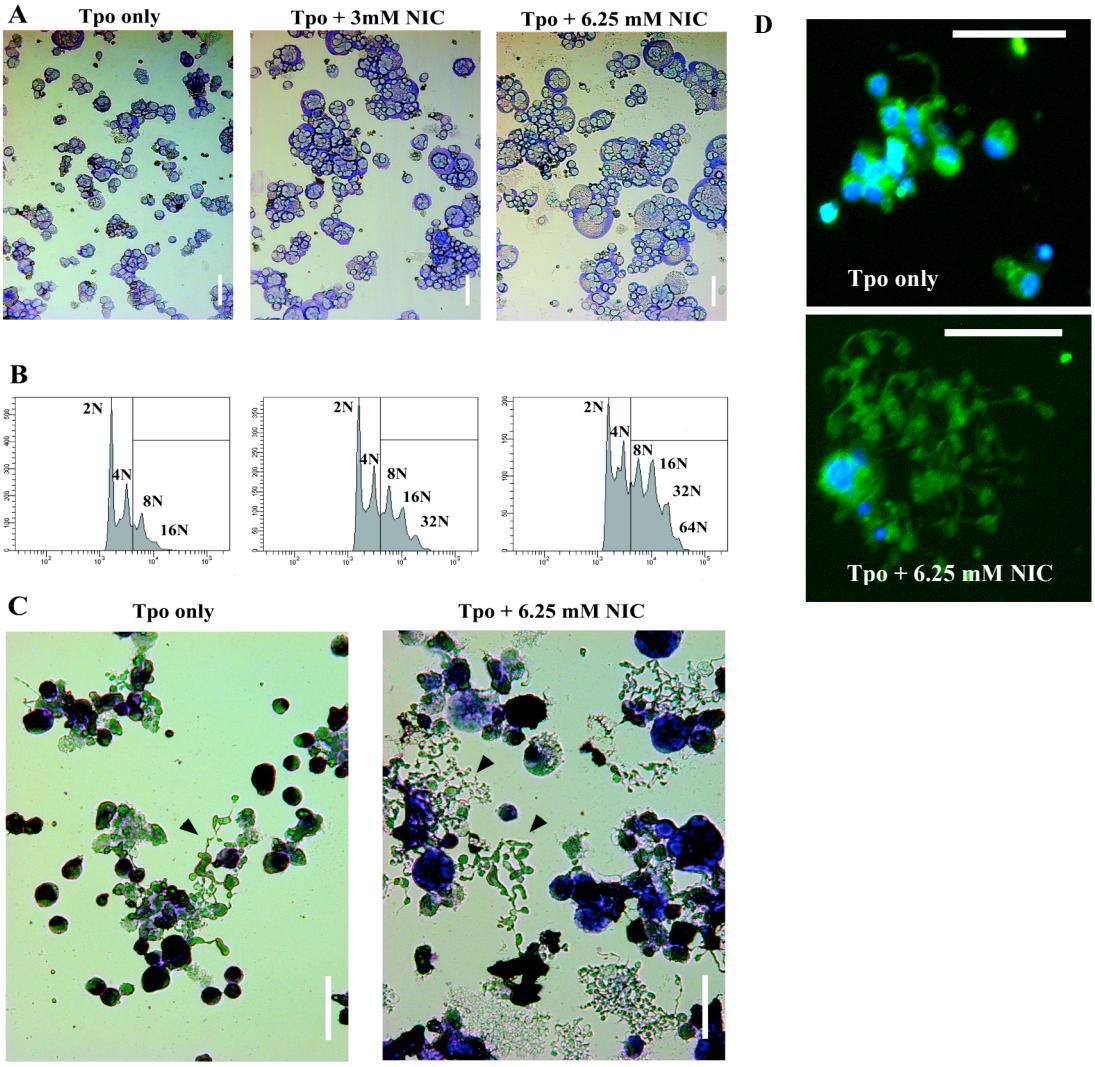
A
Tpo only
Tpo + 3mM NIC
Tpo + 6.25 mM NIC
B
2N
4N
8N
16N
32N
64N
C
Tpo only
Tpo + 6.25 mM NIC
D
Tpo only
Tpo + 6.25 mM NIC

2.3.2. Ultrastructural analysis of NIC-treated Mks

Studies were performed to evaluate whether NIC-treated Mks exhibited normal Mk morphology. The ultrastructure of Mks from Tpo only and Tpo + NIC cultures was examined by electron microscopy. Overall, the structure of cells cultured with Tpo + NIC (Fig 2.3C-F) was similar to that of cells cultured with Tpo only (Fig 2.3A-B). Alpha-granules, dense granules, and mitochondria were visible in cells from both conditions. However, NIC-treated cells were larger and generally had a more complex nuclear structure, both of which are indications of greater Mk maturation. NIC-treated cells also showed evidence of a demarcation membrane system (Fig 2.3E). Mks from both Tpo only and Tpo + NIC cultures exhibited short cytoplasmic projections. However, NIC-treated cells have a greater number of these projections and generally had a larger number of small cytoplasmic microparticles surrounding each cell. Proplatelets were present on some of the cells cultured with Tpo + NIC (Fig 2.3F) and the morphology of the proplatelets shown is similar to that obtained by Cramer *et al*. for human bone marrow $CD34^+$ cells cultured with Tpo (r-Hu-MGDF) only.[92]

Figure 2.3. NIC-treated Mks exhibit normal Mk ultrastructure.

Transmission electron microscopy of Mks cultured with Tpo only (A-B) and Tpo + NIC (C-F). The images in A-D were acquired such that the magnification gave one cell per field of view. Therefore, due to the larger cell size with Tpo + NIC, it was necessary to use a lower magnification (2500x) compared to that for Tpo only (4000x). (E) An image of 3 cells exhibiting a demarcation membrane system (2000x). (F) A proplatelet-bearing Mk (2000x). m = mitochondria, n = nucleus, g = granules, dms = demarcation membrane system, p = proplatelet. Scale bar = 2 μm.

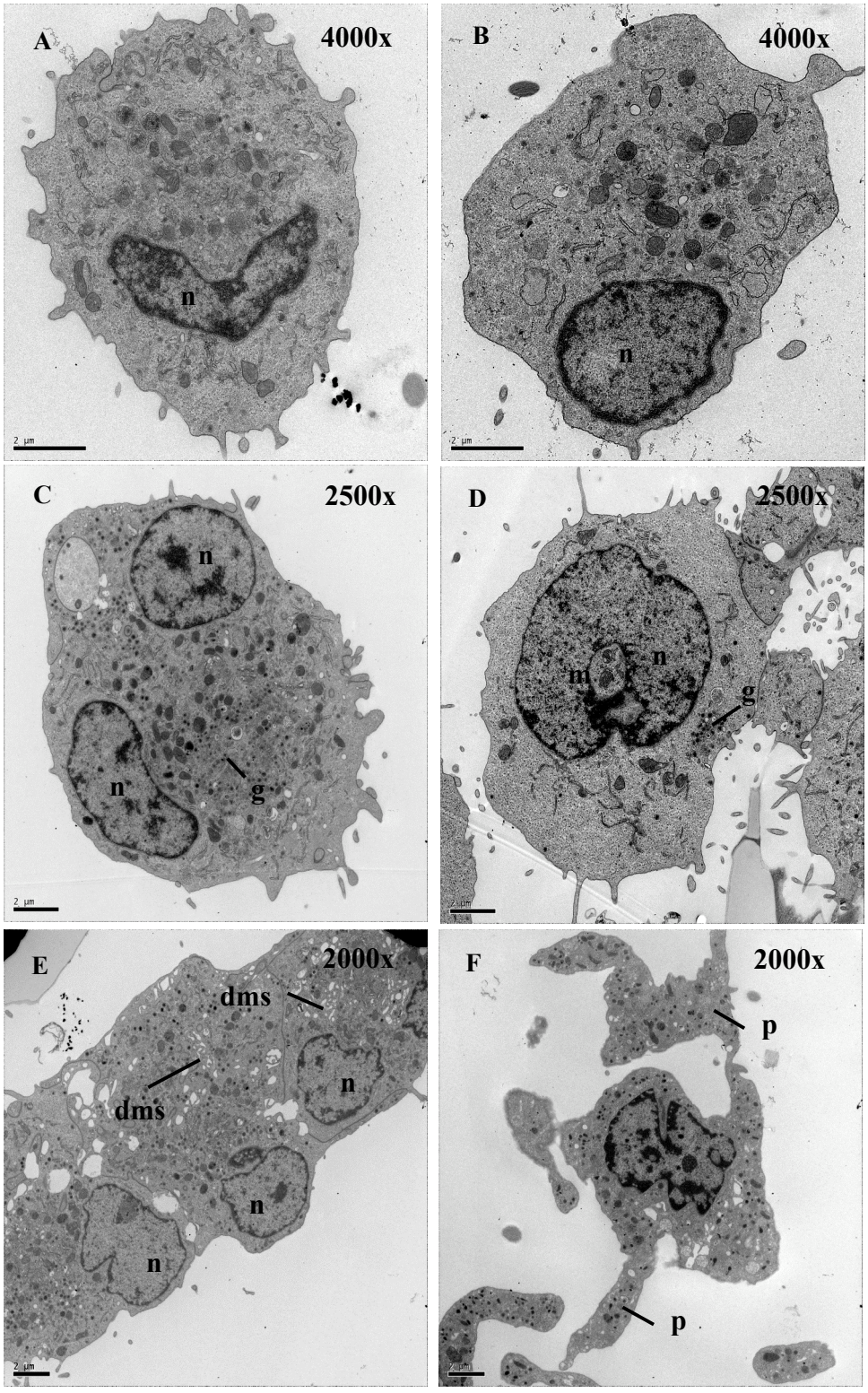
A
4000x
n
B
4000x
n
C
2500x
n
n
g
D
2500x
n
m
g
E
2000x
dms
dms
n
n
n
F
2000x
p
p

2.3.3. Consistency of NIC-enhanced Mk ploidy and proplatelet formation across donors

All further mPB $CD34^+$ cell cultures were carried out using 6.25 mM NIC. A total of 10 primary Mk cultures were initiated using cells from 7 different donors. The effects of NIC on Mk ploidy were consistent across all cell samples tested (Fig 2.4A), despite significant donor-to-donor variability in Mk maturation. The percent of high-ploidy Mks on day 11 ranged from 13.5–34.6 and 25.0–53.4 for the Tpo only and Tpo + NIC cultures, respectively. However, in all cases there was a 1.5- to 2.5-fold increase in high-ploidy Mks with 6.25 mM NIC (day 11). NIC consistently shifted the distribution of Mk ploidy towards the higher classes (Fig 2.4B). The percentages of 16N, 32N, and 64N Mks (days 11/12) were increased on average from 6.7, 1.0, and 0, respectively, for Tpo only to 14.8, 6.7, and 1.7 for Tpo + NIC cultures. Similarly, the geometric mean (GM) ploidy for $CD41^+$ cells (days 11/12) was increased by 31–81% with NIC (Fig 2.4C). Proplatelet-formation was also donor-dependent, with approximately half of the Tpo only cultures producing only a few proplatelet-forming (PPF) cells by day 13 and the other half producing a significant number by day 9 (Fig 2.4D). With the exception of one donor sample for which no PPF cells were detected, NIC increased the number of PPF Mks by approximately 5-fold (Figs 2.2C, 2.4D).

Figure 2.4. NIC consistently increases the DNA content and proplatelet formation of primary human Mks.

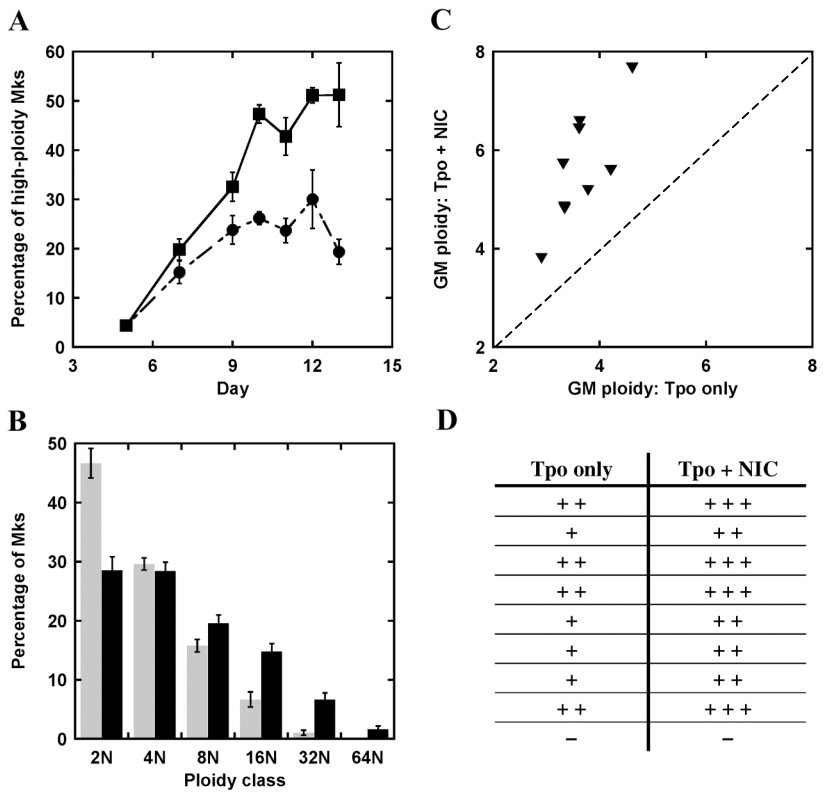

Tpo only	Tpo + NIC
+ +	+ + +
+	+ +
+ +	+ + +
+ +	+ + +
+	+ +
+	+ +
+	+ +
+ +	+ + +
–	–

(A) Percentage of high-ploidy (≥8N) CD41$^+$ Mks derived from mPB CD34$^+$ cells cultured with Tpo only (circles) and Tpo + 6.25 mM NIC (squares). Each data point represents the mean ± SEM of 2–7 separate experiments. $p <$ 0.02 for all time points except for day 12 (p = 0.13; n = 2) (B) Ploidy distribution of primary human Mks. Data represents the mean ± SEM of 9 separate experiments in which Mk ploidy was analyzed on either day 11 or 12 for cultures with Tpo only (gray) and Tpo + 6.25 mM NIC. $p < 0.05$ for all ploidy classes except for 4N (C) Relationship between the geometric mean (GM) ploidy of CD41$^+$ Mks on day 11 or 12 in cultures with Tpo only versus that with Tpo + 6.25 mM NIC for different donor samples. (D) Numbers of proplatelet-forming (PPF) Mks in cultures of mPB CD34$^+$ cells with Tpo only and Tpo + 6.25 mM NIC for different donor samples. Mks bearing 1 or more cytoplasmic extension were counted in 5 fields of view on day 11. Cultures were classified according to the number of PPF Mks: (–) 0, (+) 1–10, (++) 10–50, (+++) > 50. Counting was performed for 4 cultures and the remaining cultures were classified by estimation.

2.3.4. NIC increases polyploidization of primary murine Mks and a megakaryoblastic cell line

NIC also increased polyploidization of both primary murine Mks and a cell line model of Mk differentiation. Murine Mks derived from cultures of bone marrow mononuclear cells showed an increase in cell size and polyploidization when treated with 6.25 mM NIC. By day 4, Mks reached a maximal DNA content of 64N with NIC versus 32N for cultures with Tpo only (Fig 2.5A). 12.5 mM NIC yielded a slightly greater increase in Mk ploidy compared to that for 6.25 mM NIC (data not shown). Similar increases in Mk ploidy were obtained in a second experiment when Sca-1^{+}-selected murine bone marrow cells were treated with Tpo + 6.25 mM NIC (data not shown). NIC also enhanced polyploidization of the megakaryoblastic CHRF cell line, which undergoes polyploidization upon stimulation with PMA. Addition of NIC with PMA increased the percentage of high-ploidy CHRF cells (Fig 2.5B). By day 9, cultures treated with PMA + 12.5 mM NIC contained 47% high-ploidy cells versus 29% for cells with PMA only. A dose of 6.25 mM NIC increased Mk ploidy to a lesser extent and doses greater than or equal to 25 mM NIC were cytotoxic. NIC had no effect on ploidy in the absence of PMA, and the maximum DNA content (32N) reached by CHRF cells with PMA was not affected by NIC.

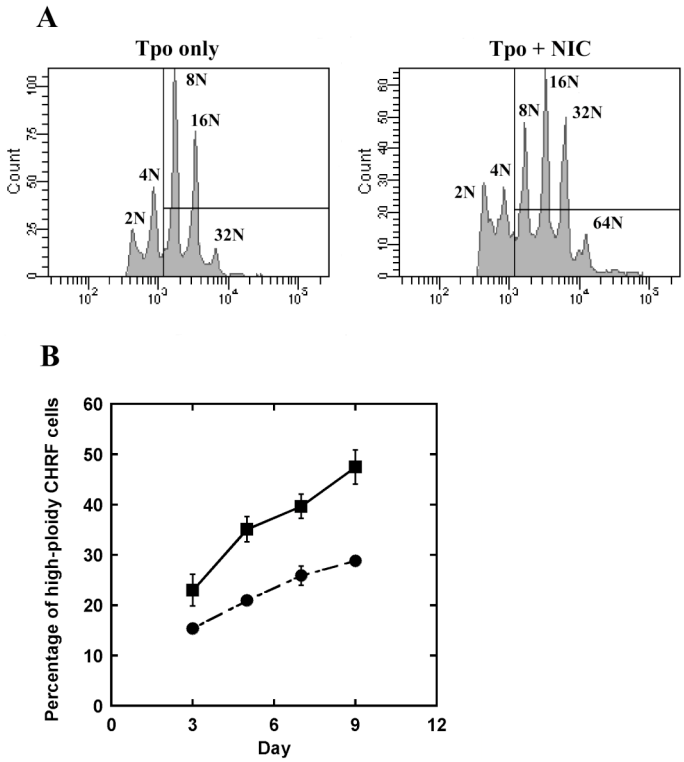

Figure 2.5. NIC enhances polyploidization of primary murine Mks and a megakaryoblastic cell line.

(A) DNA histograms of primary murine $CD41^+$ Mks. Murine bone marrow mononuclear cells were cultured with 100 ng/mL human Tpo. 6.25 mM NIC was added on day 1 after seeding, and $CD41^+$ Mk ploidy was evaluated using flow cytometry on day 4. (B) Percentage of high-ploidy CHRF cells cultured with PMA only (circles) and PMA + 12.5 mM NIC (squares). NIC was added at the time of PMA stimulation. Each data point is the mean $\pm$ SEM of 3–5 separate experiments. $p < 0.02$ for all time points.

2.3.5. NIC has no effect on primary Mk commitment or apoptosis

The kinetics of CD41 expression, total-cell expansion, and apoptosis also varied for cells from different donors. By day 11, cultures with Tpo only exhibited 3.7- to 7.6-fold total-cell expansion, whereas those with Tpo + 6.25 mM NIC exhibited only 2.4- to 4-fold cell expansion (Fig 2.6A). While it inhibited cell growth, NIC had no effect on Mk commitment, as indicated by the percentage of $CD41^+$ Mks in cultures of primary human (Fig 2.6B) or murine Mks. Of the 8 primary human Mk cultures in which CD41 expression was characterized, the percentage of $CD41^+$ cells on day 11 ranged from 68–88% for both the Tpo only and Tpo + NIC conditions. Mk polyploidization and apoptosis are typically correlated events. However, the increase in DNA content observed for cells treated with 6.25 mM NIC was not accompanied by any significant change in the kinetics of apoptosis (Fig 2.6C).

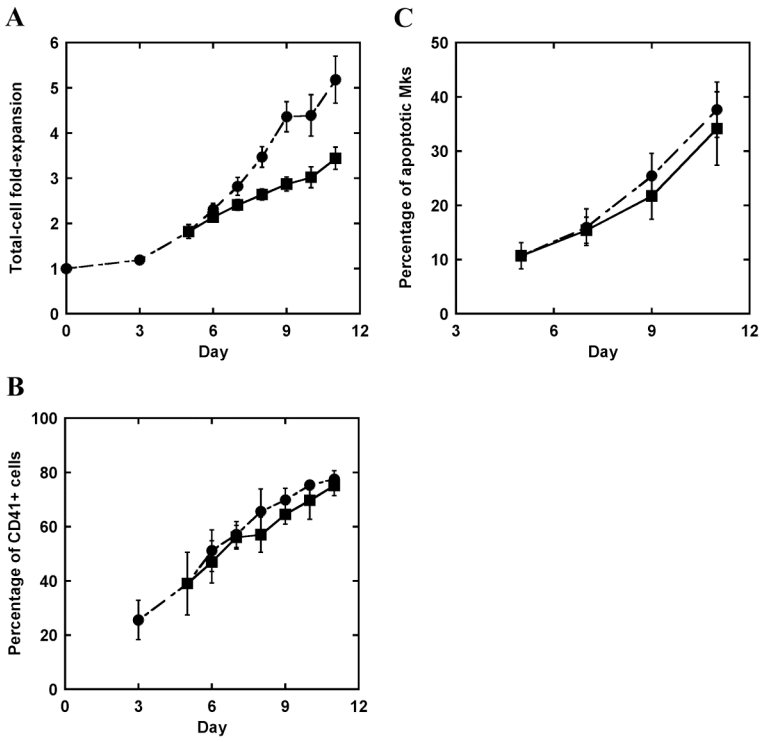

Figure 2.6. NIC inhibits cell growth but has no effect on primary Mk commitment or apoptosis.

mPB $CD34^+$ cells were cultured with 100 ng/mL Tpo (circles). 6.25 mM NIC was added to cultures beginning on day 5 (squares). (A) Cells were counted at different days of culture and are reported as the total-cell fold-expansion. Each data point represents the mean $\pm$ SEM of 5–10 separate experiments. $p < 0.01$ for all time points except for day 6 ($p < 0.05$) (B) Analysis of CD41 expression during Mk differentiation. The number of $CD41^+$ Mks as a percentage of viable cells was evaluated by flow cytometry. Each data point represents the mean $\pm$ SEM of 2–6 experiments. (C) Kinetics of $CD41^+$ Mk apoptosis as measured by AnnexinV staining. Each data point represents the mean $\pm$ SEM of 4 separate experiments.

2.3.6. NIC effects on ploidy and cell growth extend across a wide range of Mk maturation states

In order to examine whether the NIC-mediated increase in Mk ploidy varies with the stage of Mk maturation at which NIC is added, cultures initiated with mPB $CD34^+$ cells were continuously treated with 6.25 mM NIC beginning on days 0 and 3, as well as on day 5 as described above. NIC addition at day 0 or day 3 led to a similar increase in the percentage of high-ploidy Mks as that observed with day 5 addition (Fig 2.7A). Further, for NIC addition beginning at day 0 or day 3, the percentage of $CD41^+$ cells was also similar to those for NIC addition beginning at day 5 and in Tpo only cultures (Fig 2.7B). However, total-cell fold-expansion was substantially reduced by addition of NIC on day 0 (~ 30% less than for NIC addition on day 5; Fig 2.7C-D). The effect of day 3 NIC addition on cell growth was culture-dependent. For donor cells that matured slowly, reaching only 37% $CD41^+$ cells by day 7, addition of NIC at day 3 inhibited growth to a similar extent as for cells receiving NIC on day 0 (Fig 2.7C). However, for donor cells that matured more typically and reached 57% $CD41^+$ cells by day 7, adding NIC at day 3 had less of an inhibitory effect, such that the cells expanded in a similar manner to those with NIC addition at day 5 (Fig 2.7D). The effects on Mk ploidy for NIC addition on day 7, the point at which large increases in ploidy are first observed, also varied with the kinetics of cell maturation. For donor cells that matured typically with 15% high-ploidy Mks by day 7, NIC addition on day 7 decreased cell growth (Fig 2.7D) and increased Mk ploidy in a similar manner to that for cells treated on day 5 (Fig 2.7E). In contrast, for donor cells that matured more rapidly such that the percentage of high-ploidy Mks had reached 30% by day 7, there was no effect of NIC addition at day 7 and the ploidy was similar to that of cells cultured with Tpo only (Fig 2.7F). Overall, these results suggest that NIC has a similar inhibitory effect

on the growth of Mks and other myeloid cells during the proliferative phase of culture, with no effect on Mk commitment, such that earlier NIC addition more extensively decreases cell production with no change in the fraction of $CD41^+$ cells. Furthermore, NIC addition produces a similar increase in the ploidy of committed Mks until late in Mk maturation.

Figure 2.7. Effects of NIC on ploidy and cell growth extend across a wide range of Mk maturation states.

mPB $CD34^+$ cells were cultured with 100 ng/mL Tpo only. Beginning on days 0 (triangles), 3 (diamonds), 5 (squares), and 7 (open circles), 6.25 mM NIC was added to the cultures. Cells receiving no NIC (closed circles) were included for comparison. DNA content and CD41 expression were assessed by flow cytometry. (A) The percentage of high-ploidy $CD41^+$ Mks and (B) the percentage of $CD41^+$ Mks are shown for NIC addition on days 0, 3, and 5. Each data point represents the mean $\pm$ SEM of 2 separate experiments. Total-cell fold-expansion is shown for both (C) a slow-maturing culture and (D) one in which cells differentiated more typically, as determined by CD41 expression and Mk ploidy. Addition of NIC at day 7 can either result in (E) a similar percentage of high-ploidy Mks by day 11 or (F) no increase in the percentage of high-ploidy Mks compared to cultures with day 5 NIC addition.

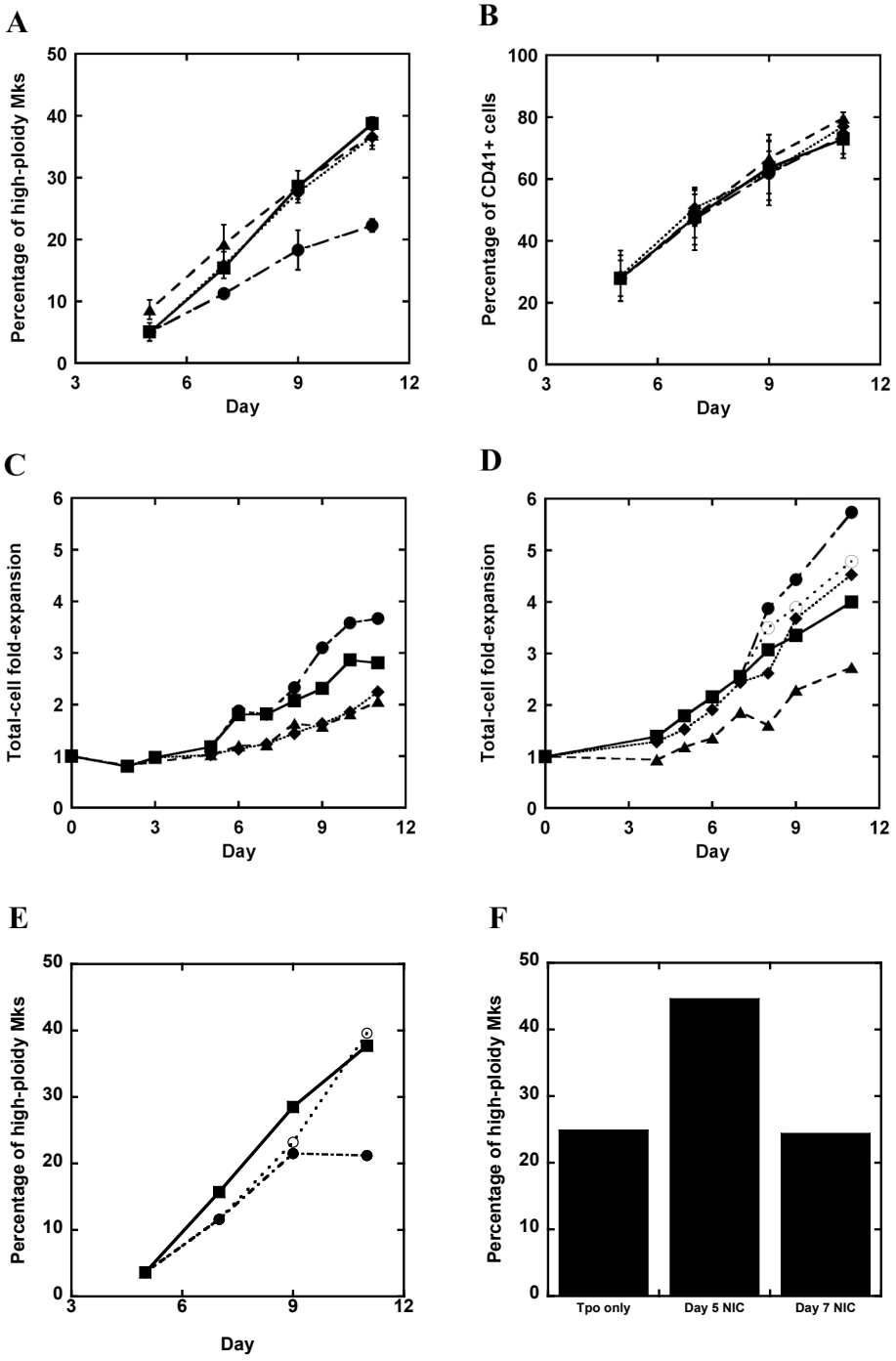
A
Percentage of high-ploidy Mks
Day
B
Percentage of CD41+ cells
Day
C
Total-cell fold-expansion
Day
D
Total-cell fold-expansion
Day
E
Percentage of high-ploidy Mks
Day
F
Percentage of high-ploidy Mks
Tpo only
Day 5 NIC
Day 7 NIC

2.3.7. Pharmacological inhibition of Sir2 or PARP does not enhance polyploidization

In order to investigate the mechanism by which NIC increases Mk ploidy and proplatelet formation, we have examined two known roles of NIC – inhibition of Sir2 and PARP activity.[39,93] As indicated above, gene expression analysis by our group revealed up-regulated expression of SIRT1, SIRT2, and SIRT7 with Mk differentiation in cultures treated with a cytokine cocktail (C. Chen, P. Fuhrken, W. Miller, and E.T. Papoutsakis, manuscript submitted April 2007). Therefore, we examined the effects of two Sir2 inhibitors – sirtinol and splitomicin, which are known to inhibit SIRT1 and SIRT2 activity.[94,95] Doses ranged from a concentration that was cytotoxic to one that had no effect on cell growth or viability (Fig 2.8A-B), but no increase in Mk polyploidization was found in mPB $CD34^+$ cell cultures at any of the concentrations tested (Fig 2.9). Additionally, the SIRT activator resveratrol had no effect on Mk differentiation (Section 6.1.1). NIC is also known to exhibit weak inhibition of PARP activity. Therefore, mPB $CD34^+$ cells were also cultured with several pharmacological inhibitors of PARP. Benzamide and 3-aminobenzamide are similar in structure to NIC and, as with NIC, both are active in the millimolar range.[96-98] In contrast, 5-iodo-6-amino-1,2-benzopyrone (INH_2BP) is more potent and is used at micromolar concentrations.[99,100] As for the Sir2 inhibitors, a wide range of concentrations was tested (Fig 2.8C-E), but none of the PARP inhibitors increased Mk polyploidization (Fig 2.9). Furthermore, the measured PARP activity was very low, even for cells cultured without NIC (Fig 2.10). This is consistent with down-regulation of PARP gene expression by approximately 2-fold during Mk maturation in cultures with or without NIC (data not shown).

Figure 2.8. Effects of Sir2 and PARP inhibitors on cell growth.

Various concentrations of Sir2 or PARP inhibitors were added to cultures of mPB $CD34^+$ cells beginning on day 5. Each graph shows the total-cell fold-expansion from a single culture with either (A) sirtinol, (B) splitomicin, (C) INH_2BP, (D) 3-aminobenzamide, or (E) benzamide. Cultures with Tpo only and Tpo + 6.25 mM NIC were included as controls. Half-media exchanges were performed every other day for inhibitor and NIC replenishment, except as noted by (s) for a single dose of inhibitor on day 5. Doses ranged from a concentration that was cytotoxic to one that had no effect on cell growth or viability. Toxic doses for each inhibitor were found to be: sirtinol, 50 μM; splitomicin, 100 μM; INH_2BP, 50 μM; 3-aminobenzamide, 1 mM; benzamide, 1 mM. Although total-cell counts in cultures containing high doses of Sir2 or PARP inhibitors may have been similar to those in cultures with 6.25 mM NIC, the cultures with high doses of inhibitors contained a large percentage of non-viable cells. In comparison, cells treated with 6.25 mM NIC remained healthy.

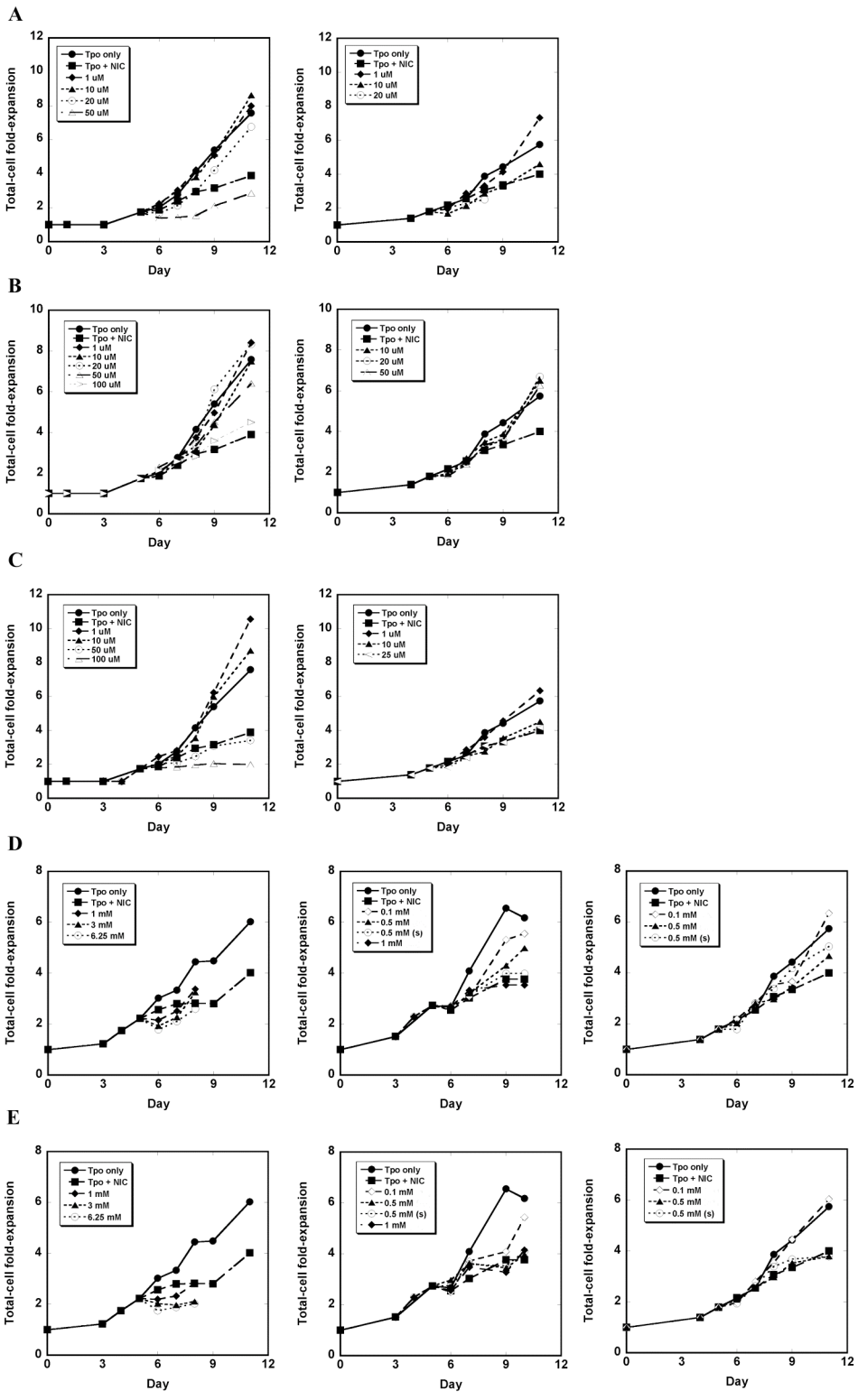
A
Tpo only
Tpo + NIC
1 uM
10 uM
20 uM
50 uM
Tpo only
Tpo + NIC
1 uM
10 uM
20 uM
B
Tpo only
Tpo + NIC
1 uM
10 uM
20 uM
50 uM
100 uM
Tpo only
Tpo + NIC
10 uM
20 uM
50 uM
C
Tpo only
Tpo + NIC
1 uM
10 uM
50 uM
100 uM
Tpo only
Tpo + NIC
1 uM
10 uM
25 uM
D
Tpo only
Tpo + NIC
1 mM
3 mM
6.25 mM
Tpo only
Tpo + NIC
0.1 mM
0.5 mM
0.5 mM (s)
1 mM
Tpo only
Tpo + NIC
0.1 mM
0.5 mM
0.5 mM (s)
E
Tpo only
Tpo + NIC
1 mM
3 mM
6.25 mM
Tpo only
Tpo + NIC
0.1 mM
0.5 mM
0.5 mM (s)
1 mM
Tpo only
Tpo + NIC
0.1 mM
0.5 mM
0.5 mM (s)
Total-cell fold-expansion
Day

			sirtinol		splitomicin		
	Tpo	Tpo + NIC	1 µM	10 µM	10 µM	20 µM	50 µM
MK12	21.20	37.70	20.90	15.60	14.10	16.70	15.00
MK8	36	52.7	37.3	36.8	38.6	36.7	32.1

			INH_2BP			3-aminobenzamide				benzamide			
	Tpo	Tpo + NIC	1 µM	10 µM	25 µM	0.1 mM	0.5 mM	0.5 mM (s)	1 mM	0.1 mM	0.5 mM	0.5 mM (s)	1 mM
MK7	24.1	49.60				25.7	25.8	26.1	26.4	25.6	26.9	29	26.4
MK12	21.20	37.70	15.1	13.2	13.1	10.70	6.60	6.50		20.30	20.40	19.50	
MK8	36	52.7	37.2	39									

Figure 2.9. No increase in Mk ploidy with Sir2 or PARP inhibitors.

Mk ploidy was assessed for non-toxic doses of Sir2 and PARP inhibitors. Data represents the fraction of high-ploidy $CD41^+$ Mks on day 11 for each experiment.

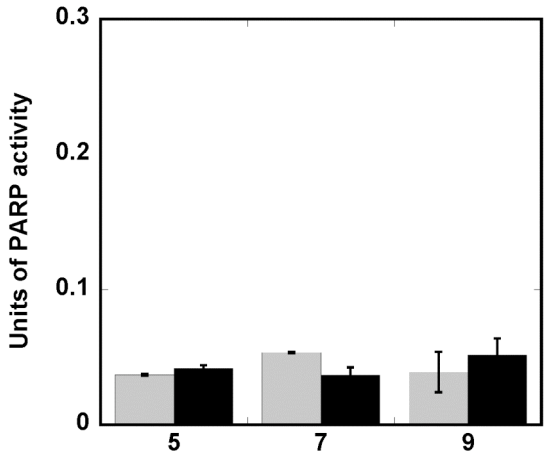

Figure 2.10. PARP activity in primary Mk cultures is low and is not affected by NIC.

Enzyme activity was determined by measuring the incorporation of biotinylated poly (ADP-ribose) onto histone-coated plates by PARP present in cell lysates. Cell extracts were prepared on days 5 (2 hrs after NIC treatment), 7, and 9 from mPB $CD34^+$ cells cultured with Tpo only (gray) and with Tpo + 6.25 mM NIC. A standard curve was prepared using the provided PARP-HSA enzyme (range 0.01–1.0 Units PARP activity).

2.3.8. Global transcriptional analysis shows similar gene expression in Mk cultures with or without NIC

Gene expression microarrays were used to identify differences in gene transcription associated with NIC-mediated increases in endomitosis and proplatelet formation. 6.25 mM NIC was added to mPB $CD34^+$ cell cultures on day 5 and cells were sampled for microarray analysis on days 5 (before NIC addition), 6, 8, and 10 from both the Tpo only and Tpo + NIC conditions. Two replicate biological experiments (MKI and MKII) were conducted. Surprisingly, although very dramatic phenotypic differences were observed with NIC addition for both experiments, the overall transcriptional patterns were very similar to those in the cultures with Tpo only. As expected, previously identified Mk-associated genes[91] were strongly up-regulated with Mk differentiation under both culture conditions in both experiments, indicating that NIC does not cause large disruptions in the normal transcriptional program of Mks (Fig 2.11A). Mk differentiation, as indicated by CD41 expression and polyploidization, occurred more slowly in MKII, and this is reflected by a delay in the up-regulation of many Mk-associated genes. Out of more than 18,000 genes probed by the microarray, only 59 genes were found to be differentially regulated by NIC (2-way ANOVA, $p<0.001$) in both cultures (Figs 2.11B, 2.12). Among these, the transcription factor MYB (also known as c-Myb), which was down-regulated with Mk differentiation in both the Tpo only and Tpo + NIC cultures (Fig 2.11B), was down-regulated to a greater extent with NIC. Greater down-regulation of c-Myb expression with NIC was confirmed by Q-RT-PCR (Fig 2.13). Mice with N-ethyl-N-nitrosourea-induced mutations in c-Myb exhibit excessive megakaryopoiesis characterized by increased numbers of bone marrow Mks and high peripheral blood platelet counts.[101] Forced expression of c-Myb results in a block

of terminal Mk differentiation, suggesting that down-regulation of c-Myb is necessary for Mk maturation.[102] Lower expression of c-Myb in NIC-treated Mks may be an indication of greater Mk maturity. Among the genes expressed higher in the presence of NIC, protein disulfide isomerase family A, member 5 (PDIA5, PDIR), was found to be up-regulated with Mk maturation (Fig 2.11B). PDIA5 is a member of the family of oxidoreductases[103] which facilitate protein folding by catalyzing the formation and reduction of disulphide bonds in the endoplasmic reticulum.[104] Greater up-regulation of PDIA5 may be related to the observation that cells cultured in the presence of NIC contain approximately 2-fold more protein by day 9 than do cells cultured with Tpo only.

Figure 2.11. Gene expression profiles of Mk-associated and NIC-regulated genes.

Profiles of gene expression for two biological replicate experiments, MKI (left) and MKII (right). Time course data is shown progressing from left to right for cells cultured with either Tpo only or Tpo + 6.25 mM NIC and analyzed on days 5 (prior to NIC addition), 6, 8, and 10. Genes are hierarchically clustered and the color denotes degree of differential expression with respect to uncultured primary human $CD34^+$ cells (averaged from 3 donors) (saturated red = 16-fold up-regulation, saturated green = 16-fold down-regulation, gray = no data). (A) Gene expression profiles for a set of 58 previously identified Mk-associated genes.[91] (B) Expression profiles for 59 genes that were found to be differentially regulated by NIC in both MKI and MKII by 2-way ANOVA ($p<0.001$).

A

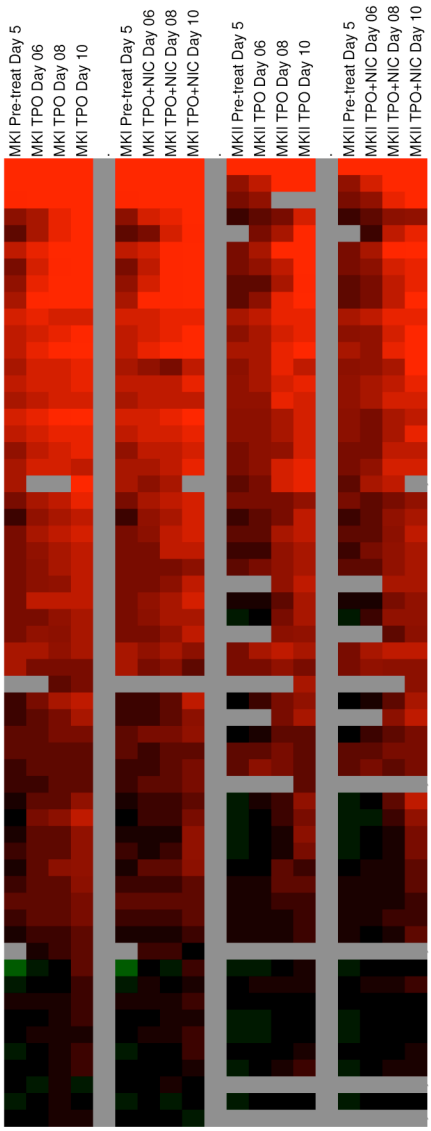

Gene Name	Description
LTBP1	Latent transforming growth factor beta binding protein 1 (LTBP1), transcript variant 1, mRNA
GNAZ	Guanine nucleotide binding protein (G protein), alpha z polypeptide (GNAZ), mRNA
ITGB5	Integrin, beta 5 (ITGB5), mRNA
VDR	Vitamin D (1,25- dihydroxyvitamin D3) receptor (VDR), transcript variant 2, mRNA
CALD1	Caldesmon 1 (CALD1), transcript variant 1, mRNA
BDNF	Brain-derived neurotrophic factor (BDNF), transcript variant 1, mRNA
CD9	CD9 antigen (p24) (CD9), mRNA
ITGB3	Integrin, beta 3 (platelet glycoprotein IIIa, antigen CD61) (ITGB3), mRNA
ABCC3	ATP-binding cassette, sub-family C (CFTR/MRP), member 3 (ABCC3), transcript variant MRP3B, mRNA
VWF	Von Willebrand factor (VWF), mRNA
ACTN1	Actinin, alpha 1 (ACTN1), mRNA
THBS1	Thrombospondin 1 (THBS1), mRNA
HGD	Homogentisate 1,2-dioxygenase (homogentisate oxidase) (HGD), mRNA
INSIG1	Insulin induced gene 1 (INSIG1), transcript variant 2, mRNA
SQLE	Squalene epoxidase (SQLE), mRNA
LAT	Linker for activation of T cells (LAT), transcript variant 1, mRNA
INSIG1	Insulin induced gene 1 (INSIG1), transcript variant 2, mRNA
CTDSPL	CTD (carboxy-terminal domain, RNA polymerase II, polypeptide A) small phosphatase-like (CTDSPL)
RAB27B	RAB27B, member RAS oncogene family (RAB27B), mRNA
DNM3	Dynamin 3 (DNM3), mRNA
CLU	Clusterin
ILK	Integrin-linked kinase (ILK), transcript variant 3, mRNA
GP9	Glycoprotein IX (platelet) (GP9), mRNA
NRGN	Neurogranin (protein kinase C substrate, RC3) (NRGN), mRNA
KIF2	Kinesin heavy chain member 2 (KIF2), mRNA
NFIB	Nuclear factor I/B (NFIB), mRNA
FYB	FYN binding protein (FYB-120/130) (FYB), mRNA
CDKN2D	Cyclin-dependent kinase inhibitor 2D (p19, inhibits CDK4) (CDKN2D), transcript variant 1, mRNA
PTGIR	Prostaglandin I2 (prostacyclin) receptor (IP) (PTGIR), mRNA
PPBP	Pro-platelet basic protein (chemokine (C-X-C motif) ligand 7) (PPBP), mRNA
PF4	Platelet factor 4 (chemokine (C-X-C motif) ligand 4) (PF4), mRNA
SLC2A3	Solute carrier family 2 (facilitated glucose transporter), member 3 (SLC2A3), mRNA
SALL2	Sal-like 2 (Drosophila) (SALL2), mRNA
GNB5	Guanine nucleotide binding protein (G protein), beta 5 (GNB5), transcript variant 2, mRNA
EMILIN1	Elastin microfibril interfacer 1 (EMILIN1), mRNA
PLEK	Pleckstrin (PLEK), mRNA
ITGA2B	Integrin, alpha 2b (platelet glycoprotein IIb of IIb/IIIa complex, antigen CD41B) (ITGA2B), mRNA
CD151	CD151 antigen (CD151), transcript variant 1, mRNA
CXCL3	Chemokine (C-X-C motif) ligand 3 (CXCL3), mRNA
ANXA3	Annexin A3 (ANXA3), mRNA
MYOM1	MRNA for skeletal muscle 190kD protein.
MYOM1	Myomesin 1 (skelemin) 185kDa (MYOM1), mRNA
GJA4	Gap junction protein, alpha 4, 37kDa (connexin 37) (GJA4), mRNA
DAB2	Disabled homolog 2, mitogen-responsive phosphoprotein (Drosophila) (DAB2), mRNA
PDLIM1	PDZ and LIM domain 1 (elfin) (PDLIM1), mRNA
PRKCD	Protein kinase C, delta (PRKCD), transcript variant 1, mRNA
EIF4G3	Eukaryotic translation initiation factor 4 gamma, 3 (EIF4G3), mRNA
DOK1	Docking protein 1, 62kDa (downstream of tyrosine kinase 1) (DOK1), mRNA
GNAZ	Guanine nucleotide binding protein (G protein), alpha z polypeptide (GNAZ), mRNA
GCKR	Glucokinase (hexokinase 4) regulator (GCKR), mRNA
FCER1G	Fc fragment of IgE, high affinity I, receptor for; gamma polypeptide (FCER1G), mRNA
PRUNE	Prune homolog (Drosophila) (PRUNE), mRNA
DIAPH1	Diaphanous homolog 1 (Drosophila) (DIAPH1), mRNA
THC2357315	[Replaced by A_23_P340848] PI2R_HUMAN (P43119) Prostacyclin receptor (Prostanoid IP receptor)
DDEF2	Development and differentiation enhancing factor 2 (DDEF2), mRNA
FLJ13491	Hypothetical protein FLJ13491 (FLJ13491), mRNA
ADCY6	Adenylate cyclase 6 (ADCY6), transcript variant 1, mRNA
WASF3	WAS protein family, member 3 (WASF3), mRNA

Saturation color = 16-fold DE

Expression ratios relative to uncultured primary CD34 cells [averaged results from three donors]

B

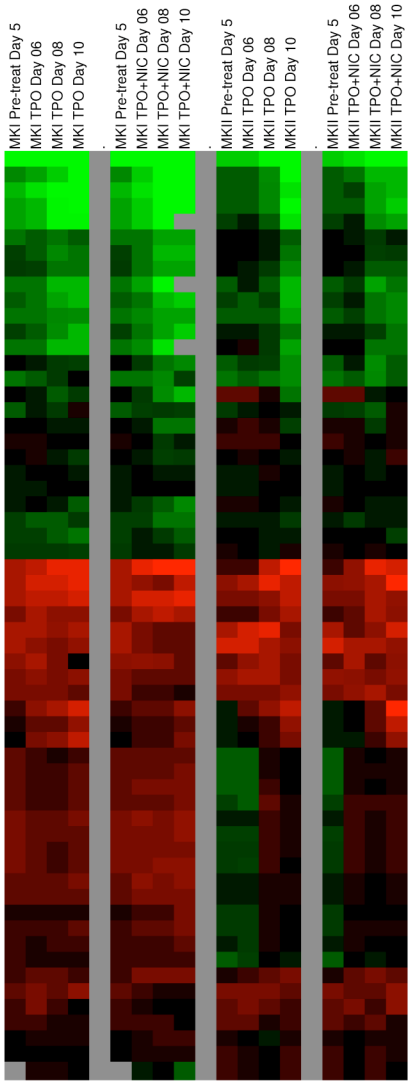

Gene Name	Description
ANXA1	Annexin A1 (ANXA1), mRNA
IGFBP7	Insulin-like growth factor binding protein 7 (IGFBP7), mRNA
ZFP36L2	Zinc finger protein 36, C3H type-like 2 (ZFP36L2), mRNA
MYB	V-myb myeloblastosis viral oncogene homolog (avian) (MYB), mRNA
ZNF521	Zinc finger protein 521 (ZNF521), mRNA
LYZ	Lysozyme (renal amyloidosis) (LYZ), mRNA
FLJ37970	Hypothetical protein FLJ37970 (FLJ37970), mRNA
KCNN4	Potassium intermediate/small conductance calcium-activated channel, subfamily N, member 4 (KCNN4), mRNA
IL3RA	Interleukin 3 receptor, alpha (low affinity) (IL3RA), mRNA
PYCARD	PYD and CARD domain containing (PYCARD), transcript variant 1, mRNA
OCIAD2	OCIA domain containing 2 (OCIAD2), transcript variant 1, mRNA
RNF130	Ring finger protein 130 (RNF130), mRNA
HLA-DRB5	Major histocompatibility complex, class II, DR beta 5 (HLA-DRB5), mRNA
CDKN1C	Cyclin-dependent kinase inhibitor 1C (p57, Kip2) (CDKN1C), mRNA
ABLIM1	Actin binding LIM protein 1 (ABLIM1), transcript variant 3, mRNA
SLC40A1	Solute carrier family 40 (iron-regulated transporter), member 1 (SLC40A1), mRNA
CTSZ	Cathepsin Z (CTSZ), mRNA
APOC1	Apolipoprotein C-I (APOC1), mRNA
S100A4	S100 calcium binding protein A4
BC064982	CDNA clone IMAGE
COX6B1	Cytochrome c oxidase subunit Vib polypeptide 1 (ubiquitous) (COX6B1), mRNA
CLDN17	[Replaced by A_23_P360924] Homo sapiens clone DNA73737 CLDN17 (UNQ758) mRNA, complete cds.
FAIM	Fas apoptotic inhibitory molecule (FAIM), mRNA
PHIP	Pleckstrin homology domain interacting protein (PHIP), mRNA
PP	Pyrophosphatase (inorganic) (PP), mRNA
EIF1AX	Eukaryotic translation initiation factor 1A, X-linked (EIF1AX), mRNA
THC2360810	Q674X7 (Q674X7) Kazrin isoform A, partial (31%)
HGD	Homogentisate 1,2-dioxygenase (homogentisate oxidase) (HGD), mRNA
PDIA5	Protein disulfide isomerase family A, member 5 (PDIA5), mRNA
TMSL8	Thymosin-like 8 (TMSL8), mRNA
CYP1B1	Cytochrome P450, family 1, subfamily B, polypeptide 1 (CYP1B1), mRNA
PRSS23	Protease, serine, 23 (PRSS23), mRNA
HIST1H4B	Histone 1, H4b (HIST1H4B), mRNA
DLC1	Deleted in liver cancer 1 (DLC1), transcript variant 1, mRNA
INCENP	Inner centromere protein antigens 135/155kDa (INCENP), mRNA
CXCL1	Chemokine (C-X-C motif) ligand 1 (melanoma growth stimulating activity, alpha) (CXCL1), mRNA
CXCL3	Chemokine (C-X-C motif) ligand 3 (CXCL3), mRNA
ANXA3	Annexin A3 (ANXA3), mRNA
LOC90313	Hypothetical protein BC004507 (LOC90313), mRNA
DUSP15	Dual specificity phosphatase 15 (DUSP15), transcript variant 1, mRNA
FKHL18	Forkhead-like 18 (Drosophila) (FKHL18), mRNA
BARX1	BarH-like homeobox 1 (BARX1), mRNA
THC2275252	AF343666 translocation associated fusion protein IRTA1/IGA1 {Homo sapiens:} , partial (81%)
SYNGR4	Synaptogyrin 4 (SYNGR4), mRNA
EGFL4	EGF-like-domain, multiple 4 (EGFL4), mRNA
GPR78	G protein-coupled receptor 78 (GPR78), mRNA
LRP1	Low density lipoprotein-related protein 1 (alpha-2-macroglobulin receptor) (LRP1), mRNA
ADAMTSL2	ADAMTS-like 2 (ADAMTSL2), mRNA
PRB3	Proline-rich protein BstNI subfamily 3 (PRB3), mRNA
NTE	Neuropathy target esterase (NTE), mRNA
AMN	Amnionless homolog (mouse) (AMN), mRNA
TNFRSF4	Tumor necrosis factor receptor superfamily, member 4 (TNFRSF4), mRNA
MRPS14	Mitochondrial ribosomal protein S14 (MRPS14), nuclear gene encoding mitochondrial protein, mRNA
ADORA2B	Adenosine A2b receptor (ADORA2B), mRNA
IRX5	Iroquois homeobox protein 5 (IRX5), mRNA
MTHFD1	Methylenetetrahydrofolate dehydrogenase (NADP+ dependent) 1, methenyltetrahydrofolate cyclohydrolase
BAX	BCL2-associated X protein (BAX), transcript variant epsilon, mRNA
RSAD1	Radical S-adenosyl methionine domain containing 1 (RSAD1), mRNA
ANP32C	Acidic (leucine-rich) nuclear phosphoprotein 32 family, member C (ANP32C), mRNA

Saturation color = 16-fold DE

Expression ratios relative to uncultured primary CD34 cells [averaged results from three donors]

Figure 2.12 NIC-associated differences in gene expression.

Profiles of NIC effects on gene expression for two biological replicate experiments, MKI (left) and MKII (right). Time course data for 59 genes that were found to be differentially regulated by NIC in both experiments (2-way ANOVA ($p<0.001$)) is shown progressing from left to right for cells analyzed on days 5 (prior to NIC addition), 6, 8, and 10. Genes are hierarchically clustered and the color denotes the ratio of expression level in Tpo + NIC cultures compared to that with Tpo only (saturated red = 2-fold up-regulation, saturated green = 2-fold down-regulation, gray = no data).

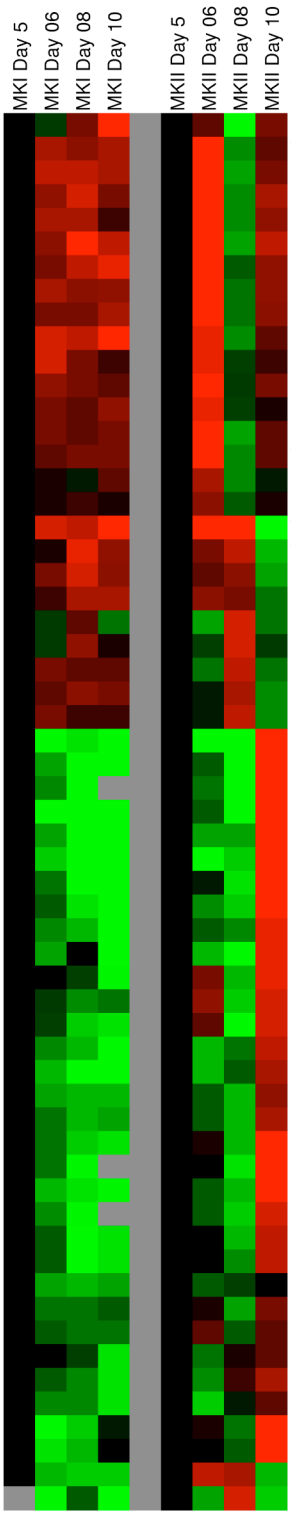

ShortName	Description
HIST1H4B	Histone 1, H4b (HIST1H4B), mRNA
THC2275252	AF343666 translocation associated fusion protein IRTA1/IGA1 {Homo sapiens;} , partial (81%)
EGFL4	EGF-like-domain, multiple 4 (EGFL4), mRNA
LOC90313	Hypothetical protein BC004507 (LOC90313), mRNA
FKHL18	Forkhead-like 18 (Drosophila) (FKHL18), mRNA
GPR78	G protein-coupled receptor 78 (GPR78), mRNA
SYNGR4	Synaptogyrin 4 (SYNGR4), mRNA
DUSP15	Dual specificity phosphatase 15 (DUSP15), transcript variant 1, mRNA
BARX1	BarH-like homeobox 1 (BARX1), mRNA
PRB3	Proline-rich protein BstNI subfamily 3 (PRB3), mRNA
LRP1	Low density lipoprotein-related protein 1 (alpha-2-macroglobulin receptor) (LRP1), mRNA
NTE	Neuropathy target esterase (NTE), mRNA
ADAMTSL2	ADAMTS-like 2 (ADAMTSL2), mRNA
AMN	Amnionless homolog (mouse) (AMN), mRNA
TNFRSF4	Tumor necrosis factor receptor superfamily, member 4 (TNFRSF4), mRNA
COX6B1	Cytochrome c oxidase subunit Vib polypeptide 1 (ubiquitous) (COX6B1), mRNA
CLDN17	Homo sapiens clone DNA73737 CLDN17 (UNQ758) mRNA, complete cds.
THC2360810	Q674X7 (Q674X7) Kazrin isoform A, partial (31%)
TMSL8	Thymosin-like 8 (TMSL8), mRNA
PP	Pyrophosphatase (inorganic) (PP), mRNA
MRPS14	Mitochondrial ribosomal protein S14, nuclear gene encoding mitochondrial protein, mRNA
MTHFD1	Methylenetetrahydrofolate dehydrogenase (NADP+ dependent) 1
BAX	BCL2-associated X protein (BAX), transcript variant epsilon, mRNA
RSAD1	Radical S-adenosyl methionine domain containing 1 (RSAD1), mRNA
PDIA5	Protein disulfide isomerase family A, member 5 (PDIA5), mRNA
EIF1AX	Eukaryotic translation initiation factor 1A, X-linked (EIF1AX), mRNA
CYP1B1	Cytochrome P450, family 1, subfamily B, polypeptide 1 (CYP1B1), mRNA
APOC1	Apolipoprotein C-I (APOC1), mRNA
IL3RA	Interleukin 3 receptor, alpha (low affinity) (IL3RA), mRNA
HGD	Homogentisate 1,2-dioxygenase (homogentisate oxidase) (HGD), mRNA
IGFBP7	Insulin-like growth factor binding protein 7 (IGFBP7), mRNA
CXCL1	Chemokine (C-X-C motif) ligand 1 (melanoma growth stimulating activity, alpha) (CXCL1), mRNA
SLC40A1	Solute carrier family 40 (iron-regulated transporter), member 1 (SLC40A1), mRNA
ANXA1	Annexin A1 (ANXA1), mRNA
ADORA2B	Adenosine A2b receptor (ADORA2B), mRNA
CTSZ	Cathepsin Z (CTSZ), mRNA
ZFP36L2	Zinc finger protein 36, C3H type-like 2 (ZFP36L2), mRNA
PYCARD	PYD and CARD domain containing (PYCARD), transcript variant 1, mRNA
CDKN1C	Cyclin-dependent kinase inhibitor 1C (p57, Kip2) (CDKN1C), mRNA
LYZ	Lysozyme (renal amyloidosis) (LYZ), mRNA
ANXA3	Annexin A3 (ANXA3), mRNA
DLC1	Deleted in liver cancer 1 (DLC1), transcript variant 1, mRNA
S100A4	S100 calcium binding protein A4, mRNA
MYB	V-myb myeloblastosis viral oncogene homolog (avian) (MYB), mRNA
ZNF521	Zinc finger protein 521 (ZNF521), mRNA
KCNN4	Potassium intermediate/small conductance calcium-activated channel, subfamily N, member 4
HLA-DRB5	Major histocompatibility complex, class II, DR beta 5 (HLA-DRB5), mRNA
FLJ37970	Hypothetical protein FLJ37970 (FLJ37970), mRNA
ABLIM1	Actin binding LIM protein 1 (ABLIM1), transcript variant 3, mRNA
FAIM	Fas apoptotic inhibitory molecule (FAIM), mRNA
OCIAD2	OCIA domain containing 2 (OCIAD2), transcript variant 1, mRNA
RNF130	Ring finger protein 130 (RNF130), mRNA
PHIP	Pleckstrin homology domain interacting protein (PHIP), mRNA
CXCL3	Chemokine (C-X-C motif) ligand 3 (CXCL3), mRNA
PRSS23	Protease, serine, 23 (PRSS23), mRNA
IRX5	Iroquois homeobox protein 5 (IRX5), mRNA
BC064982	CDNA clone IMAGE
INCENP	Inner centromere protein antigens 135/155kDa (INCENP), mRNA
ANP32C	Acidic (leucine-rich) nuclear phosphoprotein 32 family, member C (ANP32C), mRNA

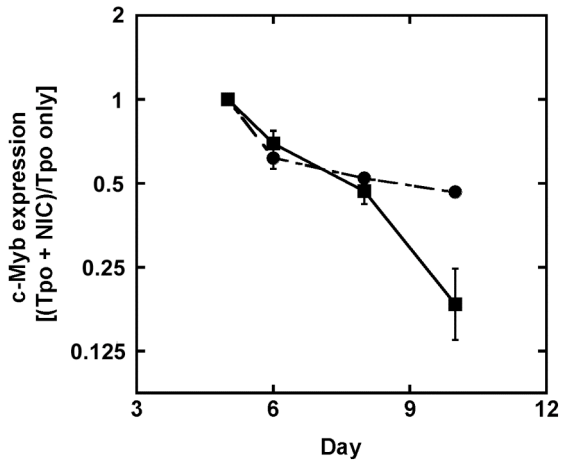

Figure 2.13. Q-RT-PCR analysis of c-Myb expression in primary human Mks from experiment MKI.

c-Myb mRNA ratios [(Tpo + NIC)/(Tpo only)] from microarray analysis (circles) and Q-RT-PCR (squares).

2.4. Discussion

It has proven difficult to obtain high-ploidy human Mks *in vitro*. Cultured primary human Mks typically reach a maximum DNA content of only 16N,[22,25,82,83] with only a few reports of cultures containing Mks with a maximum DNA content of 32N[84] or 64N.[14] Also, cultures with Tpo only typically contain 15–25% high-ploidy (≥8N) Mks.[83,84] Consistent with past results, we obtained a maximum Mk DNA content of 16N in 7 cultures and 32N in 2 cultures with Tpo only. The maximum percentage of high-ploidy Mks in these cultures ranged from 13.5–34.6%, which is similar to what is typically observed.

Some progress has been made to increase Mk ploidy based on advances in the understanding of Mk development. Although most of these studies have been performed using primary murine Mks or megakaryocytic cell lines, four recent studies with primary human cells have also demonstrated enhanced Mk maturation. Treatment with the Src kinase inhibitor SU6656 increased Mk size and the number of high-ploidy Mks in cultures of human bone-marrow-derived $CD34^+$ cells and in cultures of bone marrow mononuclear cells from patients with myelodysplastic syndromes.[25] In another study, addition of the chemokine stromal-cell-derived factor-1α (SDF-1α) to cells cultured with Tpo increased proplatelet frequency 2-fold and approximately doubled the number of Mks with both 4 and 8 nuclear lobes compared to those with Tpo only.[22] A similar increase in the number of Mks with 4 and 8 nuclear lobes was found using the MEK inhibitor PD98059.[51] However, even with SU6656, SDF-1α, or PD98059, the highest ploidy class reported was 16N. In another study, treatment of Mks with an anti-CD226 monoclonal antibody (expressed on Mks and platelets and hypothesized to play a role in Mk development as an adhesion molecule) in combination with lymphocyte-function-associated

antigen-1 (LFA-1) increased the percentage of high-ploidy Mks from 15.6% to 35.9% and increased the maximum Mk ploidy to 32N.[83]

Here, we demonstrate that Mk polyploidization and proplatelet formation are greatly increased when the water-soluble vitamin nicotinamide (NIC) is added to mPB $CD34^+$ cell cultures in the presence of Tpo, irrespective of donor-dependent differences in Mk differentiation. NIC-treated primary human Mks reach a DNA content of 64N. Also, cultures with NIC exhibit ~50% high-ploidy Mks. Together, the Mk ploidy distribution and percentage of high-ploidy Mks obtained with NIC are greater than what has been previously reported for cultured primary human Mks. The increase in ploidy with NIC more than offset the decrease in total Mk production, such that NIC addition at day 5 also led to an increase in the total Mk DNA content in all but one set of cultures (Fig 2.14). Mks in NIC-supplemented cultures also exhibited more elaborate cytoplasmic extensions and a greater frequency of proplatelet formation. NIC also increased the DNA content of both primary murine Mks and a megakaryoblastic cell line (CHRF-288-11). However, NIC did not induce polyploidization of CHRF cells in the absence of PMA, and did not alter Mk commitment or the time at which polyploidization was initiated in primary human Mk cultures, even when NIC was added on day 0 (Fig 2.7A). These results suggest that NIC does not induce endomitosis *per se*, but rather enhances the process once it has been initiated.

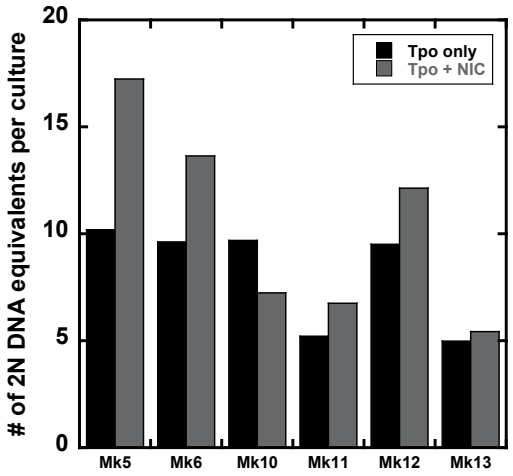

Figure 2.14. Total DNA content of Tpo only and Tpo + NIC cultures.

The percentage of Mks belonging to each ploidy class (2N, 4N, 8N, 16N, 32N, 64N) were determined from DNA histograms on either day 11 or 12 of Tpo only and Tpo + 6.25 mM NIC cultures (n = 6). Total-cell fold-expansion (exp) and the percentage of $CD41^+$ cells was used to determine the number of Mks at day 11 or 12. The number of 2N DNA equivalents in Tpo only (black) and Tpo + NIC (gray) cultures was then calculated as follows:

$$\textit{DNA content} = (\mathbf{1} * \%2N/100 * exp * \%CD41^+/100) + (\mathbf{2} * \%4N/100 * exp * \%CD41^+/100) + (\mathbf{4} * \%8N/100 * exp * \%CD41^+/100) + (\mathbf{8} * \%16N/100 * exp * \%CD41^+/100) + (\mathbf{16} * \%32N/100 * exp * \%CD41^+/100) + (\mathbf{32} * \%64N/100 * exp * \%CD41^+/100)$$

The mechanisms that underlie the ability of NIC to enhance Mk maturation have yet to be established. Surprisingly, very similar global transcriptional profiles were observed with or without NIC, despite the dramatically different phenotypes. NIC has a variety of known roles including serving as a precursor to nicotinamide adenine dinucleotide (NAD^+),[52-54] activating the PI3K/Akt signaling pathway,[45,46] and inhibiting the activity of both PARP[93] and the Sir2 family of histone/protein deacetylases (sirtuins).[39] PARP catalyzes the NAD^+-dependent addition of poly (ADP-ribose) onto nuclear proteins including histones and plays a role in DNA replication.[33] PARP-1 has been shown to interact with many cell-cycle regulators such as p21,[34] proliferating cell nuclear antigen (PCNA),[34] and p53.[35] However, several different pharmacological inhibitors of PARP including INH_2BP, which is a more potent PARP inhibitor than NIC, did not increase Mk ploidy. Sirtuins catalyze a unique NAD^+-dependent reaction and are required for a wide variety of biological processes including transcriptional silencing, regulation of apoptosis, and lifespan regulation.[37,38] NIC inhibits the ability of SIRT1 to deacetylate p53[39] and also inhibits the activity of SIRT2, which is an α-tubulin deacetylase that has been shown to play a role in cell-cycle regulation.[105] While we initially examined NIC because it is a sirtuin inhibitor, two additional chemical inhibitors of SIRT1 and SIRT2 failed to increase Mk ploidy. Therefore, we conclude that NIC does not enhance Mk maturation by inhibiting SIRT1 or SIRT2 activity. However, we are not able to rule out effects on SIRT7 because this molecule has not been well characterized. Recently, it has been shown that SIRT7 localizes to the nucleus[106,107] and is necessary for cell survival.[107] However, it is not yet known whether nicotinamide, sirtinol, and/or splitomicin inhibit SIRT7 activity.

Our results suggest several potential applications for NIC both *in vitro* and *in vivo*. We provide a novel culture system that can be used to investigate the complex process of Mk differentiation. Importantly, NIC increases the rate of endomitosis without affecting apoptosis, such that Mks reach ploidy levels closer to those observed *in vivo*. Since there is a direct correlation between Mk DNA content and the number of platelets produced,[14] these results suggest a possible therapeutic benefit of NIC in providing Mks for transplantation therapies and/or platelets for use in transfusions. NIC may be especially useful for increasing the ploidy of umbilical-cord-blood-derived Mks, which typically show less extensive polyploidization compared to Mks from other hematopoietic cell sources.[108] Furthermore, NIC has been administered safely at pharmacological doses for a variety of therapeutic applications, dating back to the late 1950s for treatment of psychiatric conditions such as schizophrenia. More recently, NIC has undergone clinical testing for use as a preventative agent for Type I diabetes.[60-62] Doses up to 3 g/day have been reported to be generally well tolerated with few side effects.[31] *In vivo* administration of NIC may have therapeutic potential for the management of Mk and platelet disorders such as essential thrombocytopenia, refractory thrombocytopenia in myelodysplastic syndromes, and megakaryoblastic leukemia.

In summary, although the molecular and cellular mechanisms through which Mks differentiate and mature remain poorly characterized, we have shown that Mk maturation *in vitro* can be dramatically enhanced by adding the water-soluble vitamin nicotinamide. Elucidating the mechanisms by which NIC increases Mk ploidy could provide the basis for clinical advances for the treatment of Mk and platelet disorders.

2.5. Acknowledgements

I am grateful to Peter Fuhrken for his data analysis expertise and help in performing the array studies. I thank Dr. Lonnie Shea, Dr. Elizabeth Eklund, Christopher Rives, Laura De Laporte, and Iwona Konieczna for their help with the mouse studies and Dr. Shea for the use of equipment. I also thank Lennell Reynolds of the Cell Imaging Facility (Chicago campus) for performing the EM sample preparations and Genentech for their kind donation of Tpo.

3. CHAPTER 3: Characterization of the mechanism(s) underlying the effects of nicotinamide on Mk differentiation

3.1. Introduction

Megakaryocytic cells (Mks) are the immediate precursors to platelets. Mk differentiation includes progression through several rounds of endomitosis to form polyploid cells with multilobated nuclei, the development of a demarcation membrane system, and the production of cytoplasmic extensions called proplatelets, from which platelets are released. We have discovered that nicotinamide (NIC, one form of vitamin B3) greatly increases Mk ploidy and proplatelet production – without affecting Mk commitment – in cultures of human mobilized $CD34^+$ cells stimulated with Tpo (Chapter 2).[109] It is possible that NIC may be used directly to increase Mk maturation and platelet production both *in vivo* and *in vitro*. However, it is important to understand the mechanism(s) underlying the effects of NIC. Doing so would lead to a greater understanding of Mk differentiation and may allow for further modulation of Mk maturation.

Despite the dramatic phenotypic differences observed with NIC addition, microarray-based gene-expression analysis revealed similar transcriptional patterns in Mk cultures with or without NIC, indicating that NIC does not disrupt the normal Mk transcriptional program (Section 2.3.8).[109] In fact, only 59 genes were found to be differentially regulated by NIC. Since this list of genes did not suggest an obvious mechanism as to how NIC may be increasing Mk maturation, we investigated the hypothesis that post-translational modifications and cellular processes, such as metabolic regulation, were largely responsible for the observed effects of NIC. Figure 3.1 is a schematic outlining two of our initial hypotheses: (1) NIC affects Mk maturation

by acting through a previously identified mechanism or (2) acts by modulating the activation of Tpo-mediated signaling pathways.

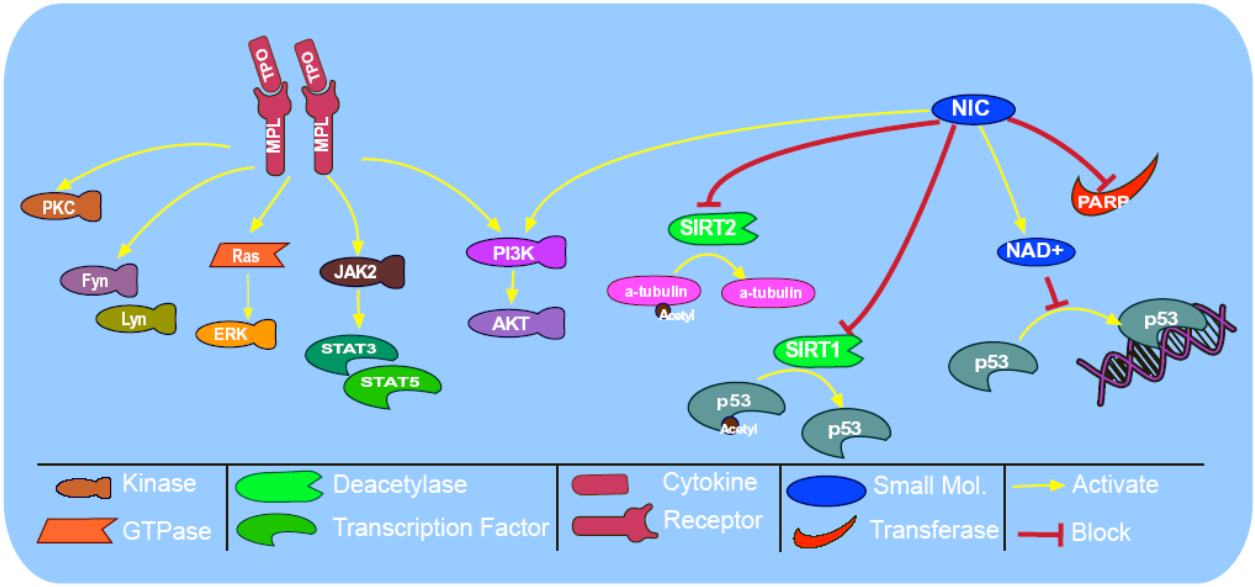

Figure 3.1. Schematic pathway depicting Tpo and nicotinamide (NIC) signaling.

Tpo, signaling through its receptor Mpl, can activate various signaling pathways, including those involving protein kinase C (PKC), the Src kinases Fyn and Lyn, the Ras/ERK branch of the MAPK pathway, the JAK/STAT pathway, and the PI3 kinase (PI3K)/Akt (PKB) pathway. NIC has also been shown to activate the PI3K/Akt pathway. Furthermore, NIC inhibits SIRT1 and SIRT2 from acetylating p53 and alpha-tubulin, respectively, while also inhibiting poly (ADP-ribose) polymerase (PARP). Finally, NIC increases intracellular NAD^+ levels, which in turn can modulate p53 binding to DNA. Pathway icons provided by Biocarta (www.biocarta.com).

Nicotinamide and Tpo are both known to affect cells via diverse signal transduction pathways. NIC has been shown to exert a protective effect against apoptosis through activation of Akt1 and Bad phosphorylation.[45,46] In addition to its role in apoptosis, Akt (protein kinase B) is a broad acting molecule affecting modulators of cytoskeleton organization such as Gsk3 (glycogen synthase kinase 3) and various cell cycle regulators with an established role in Mk maturation including p21, cyclinD1 and cyclinD3.[48-51] NIC also serves as a precursor for NAD^+. Supplementation of NIC to cultures has been shown to raise the level of intracellular NAD^+, [52,57,110,111] which can lead to a variety of effects within the cells including altering the binding of p53 to DNA.[52] NIC also inhibits the enzymes PARP and Sir2; however, culture with additional PARP and SIRT inhibitors did not mimic the effects of NIC on Mk ploidy (Section 2.3.7), tentatively ruling out inhibition of PARP or SIRT as a possible mechanism.

Tpo is the primary cytokine that regulates Mk development. The binding of Tpo to its receptor, Mpl, activates multiple signaling cascades including Ras/MAPK. The MAPKs ERK1 and ERK2 are rapidly phosphorylated after exposure to Tpo and are key regulators of cell proliferation, differentiation, and survival. A role for MAPK signaling in Mk endomitosis is suggested by a lower fraction of polyploid Mks after treatment with a MEK/ERK inhibitor;[22,112] however, results with MEK inhibitors have been variable. Tpo has also been shown to signal through the phosphatidylinositol 3-kinase (PI3K)/Akt pathway. With Tpo as the only growth factor present in our cultures, it is possible that NIC acts by enhancing Tpo signaling.

This chapter focuses on the role of intracellular NAD(H) levels and Tpo-mediated signaling in the ability of NIC to enhance Mk polyploidization. We demonstrate that although NIC can increase Mk ploidy in the absence of Tpo, the full effects of NIC on Mk

polyploidization were only obtained in cultures with Tpo. Moreover, NIC increased Tpo-mediated activation of ERK and the downstream ERK target RSK1, but did not alter Tpo-mediated Akt signaling. In addition, NIC dramatically increased the levels of intracellular NAD(H) (by as much as 5–fold) in a dose-dependent manner, and more than doubled the cell-volume-specific ($g/\mu m^3$) glucose consumption rate.

3.2. Materials and methods

3.2.1. Mk cultures

3.2.1.1. Tpo only

Unless otherwise noted, all reagents were obtained from Sigma-Aldrich (St. Louis, MO). Cultures were initiated with previously frozen human mobilized peripheral blood (mPB) $CD34^+$-selected cells (AllCells; Berkeley, CA or Fred Hutchinson Cancer Research Center; Seattle, WA). Cells were cultured in T-flasks and maintained at a density of 100,000–200,000 cells/mL with a constant liquid depth of 0.33 cm. All cultures, except where indicated, were performed using X-VIVO 20 (BioWhittaker; Walkersville, MD) supplemented with 100 ng/mL Tpo (Peprotech; Rocky Hill, NJ or generously provided by Genentech; South San Francisco, CA). Beginning at day 5, cells were continuously treated with 6.25 mM nicotinamide (NIC). Every other day, half-media exchanges were performed using fresh medium containing 100 ng/mL Tpo and 6.25 mM NIC. Cells receiving no NIC were used as a control. Cells were incubated at 37°C in a fully humidified atmosphere of 5% CO_2 and 95% air.

3.2.1.2. Alternative Mk cultures containing Tpo

mPB $CD34^+$-selected cells were cultured in X-VIVO 20 supplemented with either 100 ng/mL Tpo (Peprotech) and 0.15 μg/mL SDF-1α (R&D Systems) or Tpo (50 ng/mL; Peprotech) plus a cocktail of cytokines [IL-3 (0.005 ng/mL; Peprotech), IL-6 (10 ng/mL; Peprotech), and SCF (10 ng/mL; generously donated by Amgen)]. 6.25 mM NIC was added to the SDF1-α and cocktail cultures on days 0 and 5, respectively. Separately, cells were cultured with Tpo only or

Tpo + NIC (day 5 addition) on fibronectin-coated surfaces (BD Biocoat, BD Biosciences, Bedford, MA).

3.2.1.3. Cytokine cocktail cultures without Tpo

$CD34^+$ cells were cultured in X-VIVO 20 supplemented with IL-3 (1.5 ng/mL), IL-6 (10 ng/mL), and SCF (50 ng/mL). On day 5, cells were divided and treated to generate 4 cultures: cocktail [(IL-3, IL-6, SCF); (C)], cocktail + 6.25 mM NIC (C + N), cocktail + 100 ng/mL Tpo (C + T), or cocktail + Tpo + NIC (C + T + N).

3.2.2. Human megakaryoblastic cell line culture

The human megakaryoblastic CHRF-288-11 (CHRF) cell line[85,86] was generously provided by Dr. R. Smith (NIH; Bethesda, MD). CHRF cells were cultured in Iscove's modified Dubelcco's medium (IMDM) supplemented with 10% FBS (HyClone). Experiments performed with the CHRF cells in this chapter did not include PMA stimulation to induce Mk differentiation.

3.2.3. Mk characterization

3.2.3.1. Flow cytometric detection of surface marker expression

Cells were washed with phosphate-buffered saline (PBS) containing 2 mM EDTA (to reduce platelet adhesion) and 0.5% bovine serum albumin (BSA) [PEB], incubated with fluorescein (FITC)-labeled anti-CD41 antibody and APC-labeled anti-cmpl antibody (BD Biosciences; San Jose, CA) for 30 minutes at room temperature, and then analyzed on a Becton

Dickinson LSRII flow cytometer using FACSDiva software (BD Biosciences). DAPI was added to samples at a final concentration of 3 μM shortly prior to acquisition to exclude dead cells.

3.2.3.2. Flow cytometric analysis for Mk ploidy

Cells were labeled with FITC-conjugated anti-CD41 antibody (BD Biosciences) and fixed with 0.5% paraformaldehyde (15 minutes at room temperature), followed by permeabilization with cold 70% methanol (1 hour at 4^{o}C). Cells were treated with RNAse followed by 50 μg/mL propidium iodide to stain DNA, and analyzed by flow cytometry. The percentage of high-ploidy Mks was determined from the ratio of the number of $CD41^{+}$ Mks with 8N or higher DNA ploidy to the total number of $CD41^{+}$ Mks.

3.2.4. Measurement of intracellular NAD(H) levels

Human mPB $CD34^{+}$ cells were cultured as described with 100 ng/mL Tpo or Tpo + NIC. NAD(H) [NAD^{+} + NADH] was extracted using a slightly basic pH extraction buffer containing the detergent Triton X-100.[113] The extracts were subjected to an enzymatic cycling reaction[114] performed in a 96-microwell flat-bottom plate using a reagent mixture containing 0.1 M bicine, 0.5 M ethanol, 4.17 mM EDTA, 0.83 mg/mL BSA, 0.42 mM MTT (3--2,5-diphenyltetrazolium bromide), and 1.66 mM phenazine ethosulfate. The reaction was started by adding 2U of yeast alcohol dehydrogenase. Color was developed in the dark for 30 minutes and detected at 570 nm using an ELISA plate-reader. Each sample was run in duplicate. When necessary, samples were diluted by half with extraction buffer in order to ensure measured NAD(H) levels were within the range of the standard curve.

3.2.5. Primary Mk cultures with APO866

mPB $CD34^+$-selected cells were cultured in X-VIVO 20 supplemented with 100 ng/mL Tpo. On day 4, portions of the cells were treated with varying concentrations (0.05–1000 nM) of APO866 (provided by NIMH Chemical Synthesis and Drug Supply Program; Research Triangle Park, NC) in DMSO. NIC (3 or 6.25 mM) was added 12-24 hours after APO866 addition. Half-media exchanges were performed every other day with media containing Tpo, NIC and/or APO. NAD(H) was measured in all cultures on day 5 (4 hours after NIC addition) and on days 7 and 9. Cells cultured with Tpo only, Tpo + NIC, and Tpo + APO were used as controls. Separately, APO only and APO + 3 mM NIC cultures were also included in which full media exchanges were performed every day of the culture after APO addition on day 4. Tpo only and Tpo + 3 mM NIC cultures handled in a similar manner provided controls.

3.2.6. CHRF cell cultures with APO866

CHRF cells were seeded in 6-well plates at a density of 100,000–200,000 cells/mL in IMDM containing 10% FBS. APO866 (0.1–1000 nM) was added to cells at the time of seeding. 4-12 hours after APO866 addition, 3 or 6.25 mM NIC was added to the cultures and NAD(H) was measured two days after the cultures were initiated. Untreated CHRF cells and cells treated with either APO866 or NIC alone were used as controls. Separately, CHRF cells were treated with either 3 or 6.25 mM NIC for 24 hours before APO866 was added (10–1000 nM). NAD(H) levels were measured 24 hours after APO addition.

3.2.7. Primary Mk cultures with nicotinic acid (NA)

mPB $CD34^+$-selected cells were cultured in X-VIVO 20 supplemented with 100 ng/mL Tpo. On day 5, cells cultured with Tpo only were treated with varying doses (3 and 6.25 mM) of nicotinic acid (NA; Sigma Aldrich). NA was added to X-VIVO 20 from a stock solution of 15 mg/mL and media was pH adjusted to 7.2 before adding to cells. NAD(H) was measured on day 5 (4 hours after NA addition) and on days 7 and 9. Cells cultured with Tpo only and Tpo + 6.25 mM NIC were used as controls.

3.2.8. Analysis of glucose and lactate concentrations in cell culture media

Glucose and lactate concentrations were measured in cell culture media from Tpo only and Tpo + NIC cultures. Media was sampled on days 5, 7, 8, 9, and 11. On days when media was exchanged for NIC replacement, media samples were collected before and after the exchange. Media was analyzed with a YSI 2700 SELECT Analyzer (Yellow Springs, OH) with membranes for D-glucose (YSI #2365) and lactate (YSI# 2329). Measurements were performed in duplicate.

3.2.9. Detection of phosho-MAPKs using the Proteome Profiler Array

A commercially available antibody array (R&D Systems) was used to detect the levels of 21 phosphorylated MAPKS including Akt 1, 2, 3; ERK 1, 2; GSK3; and several p38 isoforms. Whole-cell lysates were prepared using 4.5 million cells from Tpo only and Tpo + NIC cultures 24 hours after NIC addition on day 5. It should be noted that the fraction of Mks at this time point was ~50% in both conditions and that Tpo only and Tpo + NIC cells were similar in size on day 6. Total protein yield was quantified using the BCA assay (Pierce) and was determined to

be ~200 μg total protein per 4.5 million cells. Equal amounts of protein from each condition were then used for incubation with the membranes. Capture antibodies spotted onto nitrocellulose membranes bind phosphorylated and non-phosphorylated kinases present in cell lysates. After washing away unbound material, a cocktail of phospho-site-specific biotinylated antibodies and streptavidin-HRP with chemiluminescence were used to detect phosphorylated kinases. The array consists of 21 kinases, 6 negative controls and 3 positive controls spotted in duplicate. The intensity of each spot with the local average background subtracted was determined using ImageQuant 5.2 software. An average of the 6 negative control spots was calculated and this value was subtracted from each kinase spot intensity. The resulting values for each pair of spots was then averaged and the ratio of the Tpo + NIC to Tpo only conditions was determined.

3.2.10. Intracellular flow cytometry for pERK and pAkt

Human mPB $CD34^+$ cells were cultured in serum-free medium supplemented with 100 ng/mL Tpo. Beginning on day 5 of culture, a portion of the cells was cultured with 6.25 mM NIC. pERK and pAkt levels were measured on days 6, 7, 8, and 9 in cells taken directly from culture using flow cytometry. Separately, beginning on day 5 of culture, cells without NIC were washed with X-VIVO 20 and starved of Tpo for 7 hours. Following starvation, cells were activated with either X-VIVO 20 alone, or X-VIVO 20 containing either 100 ng/mL Tpo, 6.25 mM NIC, or 100 ng/mL Tpo + 6.25 mM NIC. Levels of pERK and pAkt were assessed via flow cytometry at various time points after activation.

Briefly, cells were washed with PEB^+ (PBS containing 1% BSA and 2 mM EDTA) and fixed with 2% paraformaldehyde for 15 minutes at 4^oC. After washing, cells were permeabilized with ice cold 90% methanol for 20 minutes on ice. Cells were blocked with PEB^+ for 30 minutes at 4^oC followed by incubation with the primary antibody [Phospho-p44/42 MAP Kinase (Thr202/Tyr204) (197G2) Rabbit Monoclonal Antibody or phospho-Akt (Ser473) (193H12) Rabbit Monoclonal Antibody (Cell Signaling Technologies; Danvers, MA) or normal rabbit IgG (Santa Cruz Biotechnology; Santa Cruz, CA) as an isotype control] for 30 minutes at room temperature. After washing, cells were blocked with PEB^+ for 30 minutes at 4^oC followed by incubation with the secondary antibody [$F(ab')_2$ goat-anti-rabbit-PE antibody (Jackson ImmunoResearch; West Grove, PA)] for 30 minutes at room temperature. An LSRII cytometer (BD Biosciences) was used for acquisition and FACSDiva software (BD Biosciences) was used for analysis.

3.2.11. Western analysis

Primary human $CD34^+$ cells were cultured in X-VIVO 20 containing 100 ng/mL Tpo. On day 5, a portion of the cells was treated with 6.25 mM NIC. On days 7, 8, and 9, cells were sampled from Tpo only and Tpo + NIC cultures, and whole-cell lysates were prepared using 2-3 million cells from each condition. Samples were prepared in ice-cold cell lysis buffer (Cell Signaling Technologies) containing 1 mM phenylmethylsulphonyl fluoride (PMSF). An equal amount of total protein (20 μg) per sample was denatured with 3X sample buffer (62.5 mM Tris-HCl (pH 6.8), 2% w/v SDS; 10% glycerol; 50 mM DTT, 0.01% w/v bromophenol blue) and boiled for 5 minutes. Proteins were separated by SDS-PAGE using Ready-Gel Tris-HCl gels

(BioRad, Hercules, CA) and transferred onto PVDF membranes (BioRad). Non-specific binding of protein was blocked by incubation of the membrane in a solution of 5% w/v non-fat dry milk in TBS (20 mM Tris base, 137 mM NaCl) with 0.1% Tween-20 for 1 hour at room temperature. The membrane was then incubated with a solution of 5% BSA in TBS with 0.05% Tween-20 containing the appropriate primary antibody [phospho-p44/42 MAP Kinase (Thr202/Tyr204), Phospho-mTOR (Ser2448) Antibody, or Phospho-p90RSK (Ser380) Antibody (Cell Signaling Technologies)] overnight at 4^{o}C. After washing, the membrane was further incubated with a solution of 5% w/v non-fat dry milk in TBS with 0.1% Tween-20 containing the secondary antibody [affinity purified goat anti-rabbit IgG (H&L) antibody conjugated to horseradish peroxidase (HRP) (Cell Signaling Technologies)]. Bound antibodies were detected using chemiluminescence detection (ECL Plus, Amersham; Piscataway, NJ) and a Storm 860 fluorimager (Molecular Dynamics). For detection of total kinase protein levels, the membranes were stripped using a solution of 100% acetonitrile followed by incubation at 50^{o}C in a solution of 100 mM 2-mercaptoethanol, 2% SDS, and 62.5 mM Tris HCl pH 6.7. Membranes were then reprobed with antibodies for total ERK1/2 (Cell Signaling), total RKS1 (Santa Cruz), or total mTOR (Cell Signaling). Densitometry was performed using ImageQuant 5.2 software.

3.2.12. Mk cultures with chemical inhibitors of MEK

Synthetic inhibitors of MEK were dissolved in DMSO and added to human Mk cultures beginning on day 4. Half-media exchanges were performed every other day for inhibitor replacement. 6.25 mM NIC was added to cultures on day 5. U0126 (Calbiochem; San Diego, CA) was tested in the concentration range of 5–25 μM. PD98059 (Calbiochem) was tested in the

concentration range of 10–75 μM. Cells treated with an equal volume of DMSO were included as a control.

3.3. Results

3.3.1. Full effects of NIC on Mk ploidy are Tpo-dependent

We have previously shown that NIC increases ploidy in cultures of primary human $CD34^+$ cells supplemented with Tpo.[109] In order to examine the role of Tpo in the effects of NIC, Mk cultures were performed using a cytokine cocktail that did not include Tpo. Primary human $CD34^+$ cells were cultured with IL-6 (10 ng/mL), IL-3 (1.5 ng/mL), and SCF (50 ng/mL). On day 5, cells from the cocktail cultures were treated with either 6.25 mM NIC, 100 ng/mL Tpo, or Tpo + NIC. Cells cultured with Tpo only and Tpo + NIC were included for comparison. This cytokine combination yielded ~16% $CD41^+$ cells by day 11 (Fig 3.2A) compared to cultures with Tpo only which typically contain 80–90% $CD41^+$ cells. Furthermore, polyploidization was less extensive in cocktail cultures. On day 11, the percentage of high-ploidy ($\geq$ 8N) Mks was ~2-fold lower in cocktail cultures compared to those with Tpo only, and reached only ~9% high-ploidy Mks (Fig 3.2B). Moreover, the degree of Mk polyploidization was also lower without Tpo; and the maximum DNA content reached was only 8N in the cocktail cultures (Fig 3.2C) compared to 16N in cultures with Tpo only.

The addition of NIC to cocktail cultures increased the percentage of high-ploidy Mks by approximately 2-fold (day 11) to a level similar to that for Tpo only cultures. However, the increase was greater when NIC was added in the presence of Tpo. Cocktail cultures treated with Tpo contained ~10% high-ploidy Mks compared to 37% on day 11 in cocktail cultures treated with Tpo + NIC (Fig 3.2B). Moreover, the degree of Mk polyploidization was increased to a greater extent when NIC was added simultaneously with Tpo compared to NIC alone. NIC

increased the maximum DNA content of cocktail cultures from 8N to 16N (Fig 3.2C), whereas Mks from cocktail cultures treated with Tpo + NIC reached a DNA content of 32N. While it appears that Tpo plays an important role in the effects of NIC on Mk polyploidization, similar levels of the Tpo receptor c-mpl were measured on Mks from cultures with Tpo only and Tpo + NIC (data not shown).

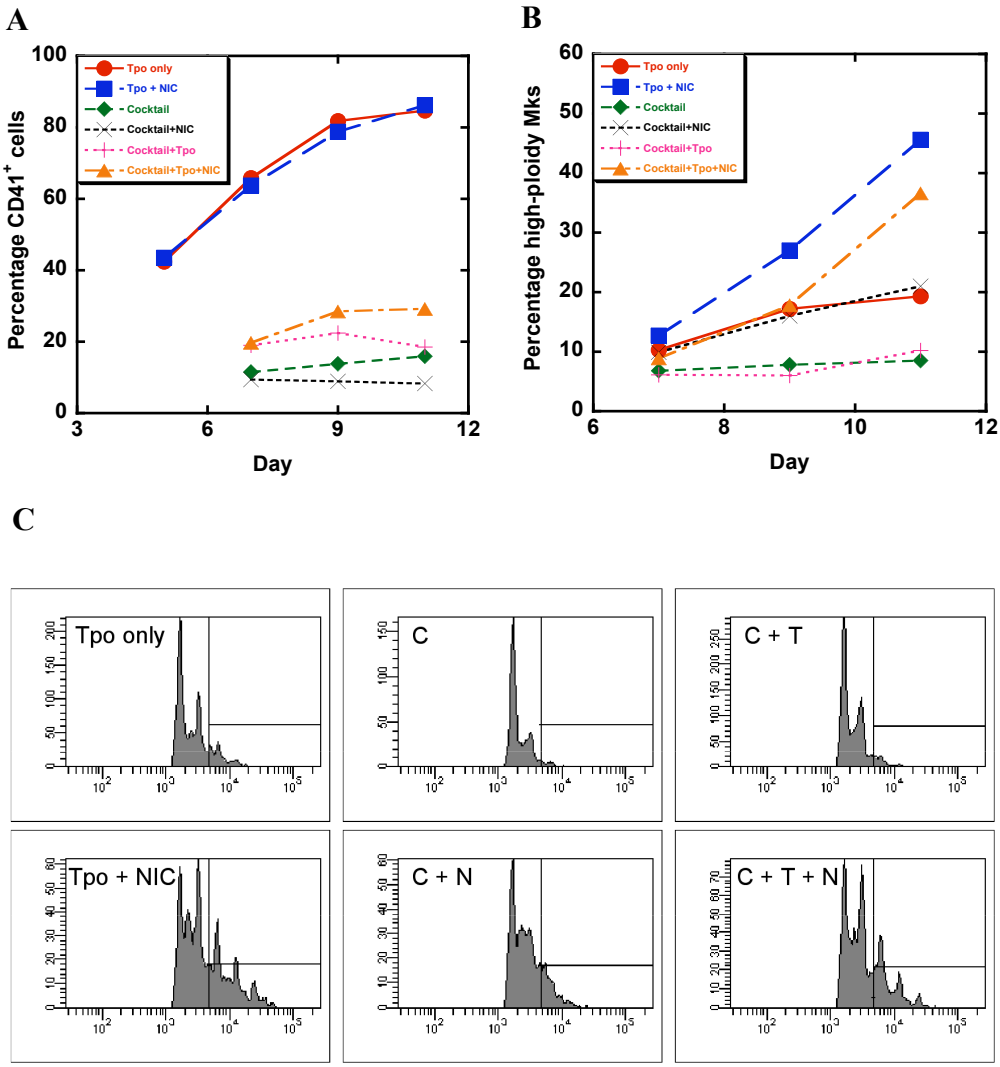

Figure 3.2. Full effects of NIC on Mk ploidy are Tpo-dependent.

Human mPB CD34$^+$-selected cells were cultured with IL-3, IL-6, and SCF (C; green). Beginning on day 5, either 100 ng/mL Tpo (C+T; pink), 6.25 mM NIC (C+N; black), or Tpo + NIC (C+T+N; orange) was added to cultures. Tpo only (red) and Tpo + 6.25 mM NIC (blue) cultures were included for comparison. (A) The number of CD41$^+$ cells as a percentage of viable cells was determined by flow cytometry. (B) DNA content was measured by staining with PI; the data shown is the percentage of CD41$^+$ cells with DNA content $\geq$ 8N. (C) DNA histograms on day 11 of all cultures. For A-C, data is representative of n = 2 for all cultures.

3.3.2. Detection of kinase activation in Mk cultures using an antibody array

Since NIC appeared to synergize with Tpo to increase Mk ploidy, we used a commercially available antibody array for phosphorylated kinases to examine the hypothesis that NIC increased Mk maturation by modulating the activity of Tpo-associated signal transduction pathways. Our studies focused on two signaling pathways that may be affected by NIC – PI3K/AKT and Ras/MAPK/ERK. This commercially available antibody array (R&D Systems) detects the level of 21 phosphorylated MAPKS including Akt 1, 2, 3; ERK 1, 2; GSK3; and several p38 isoforms. Kinase expression levels were compared between cells sampled from Tpo only and Tpo + NIC cultures. Five targets were identified to be more highly activated in the cells cultured with Tpo + NIC compared to Tpo only; including: ERK1, RSK1, GSK3, and p38α and γ isoforms (Fig 3.3A). Most changes were subtle – ranging from 1.3- to 3.5-fold over the Tpo only condition. These target spots were noticeably darker on the NIC array upon inspection of the scanned images (Fig 3.3B). A 1.4–fold increase in ERK activation was observed for the Tpo + NIC cells at 24 hours with the array. Activation of RSK1 (ribosomal protein S6 kinase), a downstream target of ERK, was also shown to be higher in the NIC culture. RSK1 has been shown to have a role in regulating cell size with overexpression of RSK1 leading to increased cell size.[115] RSK1 has also been shown to phosphorylate Gsk3, which was also present at a higher level in the Tpo + NIC cells. Gsk3 is also a downstream target of Akt; however, neither Akt1, 2, nor 3 was activated in either condition. Interestingly, two p38 isoforms were also more highly activated in Tpo + NIC cells. These results highlight the utility of using more global approaches, such as antibody arrays, to identify promising targets for additional study using more quantitative assays.

Figure 3.3. Detection of phospho-MAPKs using the Proteome Profiler Array in Tpo only and Tpo + NIC cultures.

Primary human $CD34^+$-selected cells were cultured with 100 ng/mL Tpo. On day 5, a portion of the cells was treated with 6.25 mM NIC. Whole cell extracts were prepared using 4.5 million cells from each condition on day 6. Membranes were then incubated with an equal amount of total protein from each culture. The intensity of each spot with the local average background subtracted was determined using ImageQuant 5.2 software. An average of the 6 negative control spots was calculated and this value was subtracted from each kinase spot intensity. The resulting values for each pair of spots was then averaged and the ratio of the Tpo + NIC to Tpo only conditions was determined. (A) Spot intensities (background corrected) of proteins determined to have higher activation in Tpo + NIC cells. (B) Images of MAPK antibody arrays with kinases activated to a greater extent in NIC-treated cells highlighted. Data shown is from one biological experiment. Replicates were not performed.

A

	Tpo only	Tpo + NIC	Ratio
ERK1	2194.2	3143.7	1.4
p38γ	1663.8	2106.3	1.3
RSK1	82.3	874.3	10.6
GSK3α/β	409.2	1448.8	3.5
p38α	1319.0	2290.8	1.7

B

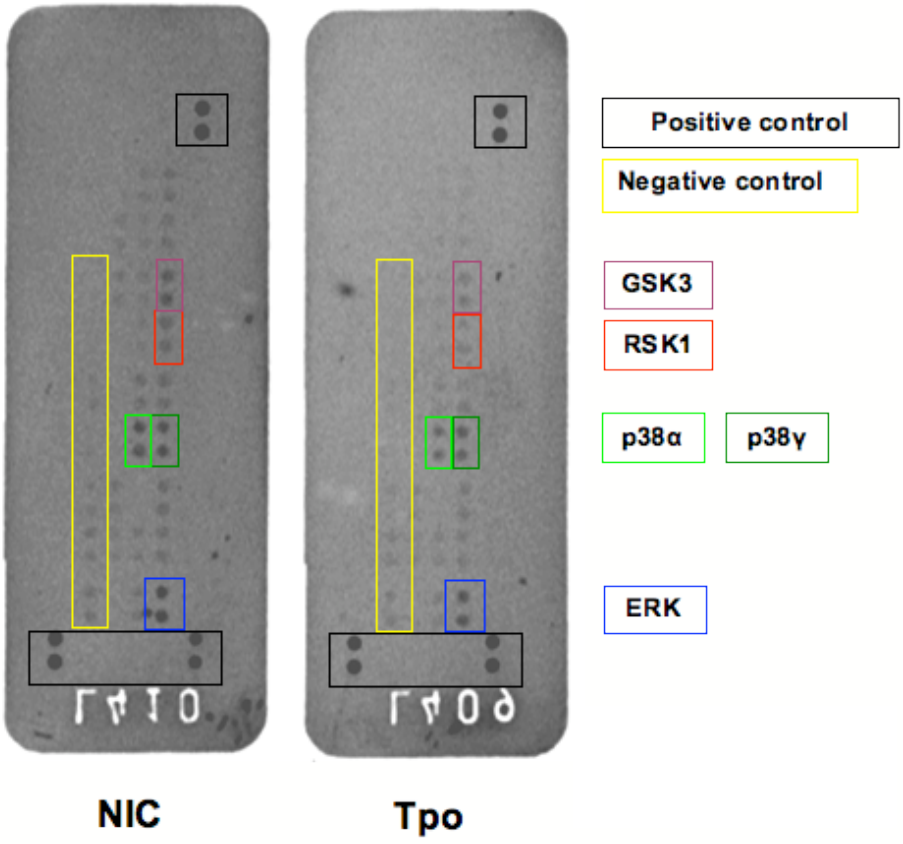

3.3.3. Effects of NIC on Tpo-mediated signaling pathways – PI3K/Akt and Ras/MAPK

Studies were performed to further characterize the effects of NIC on several target kinases identified with the antibody arrays. NIC has been shown to increase Akt activation in other cell types, therefore we measured levels of phosphorylated Akt in Mks from cultures with Tpo only and Tpo + NIC using flow cytometry. Akt was not found to be activated above background levels in cells removed from either culture (Fig 3.4A), confirming results obtained with the antibody array. Moreover, the transient increase in the level of phosphorylated Akt (pAkt) was similar in short-term studies when cells were starved of Tpo and stimulated with either Tpo only or Tpo + NIC (Fig 3.4B). Overall, NIC does not alter Akt activation in Mks.

Figure 3.4. Akt activation is not affected by NIC.

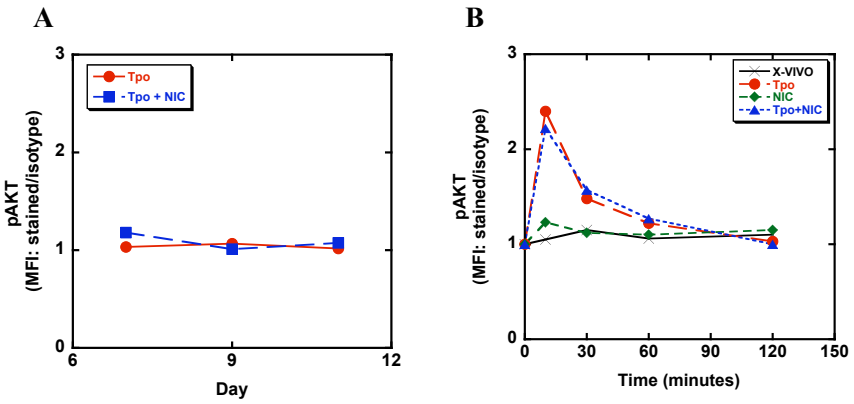

Primary human mPB $CD34^{+}$-selected cells were cultured with 100 ng/mL Tpo. Beginning on day 5, a portion of the cells was treated with 6.25 mM NIC. Cells were sampled from each of the cultures at various time points and the level of phosphorylated Akt (Ser473) was measured by intracellular flow cytometry. (A) Flow cytometric analysis of steady-state pAkt levels in Tpo only (red) and Tpo + NIC (blue) cultures. Data is representative of 2 biological replicates. (B) Separately, levels of pAkt were also measured in starved cells stimulated with X-VIVO 20 alone (black) or containing either 100 ng/mL Tpo (red), Tpo + 6.25 mM NIC (blue), or 6.25 mM NIC (green).

Levels of phosphorylated ERK (pERK) were measured in cells sampled from Tpo only and Tpo + NIC cultures using both flow cytometry and Western analysis. The level of phosphorylated ERK in cells removed directly from culture was found to peak at day 7 (Fig 3.5A), which is the point in culture when the percentage of polyploid Mks began to increase (Fig 2.4A). Levels of pERK then decreased as the cells matured. However, the level of pERK was greater in cells from Tpo + NIC cultures compared to cells cultured with Tpo only using both methods of detection (Fig 3.5A,B). Furthermore, these results are in agreement with results obtained using the antibody array described above. ERK activation was also higher in starved cells stimulated with Tpo + NIC compared to Tpo only (Fig 3.5C). These studies suggest that ERK signaling may play a role in NIC-mediated enhanced polyploidization.

Figure 3.5. Cells cultured with NIC have increased ERK activation.

Primary human mPB $CD34^+$-selected cells were cultured with 100 ng/mL Tpo. Beginning on day 5, a portion of the cells was treated with 6.25 mM NIC. Cells were sampled from each of the cultures at various time points and the level of phosphorylated ERK (p44/42) was measured by intracellular flow cytometry and Western analysis. (A) Flow cytometric analysis of steady-state pERK levels in Tpo only (red) and Tpo + NIC (blue) cultures. Kinetics of pERK expression is shown for 2 biological replicates. (B) Western analysis of steady-state pERK levels in Tpo only (T) and Tpo + NIC (N) cultures. Band density analysis with ImageQuant 5.2 is shown at the right. (C) Separately, levels of pERK were also measured in starved cells stimulated with X-VIVO 20 alone (black) or containing either 100 ng/mL Tpo (red), Tpo + 6.25 mM NIC (blue), 6.25 mM NIC (green).

A

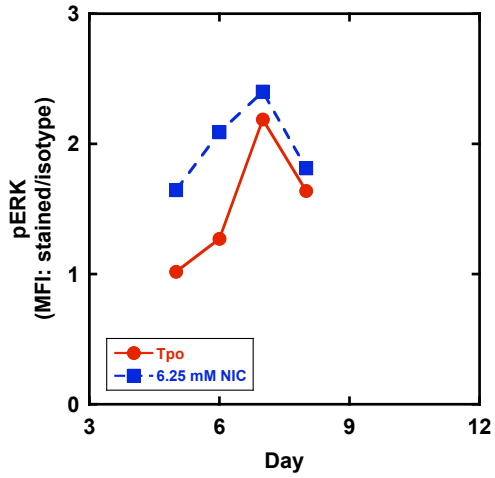
pERK
(MFI: stained/isotype)
Day
Tpo
- 6.25 mM NIC

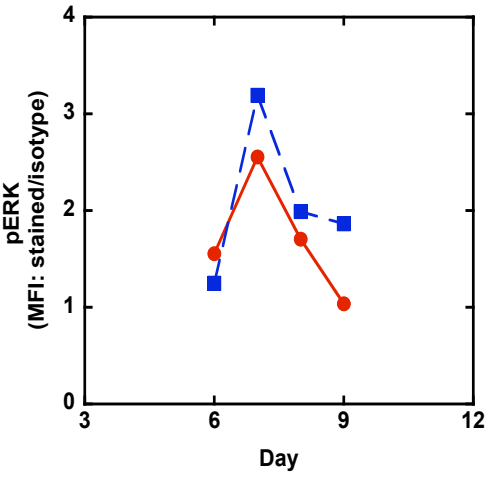
pERK
(MFI: stained/isotype)
Day

B

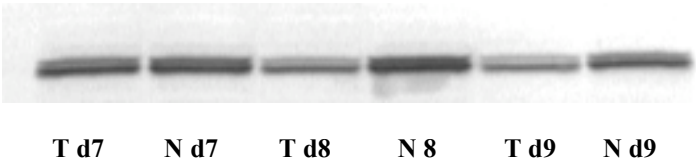
T d7
N d7
T d8
N 8
T d9
N d9

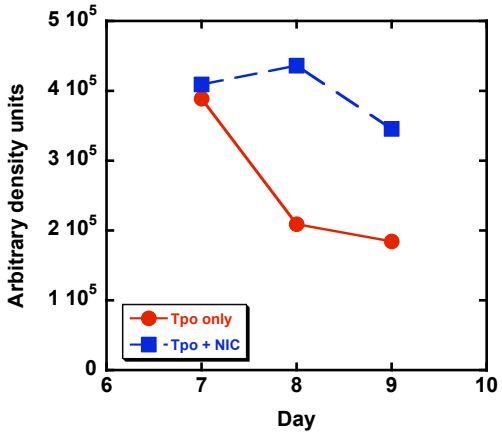
Arbitrary density units
Day
Tpo only
- Tpo + NIC

C

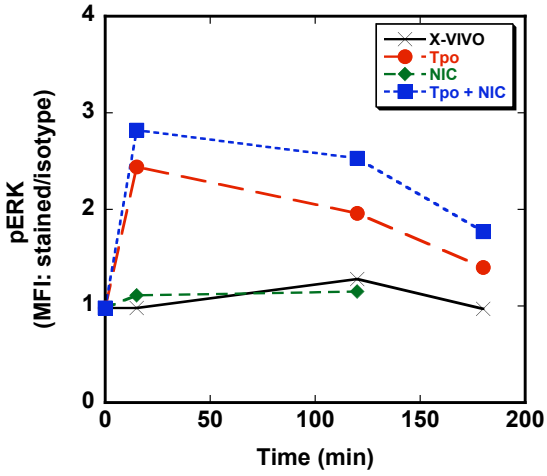
pERK
(MFI: stained/isotype)
Time (min)
X-VIVO
- Tpo
- NIC
- Tpo + NIC

3.3.4. Effects of NIC on the activation of the downstream ERK targets RSK1 and mTOR

ERK signaling activates many downstream targets. One ERK target that would be expected to play a role in increased polyploidization with NIC is mTOR (mammalian target of rapamycin). mTOR regulates cell growth and protein synthesis through its downstream targets p70S6K and 4E-BP1 and through its association with Raptor (regulatory associated protein of TOR), which serves to colocalize mTOR with 4E-BP1 and p70S6K.[116] mTor activity is negatively controlled by the tumor suppressors TSC1 (hamartin) and TSC2 (tuberin).[117,118] A role for mTOR in primary Mk endomitosis has been established through the use of its inhibitor rapamycin. Mks treated with rapamycin exhibit decreased cell size and ploidy with similar expression of Mk surface markers compared to untreated Mks.[51,82,119] This is consistent with a possible role for NIC in mTOR activation because NIC increases Mk size and ploidy without affecting Mk surface marker expression. mTOR is also a nutrient sensor and is activated by nutrient-rich conditions.[120] While signaling through PI3K/Akt controls mTOR activation,[121-123] mTOR activity can also be increased by both ERK and the ERK target RSK1 via inactivation of the mTOR repressor TSC2 (Fig 3.6).[124-126] Since NIC does not decrease Tpo-mediated Akt signaling, increased TSC2 inactivation by ERK would likely result in a net increase in mTOR activity.

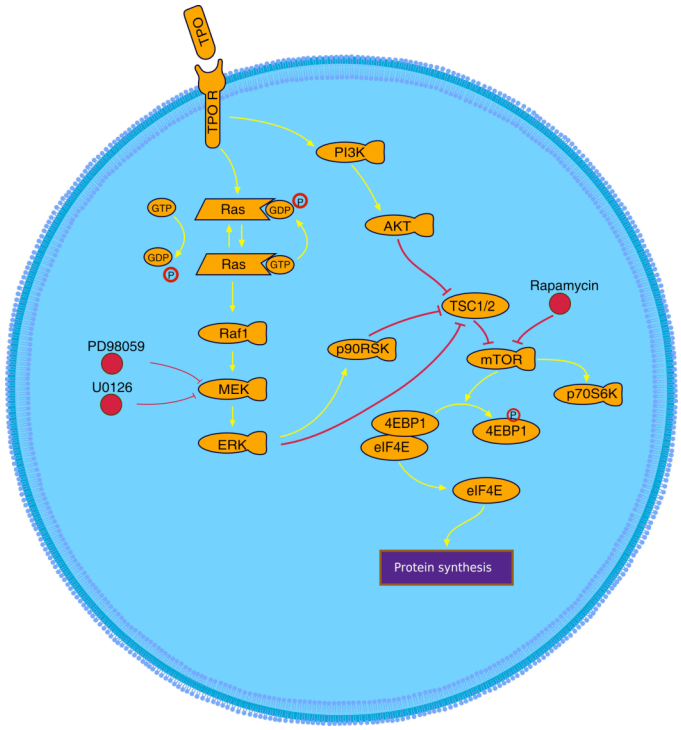

Figure 3.6. Illustration of key signaling pathways examined in Chapter 3.

Arrows and blunt-ended lines indicate positive and negative regulation, respectively. Figure composed of icons provided by Biocarta.

Since we observed increased ERK activation with NIC, we examined whether downstream targets of ERK were also more extensively activated with NIC. Western analysis was performed to measure levels of phosphorylated RSK1 (pRSK1) and phosphorylated mTOR (pmTOR) in cells sampled from Tpo only and Tpo + NIC cultures. The level of pRSK1 was found to increase with Mk maturation and was greater in NIC-treated cells (Fig 3.7A,C), further indicating a role for the ERK pathway in the NIC effects on Mk ploidy and proplatelet formation. mTOR was activated in both cultures and remained constant. Unexpectedly, pmTOR was present at similar levels in Tpo only and Tpo + NIC cells (Fig 3.7B,C).

Figure 3.7. Western analysis for the activation of downstream ERK targets RSK1 and mTOR.

Western analysis for phosphorylated and total (A) RSK1 and (B) mTOR. Primary human mPB $CD34^+$-selected cells were cultured with Tpo only (T) or Tpo + NIC (N). NIC was added on day 5 and whole-cell lysates were prepared on days 7, 8, 9, and 11 of culture. An equal amount of total protein was loaded per well. (C) Band density analysis was performed using Image Quant 5.2 software. Data shown is the ratio of phosphorylated/total protein for Tpo only (red) and Tpo + NIC (blue) cultures. Data is representative of results from 2 biological experiments.

A

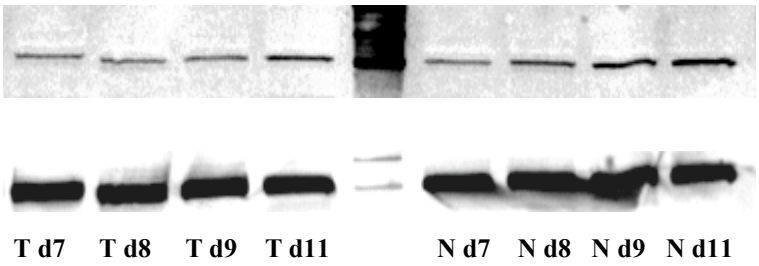
pRSK1
Total RSK1
T d7
T d8
T d9
T d11
N d7
N d8
N d9
N d11

B

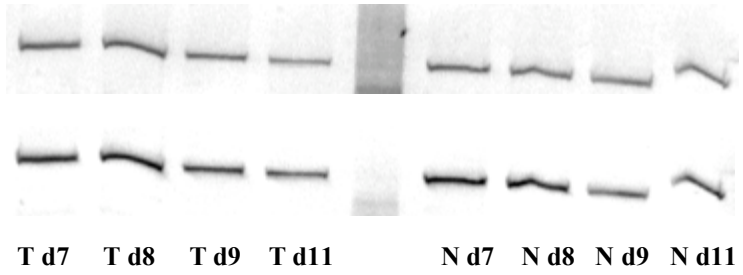
pmTOR
Total mTOR
T d7
T d8
T d9
T d11
N d7
N d8
N d9
N d11

C

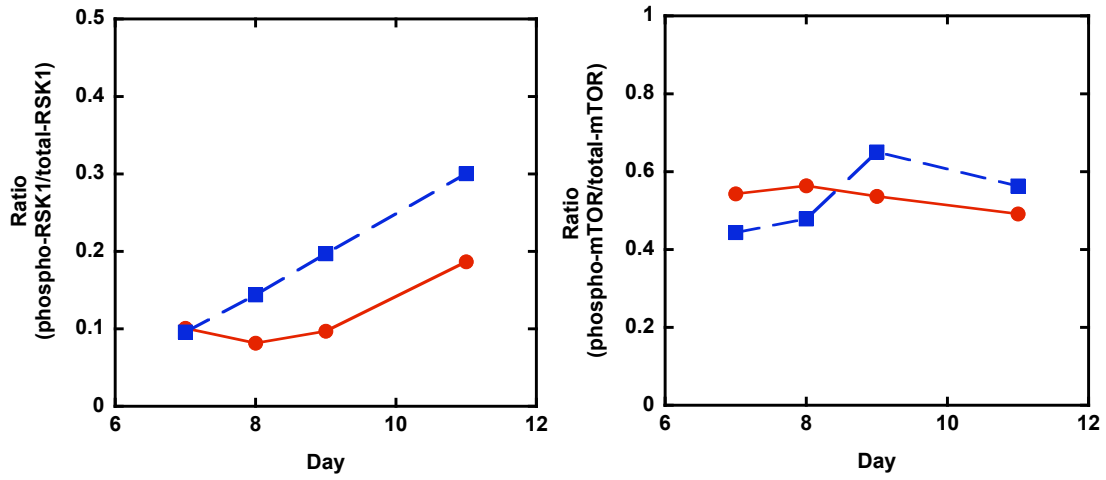
Ratio (phospho-RSK1/total-RSK1)
0.5
0.4
0.3
0.2
0.1
0
6
8
10
12
Day
Ratio (phospho-mTOR/total-mTOR)
1
0.8
0.6
0.4
0.2
0
6
8
10
12
Day

3.3.5. Chemical inhibition of MEK with PD98059 and U0126 in primary Mk cultures

Chemical inhibitors of MEK/ERK signaling (PD98059 and U0126) were used to examine whether inhibition of this pathway (1) decreases Mk ploidy in the absence of NIC and (2) decreases NIC-mediated enhancement of Mk ploidy and proplatelet formation. An important role for ERK signaling in Mk endomitosis is suggested by studies using the MEK inhibitor PD98059. Guerriero *et al*. observed a lower fraction of polyploid cells after treatment of purified hematopoietic progenitor cells with 25–50 μM PD98059.[22] Similarly, Miyazaki *et al.* reported lower ploidy with PD98059 for Mks derived from cord blood $CD34^+$ cells.[112] However, another study with cord blood $CD34^+$ cells that used a similar PD98059 level showed increased polyploidization.[127] Two other studies with mPB and cord blood $CD34^+$ cells showed greater polyploidization with PD98059 at a lower dose (6–10 μM).[51,128] Thus, whether PD98059 increases or decreases Mk ploidy remains controversial. The different effects reported are likely due in part to the different PD98059 doses and addition/exposure times used in the different studies. Another MEK/ERK inhibitor U0126 has been used less frequently in human Mk cultures. A dose of 10 μM was reported to rapidly decrease cell growth and the cells died rapidly during the first few days of culture.[51] However, another study used doses of 10 and 30 μM with no mention of cell death.[129]

Due to the conflicting results obtained by others using PD98059 in human Mk cultures and the limited use of U0126 in human Mk cultures, we initially screened a range of inhibitor concentrations (U0126: 5, 10, 25 μM; PD98059: 25, 50, 75 μM) for cytotoxicity and effects on Mk ploidy. Inhibition of ERK activation in starved cells stimulated with Tpo was demonstrated with both inhibitors (Fig 3.8A), as has been shown by others. However, we were interested in

whether these inhibitors were capable of maintaining ERK inhibition in long-term Mk cultures. Inhibitors were added to Mk cultures on day 4 because we wanted to know whether PD98059 and U0126 would offset increased ERK activation by NIC, which is added on day 5. Based on results of others, we expected to find a dose of each inhibitor that was capable of reducing Mk ploidy. However, at all doses tested, PD98059 increased Mk ploidy in a dose-dependent manner (Fig 3.8B). The increases were greater than that previously reported by others with PD98059. Cultures with 50 and 75 μM PD98059 showed signs of decreased viability towards the end of culture. Additional characterization of the non-cytotoxic doses of PD98059 (10 and 25 μM) was performed by carrying out Mk cultures with Tpo only, Tpo + 10 μM PD98059, Tpo + 25 μM PD98059, and PD98059 + NIC. The addition of NIC to cultures with 25 μM PD98059 did not further increase ploidy (Fig 3.8C), suggesting there is a limit to the benefits of NIC. In contrast, non-cytotoxic concentrations of U0126 (5–25 μM) slightly decreased Mk ploidy in Tpo only cultures (Fig 3.8B). Follow-up studies to examine the effects of U0126 in Tpo + NIC cultures have not yet been performed. While there are differences between the mechanisms by which each inhibitor acts (U0126 inhibits active and inactive MEK whereas PD98059 inhibits only the activation of inactive MEK), the conflicting effects on ploidy brings into question the specificity of the inhibitors. In summary, inhibition of ERK with chemical inhibitors was not able to provide further information as to the role of ERK in the effects of NIC on Mk ploidy. However, these studies provide a more thorough characterization of the effect of PD98059 on Mk differentiation than currently provided in the literature.

Figure 3.8. Mk ploidy in cultures with the MEK inhibitors PD98059 and U0126.

(A) mPB $CD34^+$-selected cells were cultured with 100 ng/mL Tpo. On day 3, a portion of the cells was removed and starved of Tpo overnight. Cells were then pretreated with either PD98059 or U0126 for 1 hour before being stimulated with 100 ng/mL Tpo for 10 minutes. Levels of pERK were measured using flow cytometry (blue = stained, black = isotype control). Cells not pre-treated with either inhibitor showed a 1.7-fold increase in pERK activation. Both PD98059 and U0126 completely prevented this activation. (B) mPB $CD34^+$-selected cells were cultured with 100 ng/mL Tpo. Beginning on day 4 of culture, cells were treated with varying concentrations of either PD98059 or U0126. 6.25 mM NIC was added on day 5. The percentage of high-ploidy Mks was determined in each culture on days 7 (black) and 9 (gray). (C) Kinetics of the percentage of high-ploidy Mks in cultures with non-toxic doses of PD98059 with and without NIC.

A

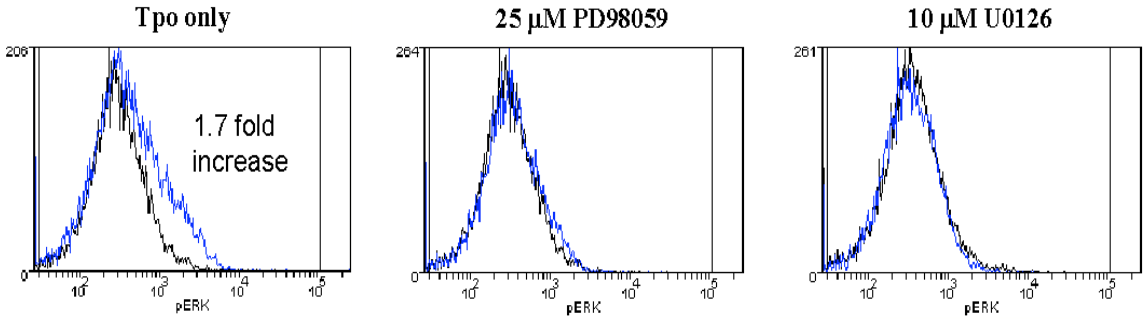
Tpo only
25 µM PD98059
10 µM U0126
1.7 fold increase
pERK
pERK
pERK

B

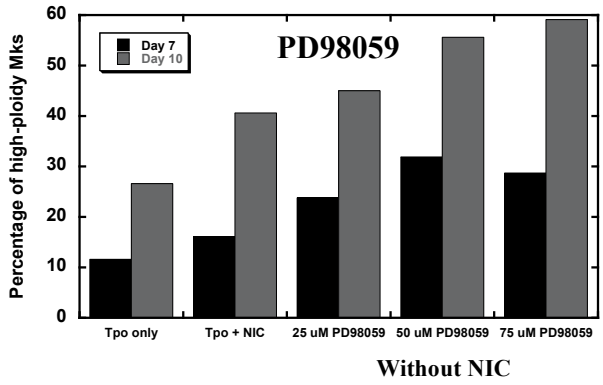
Day 7
Day 10
PD98059
Percentage of high-ploidy Mks
Tpo only
Tpo + NIC
25 uM PD98059
50 uM PD98059
75 uM PD98059
Without NIC

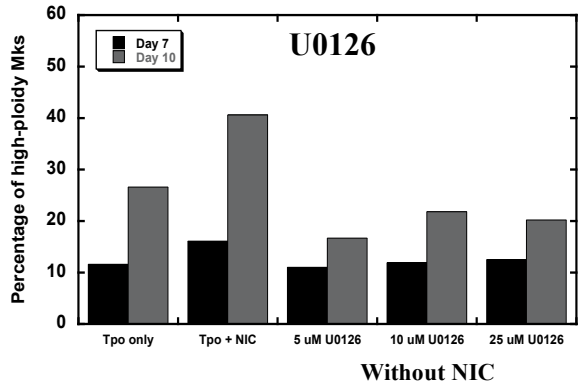
Day 7
Day 10
U0126
Percentage of high-ploidy Mks
Tpo only
Tpo + NIC
5 uM U0126
10 uM U0126
25 uM U0126
Without NIC

C

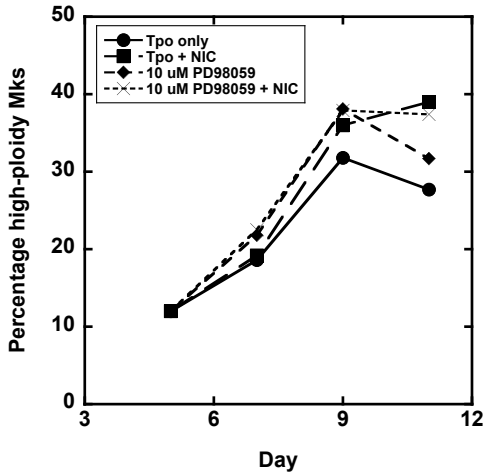
Tpo only
Tpo + NIC
10 uM PD98059
10 uM PD98059 + NIC
Percentage high-ploidy Mks
Day

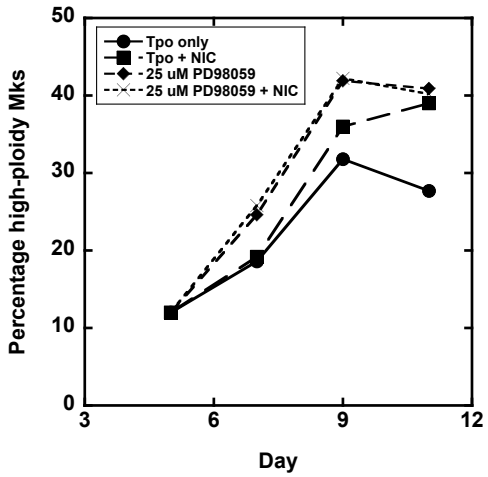
Tpo only
Tpo + NIC
25 uM PD98059
25 uM PD98059 + NIC
Percentage high-ploidy Mks
Day

3.3.6. NIC increases the level of intracellular NAD(H) and glucose metabolism in cultured primary Mks

Since NIC serves as a precursor for NAD^+ in various cell types, we measured the levels of NAD(H) [sum of NAD^+ and NADH] in primary human Mks cultured with Tpo only and Tpo + NIC (3 and 6.25 mM) at various time points in culture. NAD(H) was found to increase rapidly after the addition of NIC. Intracellular NAD(H) levels were ~3- to 6-fold higher in cells cultured with Tpo + 6.25 mM NIC compared to Tpo only after two days of NIC addition (Fig 3.9). Furthermore, the increase in NAD(H) was dose-dependent with the exception of one time point (Fig 3.9). NAD(H) levels were similar in cells cultured with both 3 and 6.25 mM NIC at day 7 in two separate biological experiments.

Figure 3.9. NIC increases the level of intracellular NAD(H) in primary human Mk cultures.

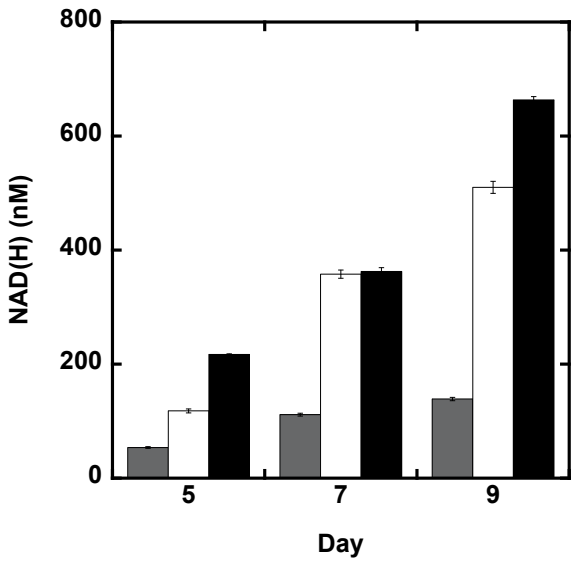

500,000 cells were sampled from Tpo only (gray), Tpo + 3 mM NIC (white), and Tpo + 6.25 mM NIC (black) cultures on days 5 (4 hours after NIC addition), 7, and 9. NAD(H) levels were determined using an enzymatic cycling assay. Data shows the average and SD of replicate samples and is representative of n = 4 for Tpo only and Tpo + 6.25 mM NIC cultures; n = 2 for Tpo + 3 mM NIC cultures.

We also measured glucose and lactate concentrations in the media of Tpo only and Tpo + NIC cultures to determine whether NIC altered the pattern of glucose consumption or the yield of lactate from glucose. Measurements were reported on a per cell volume basis to account for the increase in cell size with NIC. Overall, cells cultured with Tpo + NIC had increased glucose consumption (Fig 3.10A) and lactate production per cell volume (Fig 3.10B). However, the yield of lactate from glucose was lower in Tpo + NIC cultures compared to Tpo only after day 7 (Fig 3.10C).

Figure 3.10. Glucose and lactate metabolic quotients in Tpo only and Tpo + NIC cultures.

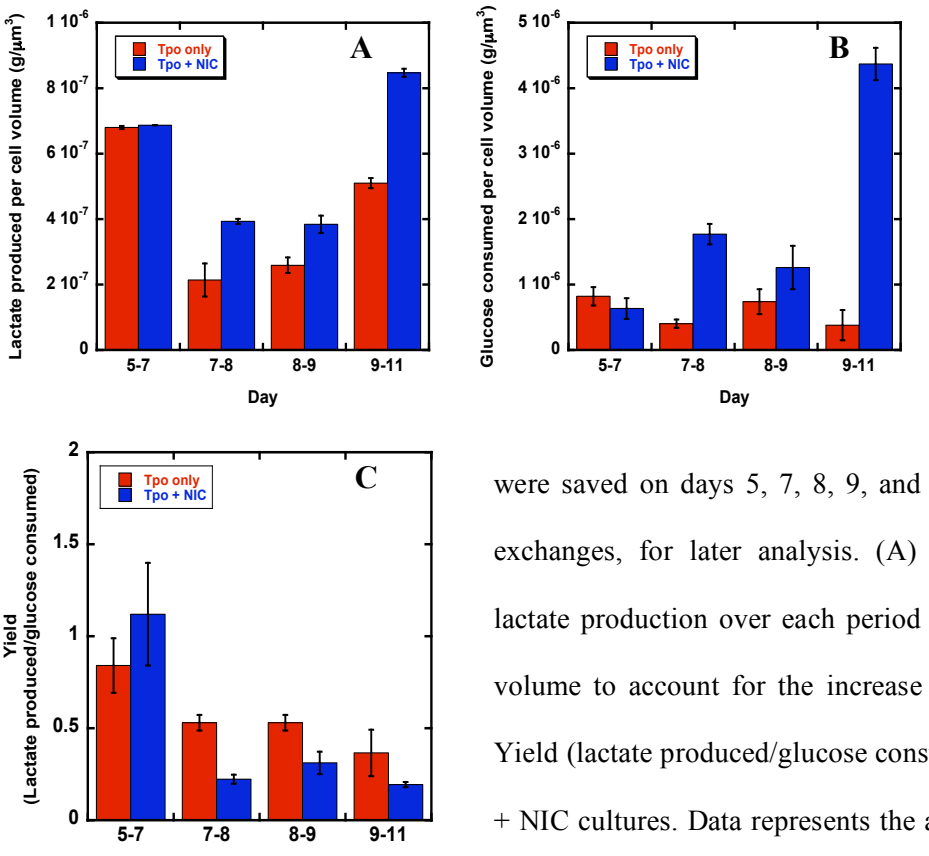

mPB CD34$^+$-selected cells were cultured with 100 ng/mL Tpo. Beginning on day 5, a portion of the cells was treated with 6.25 mM NIC. Media samples were saved on days 5, 7, 8, 9, and 11, before and after media exchanges, for later analysis. (A) Glucose consumption and lactate production over each period of time are shown per cell volume to account for the increase in cell size with NIC. (B) Yield (lactate produced/glucose consumed) in Tpo only and Tpo + NIC cultures. Data represents the average and SD of replicate measurements and is representative of 2 biological experiments.

3.3.7. Nicotinic acid is not an effective precursor for NAD(H) in cultured primary Mks

Nicotinic acid (NA), the other form of niacin, can also act as a precursor for NAD^+ and supplementation to cultures can increase the level of intracellular NAD^+ in various cell types.[57,58] If increased NAD levels are the mechanism by which NIC increases Mk ploidy, then a similar increase in NAD(H) levels from NA supplementation should also increase ploidy. Alternatively, if NA does not increase NAD(H) levels, then it would not be expected to increase Mk ploidy. Therefore, we characterized Mk maturation and NAD(H) levels in cells cultured with Tpo only or Tpo + either 3 mM or 6.25 mM NA. Doses greater than 6.25 mM were cytotoxic (data not shown). Mks from cultures with NA differentiated in a similar manner to cells cultured with Tpo only in terms of both CD41 expression and the percentage of high-ploidy Mks (Fig 3.11A). The level of intracellular NAD(H) increased only slightly by addition of either 3 mM or 6.25 mM NA (Fig 3.11B). Therefore, NA does not act as an effective NAD(H) precursor in cultured primary human Mks and does not increase Mk ploidy.

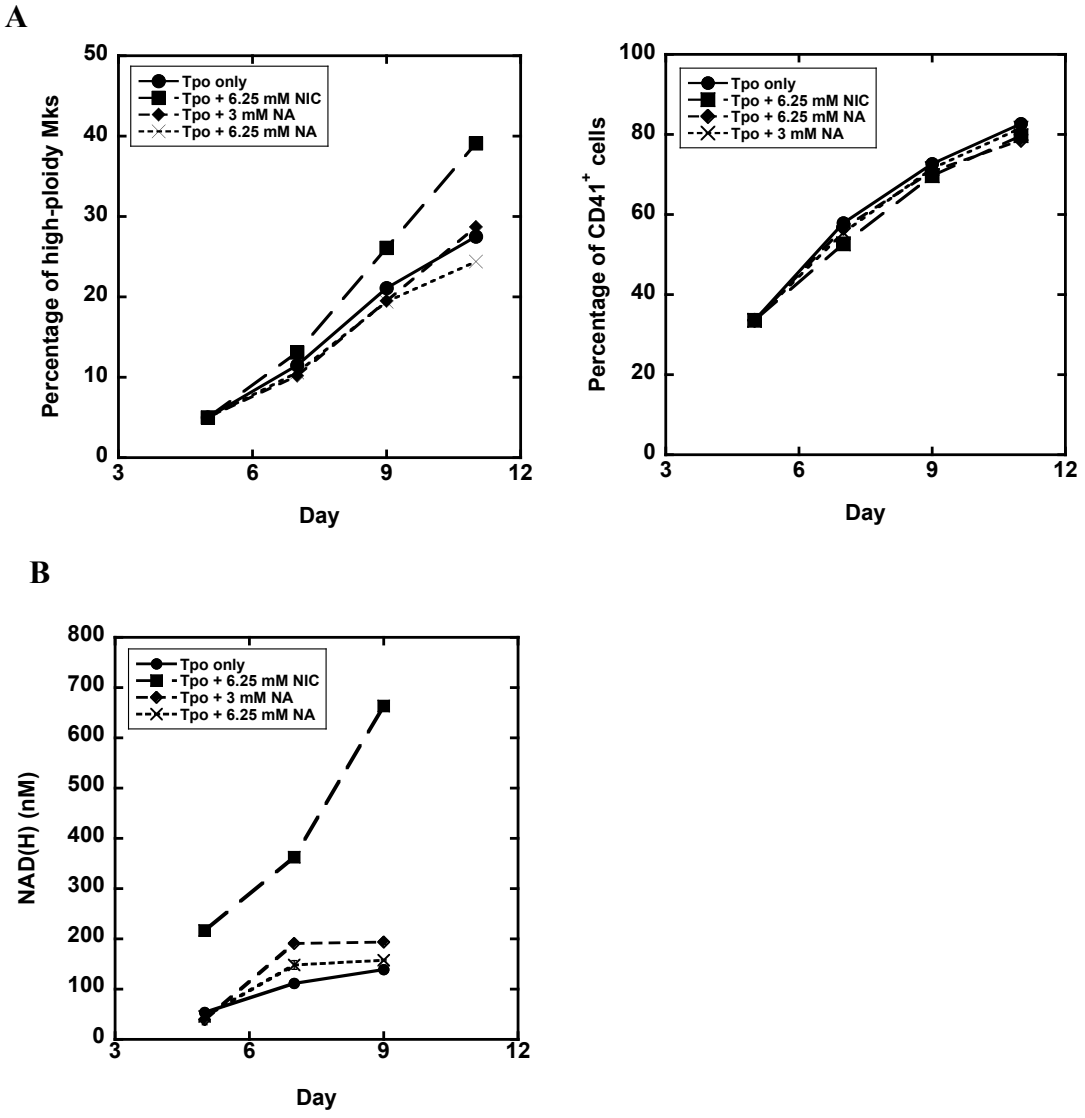

Figure 3.11. Nicotinic acid (NA) is not an effective precursor for NAD(H) in primary human Mks and has no effect on Mk ploidy.

mPB $CD34^+$-selected cells were cultured with 100 ng/mL Tpo. Beginning on day 5, cells were treated with either 6.25 mM NIC (squares), 3 mM NA (diamonds), or 6.25 mM NA (crosses). Cells cultured with Tpo only were used for a control (circles). (A) The percentage of high-ploidy Mks and $CD41^+$ cells was determined on days 5, 7, 9 and 11. (B) NAD(H) levels were measured on day 5 (4 hours after NIC/NA) addition, 7, and 9. Data shown is representative of n = 2 for NA cultures; n = 4 for Tpo only and Tpo + 6.25 mM NIC cultures.

3.3.8. Inhibition of NMPRTase in NIC-treated primary Mk cultures

In order to determine whether the increased NAD(H) levels resulting from NIC addition were responsible for enhanced Mk polyploidization, studies were carried out using APO866 – an inhibitor of nicotinamide phosphoribosyltransferase (NMPRTase), the enzyme that converts NIC to NAD^+. Doses of 1–10 nM APO866 have been found to inhibit NMPRTase in cancer cells.[130] We found that doses of 1 and 10 nM APO866 induced partial and complete cell death, respectively, in the megakaryocytic CHRF cell line after 4 days of culture, whereas CHRF cells treated with 0.1 nM APO866 remained healthy. Two days of APO treatment reduced the levels of intracellular NAD(H) almost completely in the CHRF cells (Fig 3.12A). At this time point there was no visible cell death for any of the doses.

A

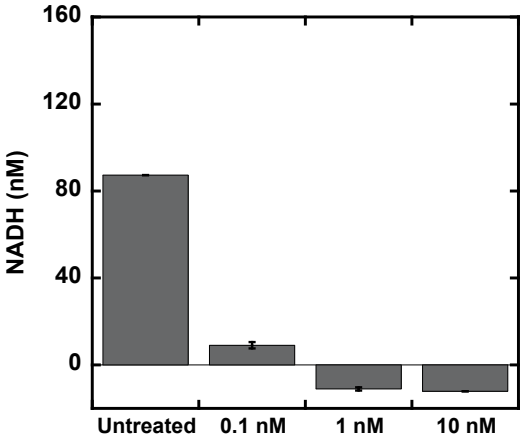

B

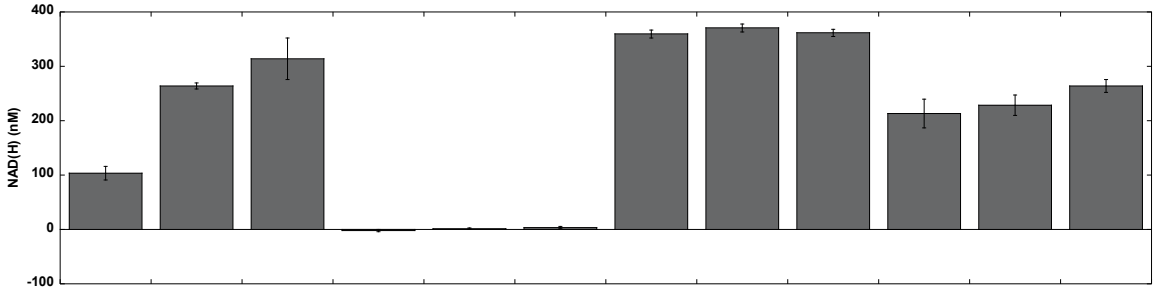

NIC (mM)	**0**	**3**	**6.25**	**0**	**0**	**0**	**6.25**	**6.25**	**6.25**	**3**	**3**	**3**
APO (nM)	**0**	**0**	**0**	**10**	**100**	**1000**	**10**	**100**	**1000**	**10**	**100**	**1000**

Figure 3.12. NAD(H) levels in CHRF cells treated with APO866.

(A) CHRF cells were treated with 0.1–10 nM APO866 for 48 hours before measuring NAD(H) levels using an enzymatic cycling assay. (B) NAD(H) levels with higher doses of APO866 (10–1000 nM) in CHRF cell cultures treated with either 3 or 6.25 mM NIC.

Based on the results of studies performed with CHRF cells, we next examined the effects of a wide range of concentrations of APO866 on primary human Mk differentiation. APO866 was added to Tpo only cultures on day 4 (12 hours prior to NIC addition; 0.05–10 nM APO866). On day 5, a portion of cells from each condition was treated with 6.25 mM NIC. In the primary Mk cultures, APO-treated Mks in Tpo only cultures started showing signs of decreased viability on day 7 of culture (1, 3, 10 nM conditions). Cells in cultures with 0.1 and 0.5 nM APO began to appear unhealthy on day 8, whereas cells treated with a dose of 0.05 nM APO866 remained viable. APO866 decreased the percentage of $CD41^+$ cells in a dose dependent manner (Fig 3.13A). On the other hand, cells treated with APO (0.05–10 nM) + 6.25 mM NIC remained healthy for the entire duration of culture and there was no difference between the percentage of high-ploidy Mks in APO + NIC and Tpo + NIC cultures (Fig 3.13B). NAD(H) levels were not measured in these cultures. Since high doses of NIC (10 mM) have been shown to reverse the effects of 10 nM APO866 in HepG2 cells,[130] it was likely that the 6.25 mM NIC concentration was too high and protected the cells against the effects of APO866.

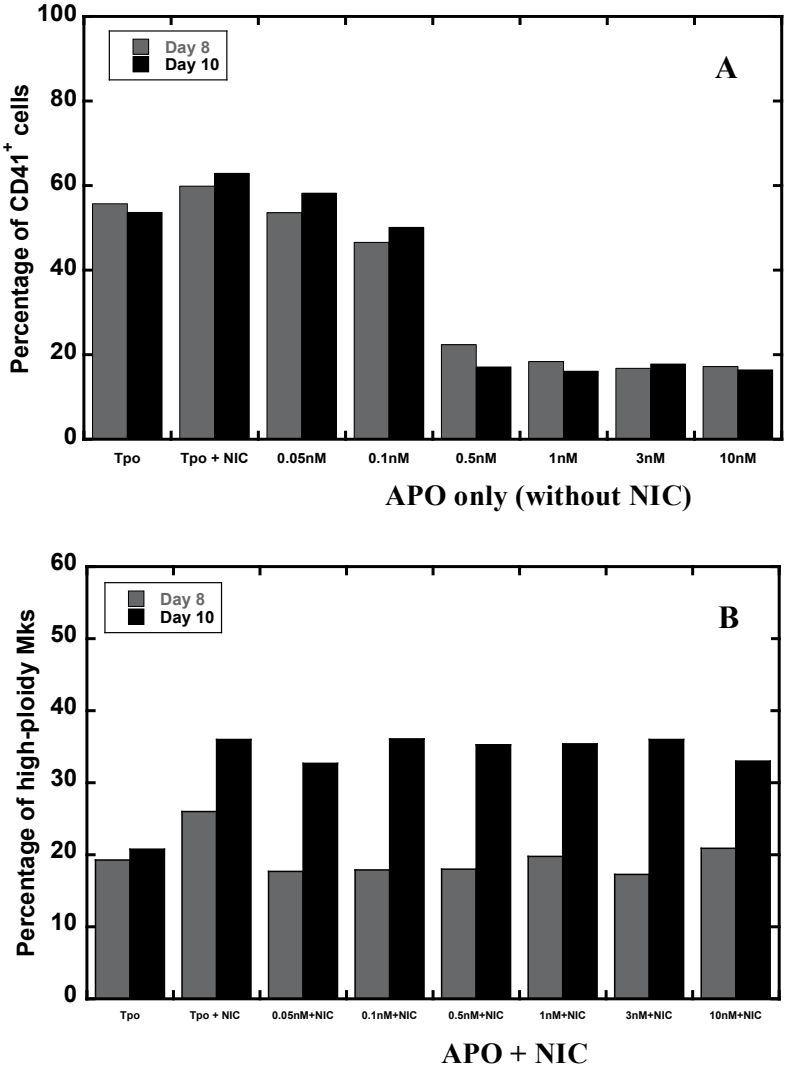

Figure 3.13. APO866 decreases the percentage of CD41$^+$ cells in Mk cultures.

mPB CD34$^+$-selected cells were cultured with 100 ng/mL Tpo. Beginning on day 4, a portion of the cells was treated with 0.05–10 nM APO866 and subsequently, 6.25 mM NIC was added on day 5. (A) Data shows the number of CD41$^+$ cells as a percentage of viable cells on days 8 (gray) and day 10 (black) in cells treated with APO only. (B) The percentage of high-ploidy Mks was similar in Tpo + NIC and APO + NIC cultures. The percentage of CD41$^+$ cells and high-ploidy Mks in Tpo only and Tpo + NIC cultures are included for comparison.

We next tested higher levels of APO866 (≥10 nM) in combination with decreased concentrations of NIC. We first carried out studies using the CHRF cell line and examined NAD(H) levels in CHRF cells treated with various concentrations of APO866 together with either 3 or 6.25 mM NIC. CHRF cells were seeded into 6-well plates and treated with 10–1000 nM APO866. Four to twenty fours after APO addition, cells were treated with either 3 or 6.25 mM NIC. Two days after the cultures were seeded, NAD(H) levels were measured using an enzymatic cycling assay. Untreated CHRF cells and CHRF cells treated with either APO or NIC alone were used as controls. The high levels of NAD(H) resulting from either 3 or 6.25 mM NIC could not be significantly reduced despite the very high concentrations of APO866 tested (Fig 3.12B). Due to the solubility of APO866, concentrations greater than 1000 nM would lead to cytotoxicity from the DMSO used to reconstitute the inhibitor.

Similar studies were also performed in primary Mk cultures. $CD34^+$ cells cultured with Tpo were treated with 10, 100, and 1000 nM APO866 together with either 3 or 6.25 mM NIC. APO decreased NAD(H) levels in cells cultured with Tpo only at all concentrations tested (Fig 3.14A). However, doses of 10–1000 nM APO866 were cytotoxic when NIC was not present. Therefore, NAD(H) was only measured on day 5 of the Tpo + APO cultures. NIC increased the level of intracellular NAD(H) in a dose-dependent manner. After 4 hours, the level of intracellular NAD(H) was increased by 2- and 4- fold with 3 and 6.25 mM NIC, respectively (Fig 3.9). The high concentrations of APO were able to reduce the NAD(H) levels in cells treated with either 3 or 6.25 mM NIC at the early time point (4 hours after NIC) (Fig 3.14B). However, by day 7, cells in the APO + NIC and NIC-only cultures had the same level of NAD(H). NAD(H) levels were reduced at day 9, likely due to a media exchange that was performed on day

7 to replace the inhibitor and NIC. Mk differentiation, as characterized by CD41 expression and percentage of high-ploidy Mks, was similar between NIC-only and APO + NIC cultures (Fig 3.14C-D).

Figure 3.14. NIC addition to primary Mk cultures treated with APO866.

Human mPB $CD34^+$-selected cells were cultured with 100 ng/mL Tpo. On day 4, cells were treated with 10 nM (green), 100 nM (black), or 1000 nM (gray) APO866. On day 5, either 3 or 6.25 mM NIC (blue) was added to the cultures. Tpo only cultures (red) were used as a control. Half-media exchanges were performed on days 7 and 9. (A) After one day of culture with APO, NAD(H) levels were completely reduced. (B) Levels of intracellular NAD(H) in APO + NIC cultures. Mk cultures were characterized for their percentage of (C) high-ploidy Mks, (D) $CD41^+$ cells, and (E) total-cell fold-expansion.

A

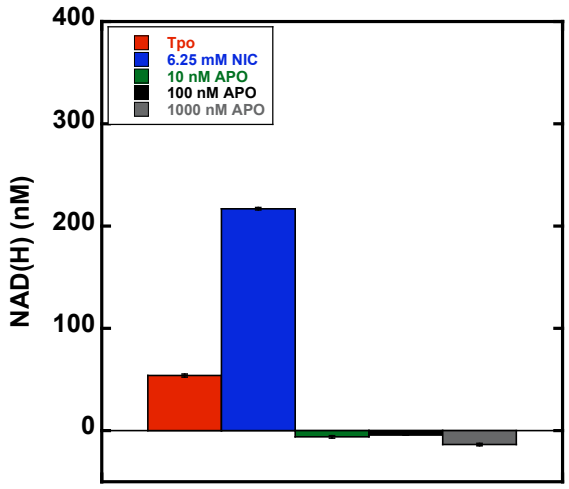
Tpo
6.25 mM NIC
10 nM APO
100 nM APO
1000 nM APO
NAD(H) (nM)
400
300
200
100
0

B

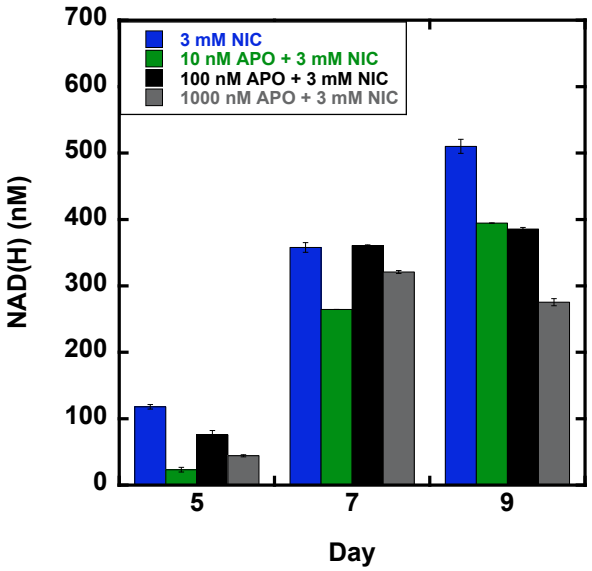
3 mM NIC
10 nM APO + 3 mM NIC
100 nM APO + 3 mM NIC
1000 nM APO + 3 mM NIC
NAD(H) (nM)
700
600
500
400
300
200
100
0
5
7
9
Day

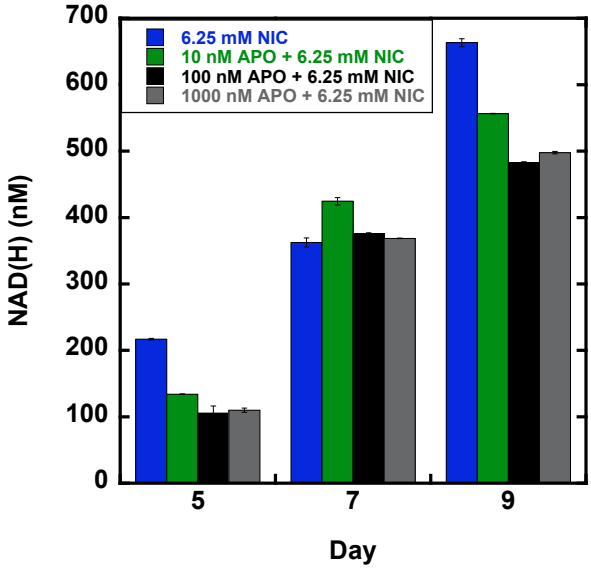
6.25 mM NIC
10 nM APO + 6.25 mM NIC
100 nM APO + 6.25 mM NIC
1000 nM APO + 6.25 mM NIC
NAD(H) (nM)
700
600
500
400
300
200
100
0
5
7
9
Day

C

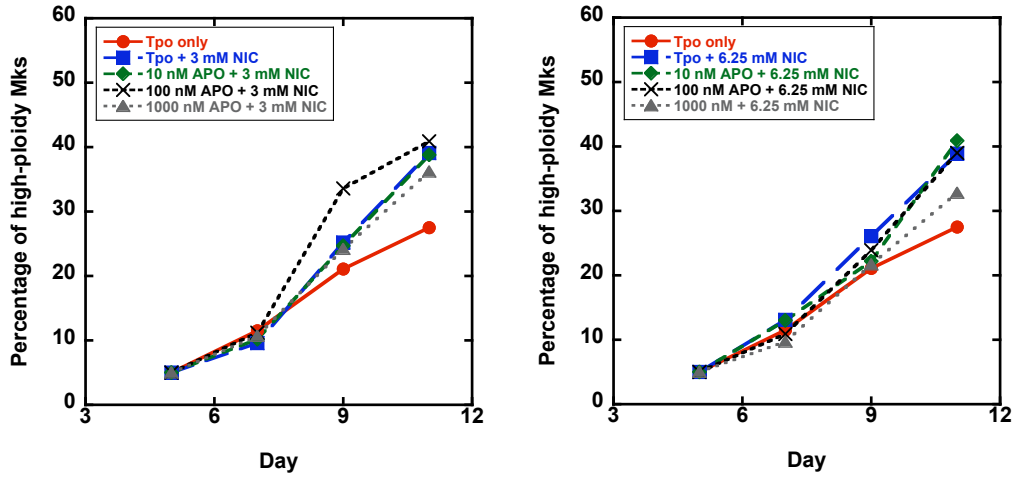
Tpo only
Tpo + 3 mM NIC
10 nM APO + 3 mM NIC
100 nM APO + 3 mM NIC
1000 nM APO + 3 mM NIC
Percentage of high-ploidy Mks
Day
Tpo only
Tpo + 6.25 mM NIC
10 nM APO + 6.25 mM NIC
100 nM APO + 6.25 mM NIC
1000 nM + 6.25 mM NIC
Percentage of high-ploidy Mks
Day

D

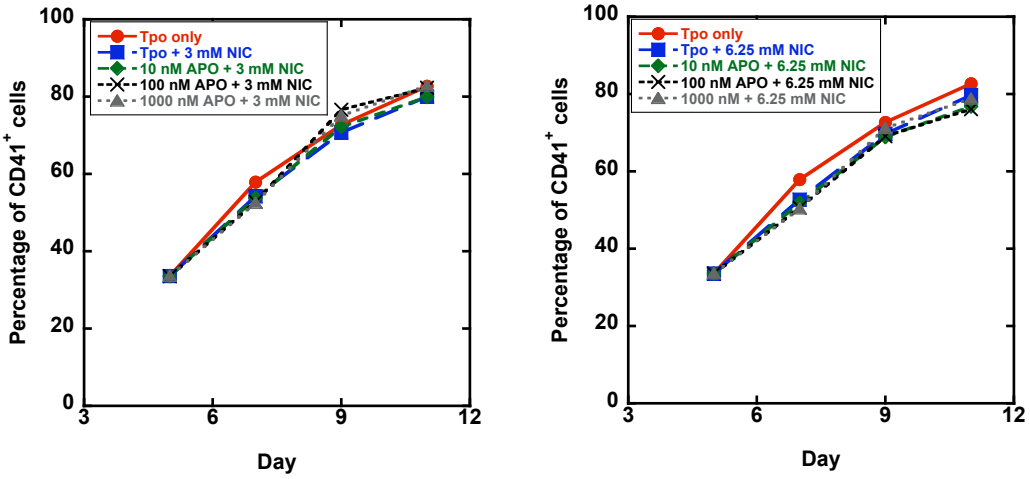
Tpo only
Tpo + 3 mM NIC
10 nM APO + 3 mM NIC
100 nM APO + 3 mM NIC
1000 nM APO + 3 mM NIC
Percentage of CD41+ cells
Day
Tpo only
Tpo + 6.25 mM NIC
10 nM APO + 6.25 mM NIC
100 nM APO + 6.25 mM NIC
1000 nM + 6.25 mM NIC
Percentage of CD41+ cells
Day

E

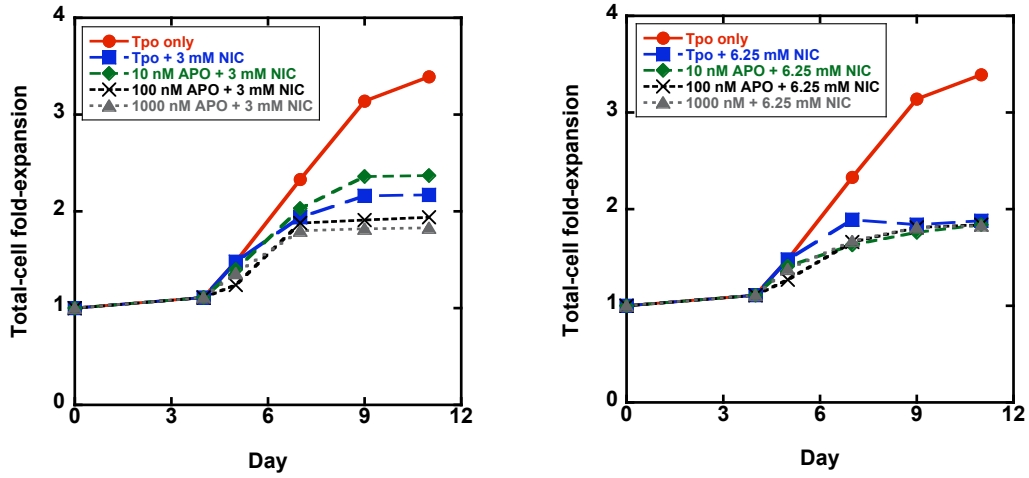
Tpo only
Tpo + 3 mM NIC
10 nM APO + 3 mM NIC
100 nM APO + 3 mM NIC
1000 nM APO + 3 mM NIC
Total-cell fold-expansion
Day
Tpo only
Tpo + 6.25 mM NIC
10 nM APO + 6.25 mM NIC
100 nM APO + 6.25 mM NIC
1000 nM + 6.25 mM NIC
Total-cell fold-expansion
Day

Since this study suggested that more frequent inhibitor replacement may maintain the reduced NAD(H) levels, cultures were then performed in which APO866 was repeatedly added to cultures to ensure levels were not lowered due to degradation. Full media exchanges were performed each day of culture. Tpo only and Tpo + NIC cultures were handled in a similar manner to provide control cultures. Again, NAD(H) levels were reduced with APO at the early time point (4 hours after NIC addition). However, by day 7 NAD(H) levels in APO + NIC cultures were similar to that of cells cultured with Tpo + NIC (Fig 3.15A). As anticipated, the percentage of high-ploidy Mks was also similar between Tpo + NIC cultures with or without APO (Fig 3.15B), as was the percentage of $CD41^{+}$ cells (Fig 3.15C).

In summary, the level of NIC that is needed to increase Mk ploidy results in such high NAD(H) levels that it cannot be significantly reduced using APO866 (1–1000 nM). Further studies can be performed to (1) determine the lowest possible NIC concentration that increases Mk ploidy and (2) characterize its effects in Mk cultures with APO866. Alternatively, we can test whether repeated addition of 100 nM APO without medium exchange is capable of reducing NAD(H) levels and Mk ploidy.

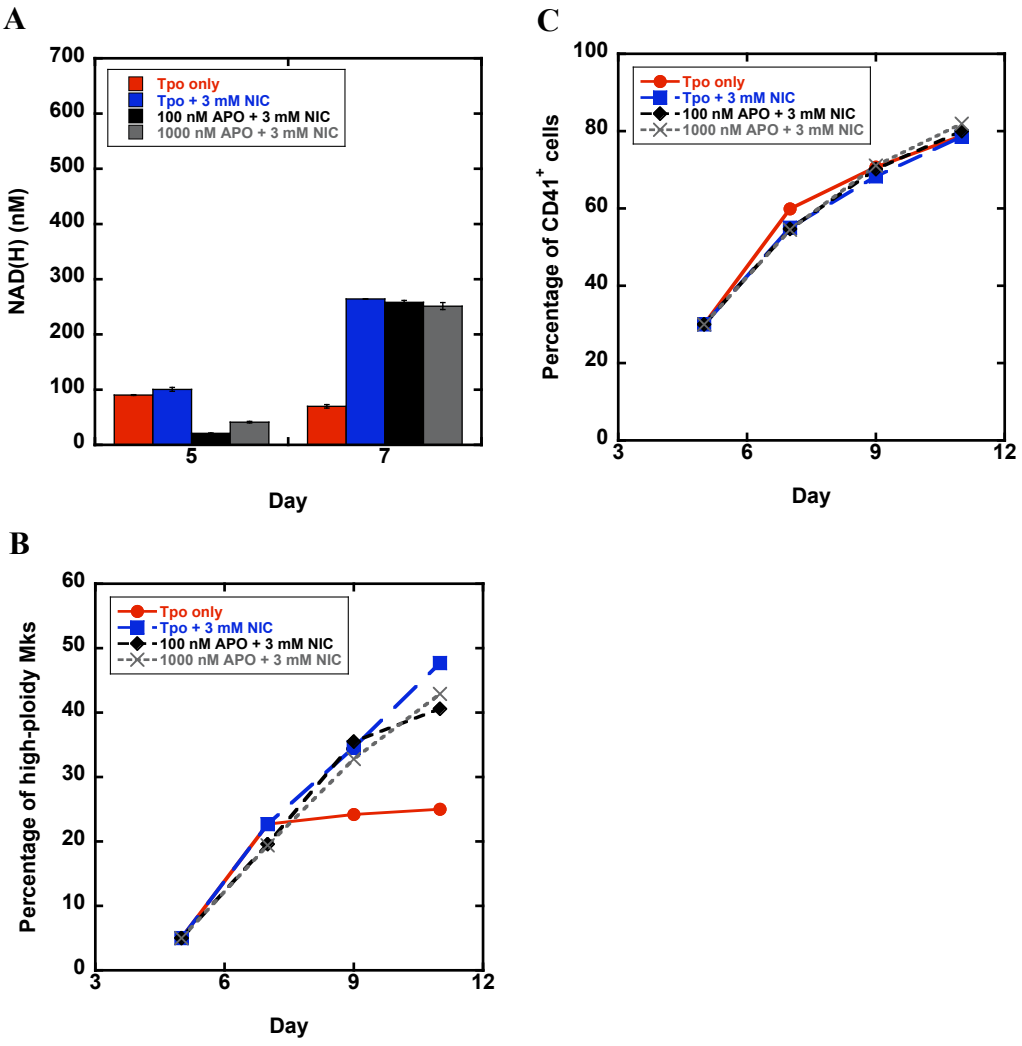

Figure 3.15. NIC addition to primary Mk cultures treated with APO866 – repeated replacement of APO866.

Human mPB $CD34^+$-selected cells were cultured with 100 ng/mL Tpo. On day 4, cells were treated with 100 nM (black) or 1000 nM (gray) APO866. On day 5, either 3 or 6.25 mM NIC was added to the cultures. Cells receiving Tpo- (red), APO-, or NIC-only (blue) were used for controls. Full media exchanges were performed every day beginning on day 5 to replace APO866. (A) Levels of intracellular NAD(H) in APO + NIC cultures. Mk cultures were characterized for their percentage of (B) high-ploidy Mks and (C) $CD41^+$ cells.

3.4. Discussion

In the present study, we provide insight as to the mechanism by which NIC enhances Mk maturation. Given the primary role of Tpo in Mk development, it is likely that NIC effects are due at least in part to modulation of Tpo-mediated signal transduction. We have previously demonstrated that nicotinamide (NIC) increases polyploidization and proplatelet formation in primary and murine Mk cultures with Tpo only (Chapter 2).[109] Additional studies demonstrate that these effects are also observed in primary human Mks cultured under a variety of Mk-promoting conditions containing Tpo. NIC increased the percentage of high-ploidy Mks by 1.5-, 1.5-, and 1.3-fold in cultures with Tpo + stromal cell derived factor 1α, a cocktail of cytokines [Tpo (50 ng/mL), SCF (10 ng/mL), IL-3 (0.005 ng/mL), IL-6 (10 ng/mL)], and in Mks cultured with Tpo on fibronectin-coated surfaces, respectively (Section 6.2.1). NIC also increased polyploidization in Tpo-dependent primary G1ME murine cells that are deficient of the transcription factor GATA1 (Section 6.2.3). Interestingly, we found that NIC appears to act independent of Tpo and can increase Mk ploidy in cells cultured with a cytokine combination of IL-3, IL-6 and SCF. However, Tpo must be present in order to achieve the full effects of NIC on Mk ploidy. Cocktail cultures that are treated with NIC on day 5 only reach a maximum DNA content of 8N, whereas if Tpo is added in combination with NIC, Mks have DNA histograms resembling cells from Tpo + NIC cultures where the maximum DNA content is 32N. Therefore, NIC appears to synergize with Tpo to enhance Mk maturation.

The binding of Tpo to its receptor, Mpl, activates multiple signaling cascades including Ras/MAPK. The MAPKs ERK1 and ERK2 are rapidly phosphorylated after exposure to Tpo and are key regulators of cell proliferation, differentiation, and survival. We have found that ERK

and its downstream target RSK1 are activated to a greater extent in cells cultured with NIC. We attempted to use pharmacological inhibitors to prevent the increase in ERK activation resulting from NIC addition in order to determine whether the increase was responsible for enhanced polyploidization. However, these studies were inconclusive due to an apparent lack of inhibitor specificity. In our hands, PD98059 increased Mk ploidy, while U0126 resulted in a small decrease in the number of high-ploidy Mks. Further studies with U0126 in cultures with Tpo + NIC may prove useful (Section 5.2.2.2). Unfortunately, until additional studies are performed, it is not possible to conclude whether the increased pERK levels are a cause or consequence of NIC increases in Mk ploidy. Alternative methods with greater specificity such as RNAi (Section 5.2.2.1) should be examined in order to fully characterize the role of ERK in NIC-mediated Mk maturation.

Tpo has also been shown to signal through the phosphatidylinositol 3-kinase (PI3K)/Akt pathway.[51,129,131] Signaling through PI3K/Akt is important for the regulation of cell cycle progression and modulates many cell cycle regulatory proteins, such as p21, p27, cdc25B and GSK3. Activated Akt also increases the post-translational stability of cyclins[132] and can function to promote cell survival; for example, via phosphorylation and inactivation of the pro-apoptotic factors Bad and caspase-9.[133] Separately, NIC has been shown in other cell types to increase Akt signaling.[45,46] However, we found the level of pAKT to be unchanged with NIC addition in both starved cells and cells sampled from long-term cultures. Moreover, expression of pmTOR, which is primarily activated by Akt, was similar in Tpo only and Tpo + NIC cells. Therefore, Akt does not likely play a role in the effects of NIC on Mk maturation.

NIC is known to act as a precursor for NAD^+ both *in vitro* and *in vivo* and has been shown to increase the level of intracellular NAD^+ in cultured cells by as much as 40% after 3 hours and up to 3-fold after 48 hours.[52-54] We found a similar increase in the level of NAD(H) when NIC was added to cultures of primary human Mks. Moreover, the increase in NAD(H) levels was dose-dependent with NIC. Interestingly, cultured Mks were not able to use nicotinic acid, the other form of niacin, as a precursor for NAD(H) and NA did not increase Mk ploidy. Other cell types (HepG2) have also been shown to have a preference for NIC as a substrate for NAD^+ generation.[130]

In order to determine whether the increased NAD(H) levels were responsible for the ability of NIC to enhance Mk polyploidization, cultures were performed with APO866 (also known as FK866) – an inhibitor of NMPRTase, the enzyme that converts NIC to NAD^+.[130] Here we showed that very low concentrations ($\geq$ 0.1 mM) of APO866 in the absence of NIC completely reduced NAD(H) levels and gradually induced cell death in cultured primary Mks. This was reflected in a dose-dependent decrease in the percentage of $CD41^+$ cells. APO alone did not appear to directly affect Mk polyploidization – DNA histograms were similar to those in untreated cultures. However, the percentage of high-ploidy Mks was reduced as a consequence of decreased cell viability. Interestingly, thrombocytopenia has been found as a side effect of APO866 administration in recent clinical trials,[134] suggesting that intracellular NAD^+ levels may play a role in Mk differentiation and platelet production. Unfortunately, APO866 was not capable of lowering the high NAD(H) levels associated with the concentrations of NIC necessary to enhance Mk ploidy. Thus, as may be expected, APO + NIC cultures contained a similar percentage of high-ploidy Mks as those treated with NIC alone. Further studies are necessary to

determine if reducing the NIC concentration would enable the APO to sufficiently lower NAD(H) levels in APO + NIC cultures and examine whether Mk polyploidization was decreased as a result (Section 5.2.2.2).

The increased NAD(H) levels from NIC addition could have several possible downstream consequences due to the multiple functions of NAD within cells. Increased levels of NAD(H) could affect NAD^+-dependent enzymes such as poly ADP-ribose polymerase (PARP)[135] and Sir2.[136] However, we have shown previously that the addition of various PARP and Sir2 inhibitors do not reproduce the effects of NIC on Mk maturation (Chapter 2).[109] Increased NAD^+ levels have also been implicated in altering the binding of p53 to the promoter DNA of select p53 target genes, including mdm2 and PIG3.[52] Since p53 is responsible for the prevention of aneuploidy and rereplication,[59] this might suggest a role for NAD^+ in modulating NIC effects on Mk DNA content via p53. Studies by others in our group demonstrate that siRNA-mediated knock-down of p53 in PMA-stimulated CHRF cells leads to an increase in both polyploidization and viability.[137] Preliminary studies have found p53 activity to be increased in Tpo + NIC Mks (Section 6.2.2); however, this data has yet to be replicated. Further studies may reveal a role of p53 in NIC-mediated increases in Mk ploidy (Section 5.2.2.3).

In summary, both Tpo-mediated signaling and the level of intracellular NAD(H) appear to have a role in the ability of NIC to increase Mk ploidy. Further studies are necessary to understand the importance of NAD(H) in Mk maturation.

3.5. Acknowledgements

I thank Jan Kemper for her help in performing the NAD(H) measurements. I am also thankful to James King for many helpful conversations regarding intracellular flow protocols and to Genentech for their donation of Tpo. I thank Peter Fuhrken for creating the pathway diagrams presented in Figures 3.1 and 3.6.

4. CHAPTER 4: Effects of nicotinamide on hematopoietic stem cell differentiation towards other lineages (erythrocytic and granulocytic)

4.1. Introduction

Myelodysplastic syndromes (MDS) encompass a heterogeneous group of malignant clonal stem cell disorders characterized by ineffective hematopoiesis, and constitute a significant clinical problem with increasing incidence.[138-140] Increased progenitor apoptosis early in the course of the disease results in low peripheral blood counts for one or more blood cell types. About 60% of MDS patients are thrombocytopenic. Chronic platelet transfusion is complicated by the development of allogeneic antibodies and approximately 30% of MDS patients die of bleeding. Increased endogenous platelet production could extend the lifespan (and increase the quality of life) for a substantial fraction of MDS patients by rescue from and/or delayed onset of clinically significant thrombocytopenia.

MDS is characterized by defective megakaryocyte (Mk) development that results in the formation of atypical "micromegakaryocytes".[141] Micromegakaryocytes are smaller in size than normal Mks and show impaired polyploidization. They have diameters up to 20 μm and a peak ploidy of 4N or 8N, as compared to normal Mks that have a diameter of 25-35 μm and mean ploidy of 16N,[142] and also often exhibit hypogranulation. Abnormal Mk maturation in MDS has also been demonstrated *in vitro*. Mk colony (CFU-Mk) formation from MDS-patient bone-marrow MNCs is reduced compared to normal bone marrow.[143] It has been hypothesized that decreased platelet production by abnormal Mks is partly responsible for the peripheral thrombocytopenia associated with MDS.[144] Besides low platelet counts, MDS patients often exhibit circulating platelets with defective activity.[145] Treatment with the Src kinase inhibitor

SU6656 has been shown to increase Mk ploidy in *in vitro* cultures of both normal and MDS bone marrow samples,[25] suggesting that normal levels of polyploidization can be restored in MDS Mks with appropriate treatments.

We have discovered that nicotinamide (NIC, one form of vitamin B3) greatly increases the *in vitro* maturation of human Mks derived from mobilized peripheral blood $CD34^+$ cells (Chapter 2). NIC-treated Mks are larger in size, reach higher ploidy levels, and have increased proplatelet formation compared to cells cultured with Tpo only. As a result, we hypothesize that NIC may increase Mk ploidy in MDS patients (Section 5.3.2.2). Since Mk ploidy directly correlates with platelet production,[14] we also hypothesize that NIC could be used to increase platelet production in MDS patients. However, prior to *in vivo* administration of NIC, it is important to understand the effect of NIC on cells from other hematopoietic lineages. Therefore, we have begun preliminary studies to examine the effects of NIC on erythrocytic and granulocytic maturation. We demonstrate that in addition to enhancing Mk polyploidization and proplatelet formation, NIC also increases erythroid maturation. NIC does not appear to alter granulocyte differentiation beyond significant inhibition of cell expansion. Additional studies to replicate these findings and further characterize the effects of NIC on erythroid differentiation are needed (Section 5.3.2.1).

4.2. Materials and Methods

4.2.1. Human erythroid (E) culture

Unless otherwise noted, all reagents were obtained from Sigma-Aldrich (St. Louis, MO). Cultures were initiated with previously frozen human mobilized peripheral blood (mPB) $CD34^+$ cells (AllCells; Berkeley, CA). Cells were cultured in T-flasks and maintained at a density of 100,000–400,000 cells/mL with a constant liquid depth of 0.33 cm. Cultures were performed using HLTM media (prepared as described in Sandstrom *et al.*[146]) containing Epo (3 U/mL; Amgen), SCF (50 ng/mL; Amgen), IL-3 (5 ng/mL; Peprotech), and IL-6 (10 ng/mL; Peprotech) with the initial pH adjusted to 7.4 with NaOH or HCl. Beginning at either day 3, 6, or 9, cells were continuously treated with 6.25 mM NIC. Cells not receiving NIC were used as a control. When needed, the cell concentrations were reduced by dilution with fresh media containing cytokines and 6.25 mM NIC if applicable. Cells were incubated at 37°C in a fully humidified atmosphere of 5% CO_2 and 95% air. Only one biological experiment was conducted.

4.2.2. Human granulocyte (G) culture

Cultures were initiated with previously frozen human mPB $CD34^+$ cells (AllCells; Berkeley, CA). Cells were cultured in T-flasks and maintained at a density of 30,000–300,000 cells/mL with a constant liquid depth of 0.33 cm. Cultures were performed using HLTM media containing IL-3 (10 ng/mL; Peprotech), IL-6 (10 ng/mL; Peprotech), SCF (50 ng/mL; Amgen), and G-CSF (10 ng/mL; Amgen) with the initial pH adjusted to 7.1 with NaOH or HCl. Due to the short half-life, 10 ng/mL G-CSF was added to cultures every 2 days. Beginning at either day 3, 6, or 9, cells were continuously treated with 6.25 mM NIC. Cells not receiving NIC were used

as a control. When needed, the cell concentrations were reduced by dilution with fresh media containing cytokines and 6.25 mM NIC if applicable. Cells were incubated at 37^{o}C in a fully humidified atmosphere of 5% CO_2 and 95% air. Only one biological experiment was conducted.

4.2.3. Colony assays

MethoCult media (Stem Cell Technologies) was prepared as instructed by the manufacturer. GM-CSF (Peprotech), G-CSF (Amgen), IL-6 (Peprotech), Epo (Amgen), SCF (R&D Systems), IL-3 (Peprotech), and ~1000 cell/mL was added to 4 mL of MethoCult media. One mL aliquots of MethoCult containing cells and cytokines was dispensed in duplicate gridded-35 mm petri dishes (Nunc). Dishes were incubated at 37^{o}C in a fully humidified atmosphere with 5% CO_2, 5% O_2 in N_2. After 14 days, plates were scored for erythroid (CFU-E), granulocyte, and monocyte (CFU-G+M) colonies using a dark-field stereomicroscope.

Colony assays were performed for 3 biological experiments. Cells were sampled from Tpo only cultures on day 0 or 1 and on day 3. Cells were put into the colony assay with or without 6.25 mM NIC. In Experiments 1 and 2, an equal number of cells were put into untreated and NIC-treated assays. Since NIC inhibits cell growth, assays without NIC contained higher cell numbers and led to pH differences of the MethoCult media between assays with and without NIC. pH has been shown to be an important regulator of erythroid differentiation.[147] Therefore, in Experiment 3, the input cell numbers were adjusted in attempt to obtain an equal number of cells per plate in conditions with and without NIC. Images of erythroid colonies were obtained with a Leica DM IL inverted contrasting microscope (Heidenheim, Germany) fitted with a SPOT

Insight 2MP Firewire Color Mosaic camera (Diagnostic Instruments; Sterling Heights, MI). Images were captured using SPOT software (Diagnostic Instruments).

4.2.4. Culture characterization

4.2.4.1. Flow cytometric detection of surface marker expression

Cells were washed with phosphate-buffered saline (PBS) containing 2 mM EDTA and 0.5% bovine serum albumin (BSA) [PEB], incubated with fluorophore-conjugated antibodies (Becton Dickinson; San Jose, CA) for 30 minutes at room temperature: G cultures – CD66b-FITC, CD11b-PECy5, CD15-FITC, CD34-APC; E cultures – GlyA-PE, CD71-FITC, CD34-APC. Cells were then analyzed on a Becton Dickinson LSRII flow cytometer using FACSDiva software (Becton Dickinson). DAPI was added to samples to give a final concentration of 1.4 μg/mL shortly prior to acquisition to exclude dead cells.

4.2.4.2. Benzidine staining

Cells expressing hemoglobin were identified by benzidine staining according to the methods described by Lam *et al*.[148] Briefly, 100,000 cells were harvested from each erythroid culture and were washed two times with cold PBS. Cells were resuspended in 27 μL of PBS and 3 μL of benzidine solution (2% benzidine in 0.5 M acetic acid) was added. 1 μL of 30% H_2O_2 was then added and cells were incubated at room temperature for 5–10 minutes. Cells were transferred to a hemacytometer and the number of positive (blue) cells were enumerated and expressed as a percentage of the total number of cells counted.

4.3. Results

4.3.1. NIC enhances erythroid differentiation

mPB CD34$^+$-selected cells were cultured in HLTM containing IL-3, IL-6, SCF and Epo to induce erythroid differentiation. NIC was added to the cultures at various time points (days 3, 6, and 9). In general, erythrocytes are more proliferative than Mks. Untreated cells reached ~1200-fold expansion (Fig 4.1) compared to Tpo only Mk cultures where ~5-fold total-cell expansion is typically obtained (Fig 2.6). NIC inhibited erythrocyte expansion, and the level of growth inhibition was dependent on the day of NIC addition. Addition of NIC on days 3, 6, and 9 reduced cell growth ~31-, 27-, and 10-fold, respectively, from untreated cells (day 19).

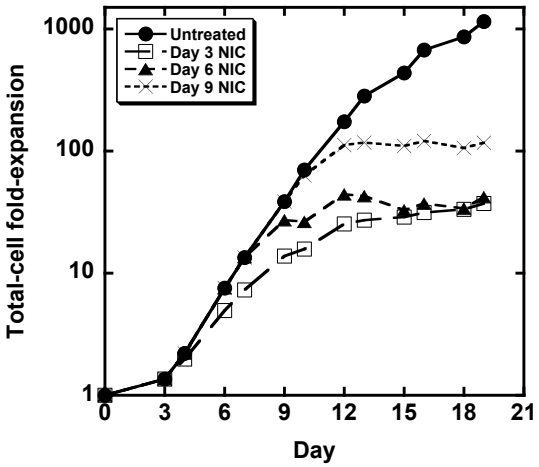

Figure 4.1. Total-cell fold-expansion of erythroid cultures with and without 6.25 mM NIC.

mPB CD34$^+$-selected cells were cultured with IL-3, IL-6, SCF and EPO. Total-cell fold-expansion was determined for cultures in which 6.25 mM NIC was added beginning on either day 3 (open squares), day 6 (triangles), or day 9 (crosses). Untreated cultures were included for controls (circles). Only one biological experiment was performed.

NIC enhanced erythroid differentiation. Cells lost expression of the primitive marker CD34$^+$ more rapidly (Fig 4.2A). In the untreated culture, the percentage of CD34$^+$ cells declined from 100 to 20% over the duration of 19 days. In contrast, the percentage

of $CD34^+$ cells had already dropped to 20% by day 12 in cultures treated with NIC (day 3 and 6 addition). The day 3 NIC-treated culture also reached its maximum percentage of $GlyA^+$ cells more quickly compared to untreated cells (Fig 4.2B). Untreated cultures contained ~60% of $GlyA^+$ cells on day 12 compared to day 9 for cultures with day 3 NIC addition. Cultures with day 3 NIC addition also contained an ~2-fold greater percentage of benzidine positive cells, a marker for hemoglobin production (Fig 4.2C). Similarly, erythroid colonies were redder in color with NIC, which is an indication of greater hemoglobin expression (Fig 4.3A). The number of CFU-E was not significantly affected when NIC was added to the assay (Fig 4.3B); however, colonies were much smaller with NIC present (Fig 4.3A). CD71, the transferrin receptor, is present on early erythroid cells but is lost as reticulocytes differentiate into mature erythrocytes. The percentage of $CD71^+$ cells in untreated cultures only declined from 90 to 85% during days 6 through 19, whereas NIC-treated cultures lost CD71 expression much more rapidly, decreasing to 30-35% by day 19 (Fig 4.2D). This is additional evidence of increased maturation with NIC. However, erythrocytes cultured with NIC also appeared to lose viability more rapidly compared to untreated cells (data not shown). This is reflected by a decrease of the percentage of $GlyA^+$ cells towards the end of culture and may be the result of more rapid maturation with NIC.

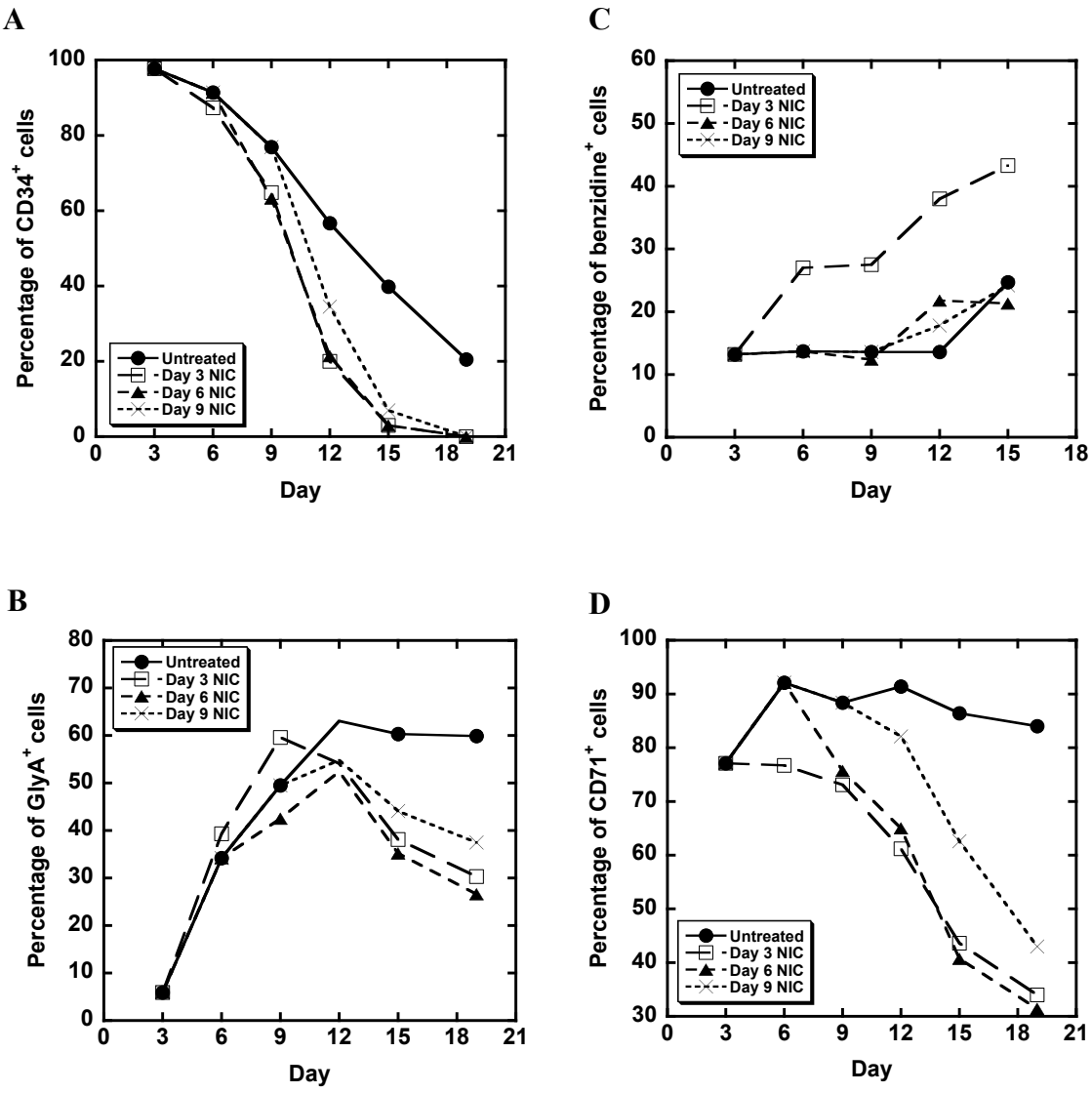

Figure 4.2. Expression of erythroid surface markers in NIC-treated cultures.

mPB $CD34^+$-selected cells were cultured with IL-3, IL-6, SCF and EPO. Beginning on either day 3 (open squares), day 6 (triangles), or day 9 (crosses), 6.25 mM NIC was added to the culture. Cells receiving no NIC were included as a control (circles). The percentage of (A) $CD34^+$ and (B) $GlyA^+$ cells was assessed using flow cytometry and is shown as the percentage of viable ($DAPI^-$) cells. (C) The percentage of cells staining positive for hemoglobin expression were determined using benzidine staining. (D) The percentage of $CD71^+$ cells decreases more rapidly in cultures with NIC. Only one biological experiment was performed.

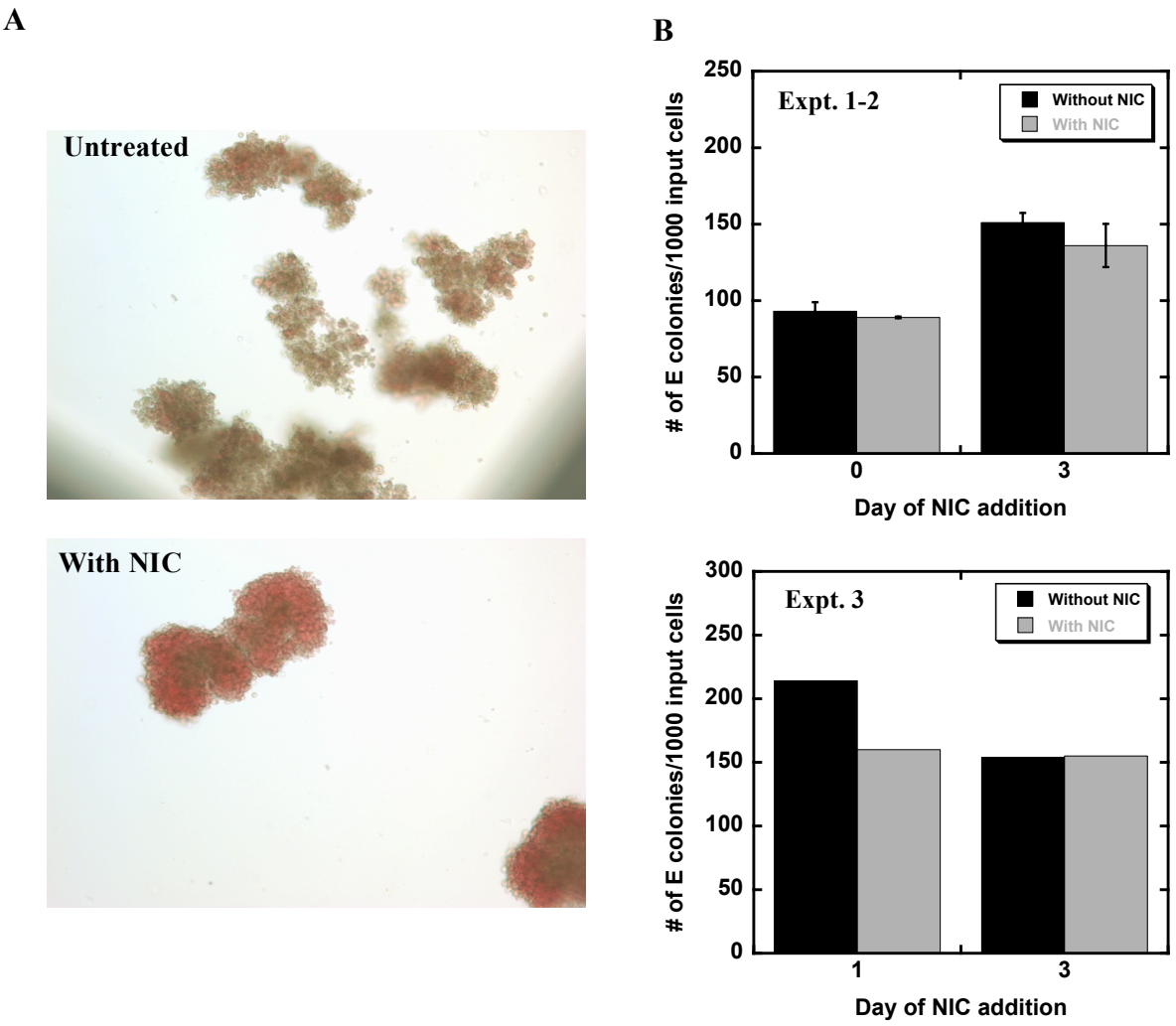

Figure 4.3. Effect of NIC on erythroid colony formation.

Cells were sampled from Tpo only cultures on either day 0 or 1 and on day 3 and put into colony assays containing a combination of cytokines. CFU-E were enumerated 14 days after assays were initiated. A total of 3 biological experiments were performed: Expts 1 & 2 – an equal number of cells were put into the assay with and without NIC; Expt 3 – the input number of cells was adjusted to account for growth inhibition with NIC. (A) Images of erythroid colonies (day 0 NIC addition) demonstrating smaller and redder colonies with NIC. (10x magnification) (B) NIC did not alter the total number of erythroid colonies formed per input cell.

4.3.2. NIC inhibits granulocyte expansion, but does not appear to alter differentiation

mPB CD34$^+$-selected cells were cultured in HLTM containing IL-3, IL-6, SCF and G-CSF to induce granulocyte differentiation. The effects of NIC addition at various points in culture (days 3, 6, 9) was examined. Unfortunately, the untreated G culture behaved abnormally (there was a high percentage of E cells contaminating the culture) and this culture could not be used for direct comparison to the NIC-treated G cultures. This necessitated the use of historical data for comparison. As with Mks and erythrocytes, NIC also inhibited expansion in granulocyte cultures (Fig 4.4). Total-cell expansion typically reaches ~7000-fold in a 21-day untreated granulocyte culture. In comparison, day 3, 6, and 9 NIC cultures reached 183-, 618-, and 628-fold expansion, respectively. Moreover, granulocyte and monocyte colony formation was inhibited with NIC; the number of colonies was reduced (Fig 4.5), along with their size, when NIC was added to the assay. Additionally, there were almost no monocyte colonies present with NIC. However,

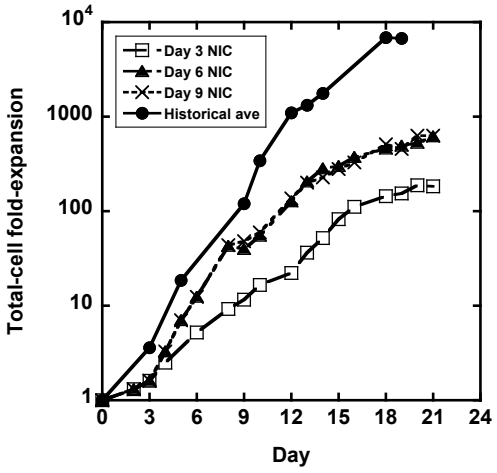

Figure 4.4. Total-cell expansion in granulocyte cultures is inhibited by NIC. mPB CD34$^+$-selected cells were cultured with IL-3, IL-6, SCF and G-CSF. Total-cell fold-expansion was determined for cultures in which 6.25 mM NIC was added beginning on either day 3 (open squares), day 6 (triangles), or day 9 (crosses). The historical average (n = 13) for granulocyte cultures performed by our group is shown for comparison (circles). Only one biological experiment was performed for cultures with NIC.

NIC did not significantly alter granulocyte differentiation in the liquid cultures in terms of surface marker expression and morphology. The kinetics of CD11b, CD15, and CD66b expression was similar in the NIC-treated cultures compared to historical data from previous G cultures conducted by others in our group[149] (Fig. 4.6). There was a slight delay in maturation when NIC was added early on day 3; however, all NIC cultures reached the same final percentages of $CD11b^+$, $CD15^+$, and $CD66b^+$ cells. This delay may be increased further if NIC was added earlier in culture before day 3. Replicate experiments are necessary; however, it is likely that those experiments will confirm that NIC does not alter granulocyte maturation.

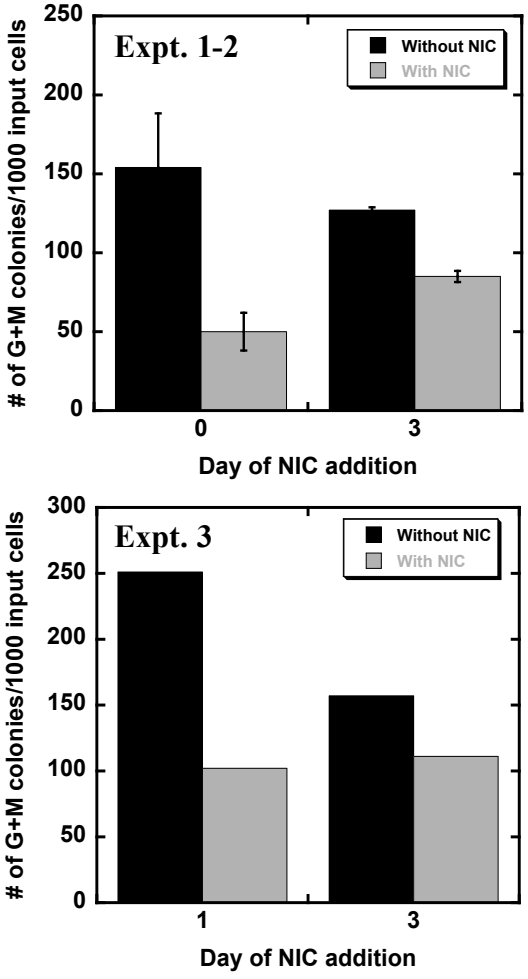

Figure 4.5. NIC inhibits granulocyte and monocyte colony formation.

Cells were sampled from Tpo only cultures on either day 0 or 1 and on day 3 and put into colony assays containing a combination of cytokines. CFU-G+M were enumerated 14 days after assays were initiated. A total of 3 biological experiments were performed: Expts 1 & 2 – an equal number of cells were put into the assay with and without NIC; Expt 3 – the input number of cells were adjusted to account for growth inhibition with NIC. A significant reduction in the size of G and M colonies was observed along with a large decrease in the number of G+M colonies formed per input cell.

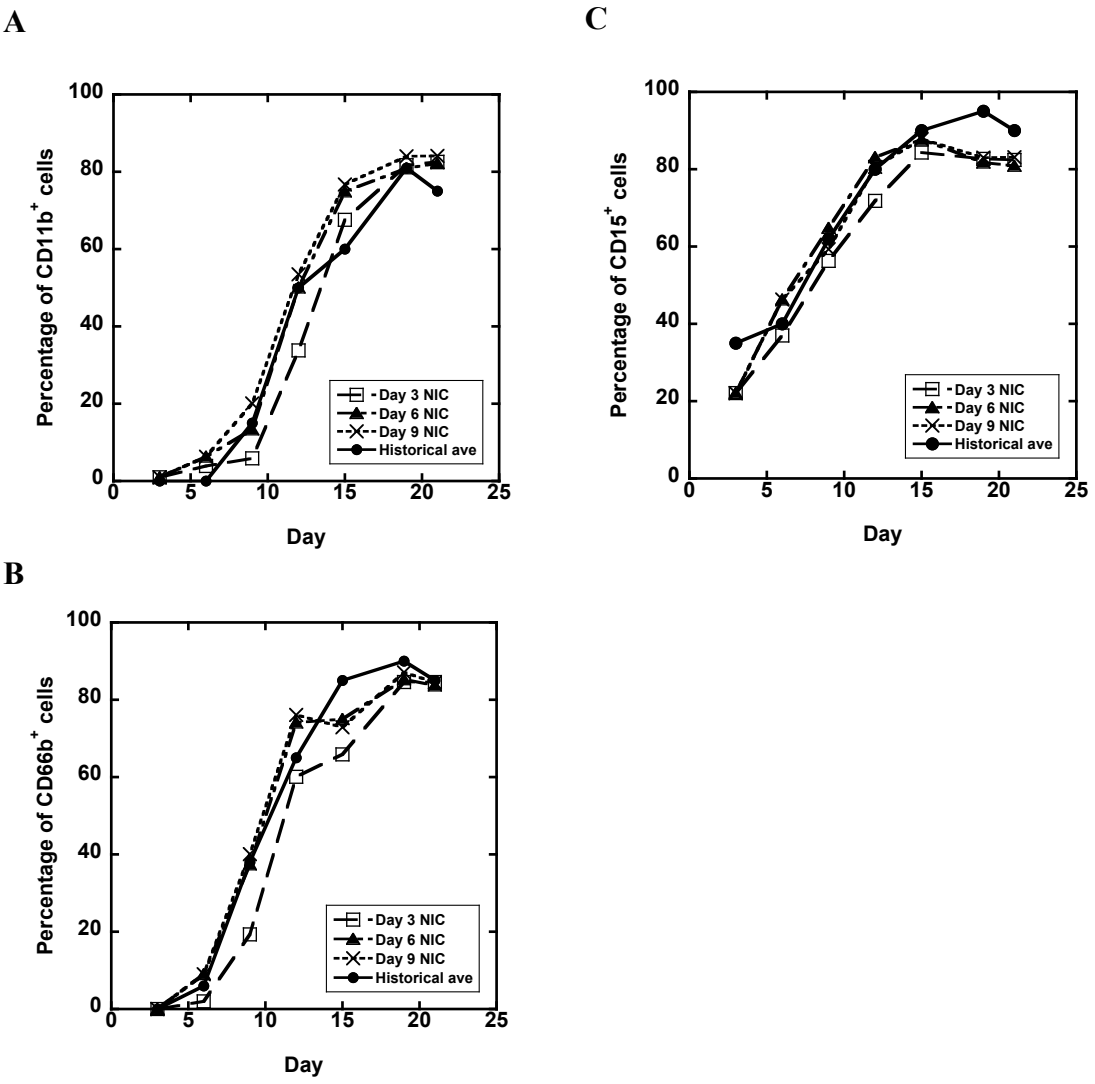

Figure 4.6. Surface marker expression in granulocyte cultures is not affected by NIC.

mPB $CD34^+$-selected cells were cultured with IL-3, IL-6, SCF and G-CSF. The total percentage of (A) $CD11b^+$, (B) $CD66b^+$, and (C) $CD15^+$ cells was determined using flow cytometry in cultures with 6.25 mM NIC added beginning on either day 3 (open squares), day 6 (triangles), or day 9 (crosses). The historical averages (n = 13) in granulocyte cultures performed by our group are shown for comparison (circles). Only one biological experiment was performed for cultures with NIC.

4.4. Discussion

In this study we demonstrate that in addition to increasing megakaryocyte (Mk) maturation, NIC also enhances erythroid differentiation. This was observed both with colony assays containing NIC and in liquid cultures of mPB $CD34^+$-selected cells treated with NIC. Enhanced erythroid differentiation was characterized by an increased percentage of benzidine positive cells, a more rapid loss of CD34 and CD71 expression, and faster gain of GlyA expression. Erythroid differentiation was enhanced to a much greater extent when NIC was added early in culture (day 3) compared to days 6 and 9. It would be of interest to examine whether earlier addition of NIC on day 0 could enhance maturation further. In contrast, day 3 addition of NIC only led to a slight delay in granulocyte differentiation. However, cell growth was significantly inhibited in these normally highly proliferative G cultures. Overall, the lack of an effect on granulocyte differentiation with NIC suggests that NIC is not simply a general hematopoietic differentiation agent. Furthermore, the lack of large polyploid E or G cells demonstrates that NIC does not act by inducing general chromosome instability and polyploidization and reaffirms that NIC only enhances the process of polyploidization in Mks as opposed to initiating endomitosis.

Further studies to characterize the effects of NIC on erythroid differentiation could reveal insight about the mechanism by which NIC increases megakaryocyte maturation. It is believed that erythrocytes and Mks arise from a common progenitor cell. Therefore, a common mechanism for enhancing differentiation towards both lineages by NIC may exist. Tpo and Epo have a high degree of sequence homology and structural similarity. Both cytokines also have similar receptor binding domains.[150,151] This suggests that perhaps the effects of NIC are in part

due to Epo/Tpo signaling. Alternatively, one early study found that NIC enhanced the differentiation of a murine erythroid cell line and increased the level of intracellular NAD two-fold.[152] However, a limited number of studies have been performed to further characterize the role of NIC and NAD levels in erythroid maturation. As discussed in Section 3.3.6, increased Mk maturation due to NIC is accompanied by greatly increased levels of NAD(H). Further studies may reveal that intracellular NAD(H) levels also play an important role in erythroid maturation.

4.5. Acknowledgements

I thank Swapna Panguanti for her help in maintaining the granulocyte cultures and Amgen for their kind donation of SCF.

5. CHAPTER 5: Conclusions and Recommendations

5.1. Chapter 2: Phenotypic characterization of the effects of nicotinamide on megakaryopoiesis

5.1.1. Conclusions

Nicotinamide (NIC) enhances megakaryocyte (Mk) differentiation in cultures of primary human and murine cells under a variety of different Mk-promoting culture conditions. NIC dramatically increases cell size, polyploidization, and proplatelet formation without affecting other aspects of Mk differentiation such as apoptosis or Mk commitment as defined by the percentage of $CD41^+$ cells in a culture. Importantly, NIC-treated cells exhibit normal Mk morphology and gene expression microarrays revealed a minimal effect of NIC on the Mk transcriptional program. Overall, these studies demonstrate that NIC could be useful as a supplement to increase the productivity of *ex vivo* Mk cultures. Furthermore, NIC-treated Mks could serve as a novel model for studying Mk polyploidization in which cells reach ploidy levels closer to those observed *in vivo*. Lastly, our results suggest that *in vivo* administration of NIC may be used to enhance Mk maturation and platelet production in patients with Mk disorders such as myelodysplastic syndromes (MDS) (Section 5.3.2.2).

5.1.2. Recommendations

NIC increases two aspects of Mk maturation – polyploidization and proplatelet formation. Since DNA content is directly proportional to the number of platelets produced per Mk, this suggests that NIC-treated Mks have a greater platelet-producing potential. However, we have not yet measured the number of platelets produced or assessed their functionality. This

requires the development of a flow cytometric assay that allows the discrimination of cultured platelets from cellular debris. It is also important to demonstrate platelet function via activation in response to agents such as PMA and ADP. Some work in developing such an assay was performed by a former Master's student in our group (Jay Cuenca); however, these studies were never brought to completion. Additionally, electron microscopy can be performed to examine whether platelets in NIC-treated Mk cultures have similar morphology to those in cultures with Tpo only.

Additional characterization can be conducted to further explore the effects of NIC on Mk apoptosis and cell-cycle regulation. We have found no effect of NIC on phosphatidyl serine inversion by Annexin V binding, a widely used marker of apoptosis. However, it is possible that other indicators of apoptosis such as caspase activation, loss of mitochondrial transmembrane potential, or DNA strand breakage may reveal important differences brought on by NIC. We can also examine whether the level and localization of key cell-cycle and cytokinesis-related proteins (cyclin D3,[153-155] cyclin E,[156,157] Aurora kinase B (AURKB),[158,159] MgcRacGAP, and RhoA[160]) are affected by NIC.

5.2. Chapter 3: Characterization of the mechanism(s) underlying the effects of NIC on Mk differentiation

5.2.1. Conclusions

In order to understand the mechanism by which NIC increases Mk maturation we examined several known roles of NIC. While NIC is known to inhibit the NAD-dependent enzymes PARP and Sir2 in other cell types, culture with additional PARP and Sir2 inhibitors was not able to mimic the effects of NIC on Mk ploidy. This suggests that the increased

polyploidization with NIC may not be due to inhibition of these enzymes. NIC also increases NAD(H) levels in a variety of cell types. We found similar increases when NIC was added to primary Mk cultures. Interestingly, the other form of niacin, nicotinic acid, only slightly increased NAD(H) levels and did not have any effect on Mk ploidy. Additional studies are necessary to examine the downstream effects of high NAD(H) levels in NIC-treated Mks.

Separately, we examined the hypothesis that Tpo-mediated signaling may play a role in the effects of NIC on Mk maturation. We found that, while NIC could increase polyploidization without Tpo present, Tpo was necessary to achieve the full effects of NIC on Mk polyploidization. In Mks, Tpo activates both the ERK and Akt signaling pathways. NIC-treated cells were found to have higher levels of ERK activation. Moreover, the downstream ERK target RSK1 also more highly activated with NIC. In contrast, Akt activation was not affected by NIC, nor was activation of mTOR, a downstream target of pAkt. Further studies are needed to fully understand the role of ERK signaling in the effects of NIC on Mk ploidy.

5.2.2. Recommendations

5.2.2.1. Further investigation of the role of ERK in the effects of NIC on Mk ploidy

RNAi for ERK

Tpo + NIC cells exhibit increased activation of ERK and its downstream target RSK1 suggesting a role for ERK signaling in the effect of NIC on Mk polyploidization. Several studies were performed using chemical inhibitors of MEK/ERK signaling (PD98059 and U0126) to examine whether inhibition of this pathway (1) decreases Mk ploidy in the absence of NIC and (2) decreases NIC-mediated enhancement of Mk ploidy and proplatelet formation. However, studies were inconclusive due to lack of inhibitor specificity. As a result, alternative methods for

gene knock down such as RNAi can be used to better understand the role of ERK signaling in NIC-treated Mks. Although, ERK knock down in primary human Mks has not yet been reported, RNAi for ERK has been successful in various cell types.[161,162] Methods for the construction of siRNA lentiviral vectors have been established in our lab and knock down studies have been demonstrated successfully in the CHRF cell line.[137] However, the methods for efficient lentiviral transfection of primary human $CD34^+$ cells have not yet been determined in our lab. Transfection is feasible, with others reporting methods that result in a transfection efficiency of ~40–50% in cord blood $CD34^+$ cells.[163,164] Therefore, prior to ERK siRNA studies, effort would need to be directed towards developing efficient primary cell transfection methods. However, preliminary studies could be performed using the CHRF cell line.

Additional studies with U0126

As described in Section 3.3.5, the MEK inhibitors U0126 and PD98059 gave conflicting results in primary Mk cultures. While PD98059 increased Mk ploidy at all concentrations tested, U0126 slightly decreased the percentage of high-ploidy Mks. However, studies with U0126 need replication. Furthermore, studies with U0126 in Tpo + NIC cultures have not yet been performed to determine whether inhibition of ERK by U0126 could reduce the effects of NIC on Mk ploidy. U0126 exhibits poor stability in solution and is often only used in short-term signaling studies. Therefore, different replacement frequencies should be examined to ensure inhibitor activity is maintained. Mk ploidy and steady-state levels of pERK should be measured in all cultures.

5.2.2.2. Further exploration of the role of NAD in the effects of NIC on Mk ploidy

Mk cultures with additional NAD^+ precursors

We have shown that NIC greatly increases the level of intracellular NAD(H) in cultured CHRF cells and primary Mks. In order to test the hypothesis that the increased NAD(H) level is responsible for the effects of NIC on ploidy, cultures with additional precursors of NAD^+ can be performed. Increased NAD(H) levels with compounds such as nicotinic acid, quinolinic acid, and NAD^+ should result in a similar increase in Mk ploidy. We have already shown that nicotinic acid is not capable of increasing intracellular NAD levels to the extent of NIC and does not increase Mk ploidy. Quinolinic acid has been demonstrated to increase intracellular NAD levels in cultured glial cells.[57] Therefore, we can examine NAD(H) levels and ploidy in Mk cultures with quinolinic acid. We can also test the effects of direct addition of NAD^+ to cultures.

Mk cultures with APO866

Thus far, conditions that provide sustained inhibition of NAD(H) levels in primary Mks with APO866 have not yet been determined. This could be key to demonstrating that the increased NAD(H) levels are responsible for the increased polyploidization with NIC. Further studies can be performed to determine the lowest possible NIC concentration that increases Mk ploidy, and then subsequently test APO with that concentration of NIC. Alternatively, frequent repeated addition of APO without media exchanges to replace NIC can be tested. For this, a dose of 100 nM APO would be added to cultures every 8-12 hours and cells assessed for NAD(H) levels and percentage of high-ploidy Mks.

5.2.2.3. Role of p53 in the effects of NIC on Mk ploidy

The effects of NIC on Mk polyploidization may be mediated directly by elevated levels of intracellular NAD^+. For example, increased levels of intracellular NAD^+ have been shown to alter the DNA binding specificity of p53, leading to decreased radiation-induced expression of p53 targets (mdm2 and PIG3) and an increased frequency of aneuploid cells.[52] Since p53 is responsible for the prevention of aneuploidy and rereplication,[59] this suggests that NAD^+ levels may modulate cellular DNA content via p53.

The possibility that elevated levels of NAD^+ affect Mk maturation via modulation of p53 binding specificity to DNA can be evaluated by comparing effects of NIC to those of thiamine (vitamin B1). Thiamine is rapidly converted to TDP (thiamine diphosphate), which is a coenzyme used in carbohydrate metabolism.[165] Supplementation of NIC and thiamine result in increased levels of NAD^+ and TDP, respectively. Increased NAD^+ and TDP both result in decreased p53 binding to the DNA binding site of mdm2.[52] Mdm2 is a nuclear phosphoprotein that is activated by p53 and functions as a negative regulator of p53 by targeting it for degradation.[166] Lower levels of mdm2 protein were also observed and led to an increase in the level of p53.[52] Interestingly, TDP also inhibits binding of p53 to the p21 DNA binding site, while NAD^+ does not.[52] Also, in contrast to NIC, thiamine does not affect p53 acetylation. Therefore, levels of total and acetylated p53 can be measured in Tpo only and Tpo + NIC cells. Additionally, the effect of elevated NAD(H) levels on p53 binding can be analyzed by chromatin immunoprecipitation of genomic DNA sites bound to endogenous p53 protein using previously described methods.[52] It is well established that p53 deficiency leads to genomic instability and

polyploidization in variety of cell types.[167,168] Therefore, it is not unexpected that the knockdown of p53 in CHRF cells further increases polyploidization.[137] Based on this observation and the previously identified connection between NAD^+ levels and p53 activity, inhibition of p53 by NIC could be responsible to enhanced polyploidization.

5.2.2.4. Role of the NADH/NAD^+ ratio and ROS levels in the effects of NIC on Mk ploidy

Individual measurements of NAD^+ and NADH

Thus far, all studies performed to examine the role of NAD^+ in Mk differentiation have relied on the measurement of NAD(H) which is the sum of NAD^+ and NADH. NAD(H) was measured in whole-cell extracts using an enzymatic cycling assay[114,169] whose feasibility was demonstrated using the CHRF cell line. A single extraction method[170] was used in which cells are incubated with a neutral or slightly basic extraction buffer which contains a detergent such as Triton X-100. The cycling reaction then measures total NAD(H). To measure NAD^+ and NADH individually, an aliquot of sample can be subjected to heating at 60°C for 30 minutes to degrade the NAD^+. From this, the NADH/NAD^+ ratio can be determined. Further studies need to be conducted to verify that NADH remains intact and is not affected by the heating process. This can be done by spiking NADH of a known amount into samples prior to heating and determining the percent recovery. These validation studies can be carried out using the CHRF cell line. Additionally, if this assay is to be used further, studies should be performed to reduce the number of cells needed at each time point per condition. Presently, the assay calls for 500,000 cells per condition. This is a large number of cells when performing primary Mk cultures. Reducing the number of cells needed would allow for the use of fewer cells and more frequent time points.

Alternatively, HPLC methods[52,171] can be used to measure both NAD^+ and NADH simultaneously; however, this would require additional method development.

NADH/NAD^+ ratio and ROS levels

Since we have observed that the level of intracellular NAD(H) [sum of NAD^+ and NADH] is greatly increased by NIC, it is possible that the effects of NIC on Mk ploidy are mediated by the NADH/NAD^+ ratio, which is emerging as an important regulator of signal transduction.[172-174] The NADH/NAD^+ ratio can be determined by separate measurements of NADH and NAD^+ using the enzymatic assay described above and compared between cells cultured with Tpo only and Tpo + NIC. Alternatively, the ratio of cellular lactate to pyruvate, which is near equilibrium with the NADH/NAD^+ ratio, can be measured. The NADH/NAD^+ ratio is also an indicator of intracellular ROS (reactive oxygen species).[172,173] More specifically, a higher NADH/NAD^+ ratio is associated with increased ROS generation.[175] Changes in the NADH/NAD^+ ratio would suggest changes in ROS levels and thus changes in mitochondrial metabolism, protein phosphorylation and ROS-related regulation and events.[173,174,176,177] Therefore, we can directly measure ROS levels in Mks cultured with and without NIC. Intracellular H_2O_2 and superoxide (O_2^-) levels are measured by flow cytometry using the dyes CM-H_2DCFDA and dihydroethidium (DHE), respectively, based on specific fluorescence activation.[178,179] In other cell types, NIC has been shown to have antioxidant properties. NIC protected cells against H_2O_2-[180] and ascorbate-Fe^{+2}-induced ROS production[181] and also protected neuronal cells from hypoxia.[182] NIC reduced ROS generation associated with cellular senescence[183] and oxygen-glucose deprivation.[182] Therefore, we would expect NIC to decrease

the NADH/NAD^+ ratio and decrease ROS levels in cultured Mks. However, the protective effects of NIC are often associated with inhibition of PARP, an enzyme with a role in DNA repair (ROS initiate DNA strand breaks which then activate PARP). We did not observe any effects on Mk ploidy when cells were cultured with additional PARP inhibitors.

5.3. Chapter 4: Effects of NIC on hematopoietic stem cell differentiation towards other lineages (erythrocytic and granulocytic)

5.3.1. Conclusions

In addition to enhancing Mk polyploidization and proplatelet formation, NIC also increased erythroid maturation. Cells differentiated more quickly with NIC as indicated by a greater percentage of benzidine positive cells, a more rapid loss of CD34 and CD71 expression, and faster gain of GlyA expression. These effects were greatest when NIC was added early to cultures (day 3). In contrast, NIC addition to granulocyte cultures on day 3 significantly inhibited cell expansion, but only led to a slight delay in differentiation. These studies demonstrate that NIC is not simply a general hematopoietic differentiation agent nor does it initiate polyploidization in non-Mk cells. *In vivo* administration of NIC would likely lead to significant inhibition of megakaryocyte, erythrocyte, and granulocyte expansion, while enhancing the maturation of both E and Mk cells. Additional studies are necessary to replicate the data shown for both E and G cultures and also to further characterize the effects of NIC on erythroid differentiation.

5.3.2. Recommendations

5.3.2.1. Additional characterization of the effects of NIC on erythroid differentiation

Preliminary data indicates that NIC enhances erythroid differentiation. However, these studies need replication. Addition of NIC on day 0 should also be examined to determine whether erythroid maturation can be increased further. Similar to Mk studies, we can examine both the role of NAD(H) levels and Epo-mediated signaling in the effects of NIC on erythroid maturation. Levels of NAD(H) can be measured to examine whether the enhanced maturation is accompanied by increased NAD(H) levels as was observed in Mk cultures. Both Tpo and Epo have been found to activate the ERK pathway in their respective cell types. Several studies show that erythroid differentiation is associated with inhibition of ERK.[184 185 186] Therefore, we would expect that NIC-treated erythroid cells would have lower levels of pERK compared to untreated cells. However, this would be in contrast to the effects of NIC on pERK in Mks.

5.3.2.2. Characterize the effects of NIC on MDS patient bone marrow samples

We have shown that NIC enhances both erythroid and Mk maturation without significantly altering granulocyte differentiation. Our studies with Mk cultures suggest that NIC has the potential to increase platelet counts in patients with myelodysplastic syndromes (MDS) patients. Also, as discussed in Chapter 1, prolonged exposure to NIC is well tolerated by humans at doses that produce NIC plasma concentrations in the millimolar range. Currently, there is not a well-accepted mouse model of MDS. More importantly, MDS is a very heterogeneous disease,[138-140] so that one or a few mouse models of MDS would not capture the diversity of the

disease. Therefore, studies can be performed to evaluate the effects of NIC on Mk cultures initiated with bone marrow cells from MDS patient aspirates. We can also evaluate the effects of NIC on bone marrow MNCs from normal donors to allow a direct comparison with the responses of MDS patient bone marrow MNCs. In an effort to identify unanticipated problems that may be associated with a clinical trial, we can also evaluate the effects of NIC on the differentiation of MDS patient and healthy donor bone marrow MNCs along the granulocytic and erythroid lineages, similar to the experiments described in this chapter with cultures of mPB $CD34^+$ cells. As part of the analysis, we can investigate whether NIC effects vary for MDS patients with different prognostic indicators. More extensive Mk maturation would support the hypothesis that NIC will decrease the severity of thrombocytopenia in MDS patients.

6. Appendix

6.1. CHAPTER 2

6.1.1. Effects of the SIRT activator resveratrol (RES) on primary Mk maturation

Aims

One approach to improve Mk culture productivity is to identify conditions that allow decoupling of Mk apoptosis and polyploidization. Previous microarray analyses of Mk differentiation performed by our group have shown the upregulation of various apoptosis related genes with Mk differentiation including several members of a class of histone deacetylases, sirtuins (C. Chen, P. Fuhrken, W. Miller, E. T. Papoutsakis, manuscript submitted April 2007). As a result, we were interested in determining whether a SIRT activator such as resveratrol (RES)[187] or SIRT inhibitor such as nicotinamide (NIC)[188,189] could be used to alter the balance between apoptosis and polyploidization in Mks. This was the primary experiment responsible for the finding that NIC dramatically increases Mk polyploidization and proplatelet formation.

Methods

Frozen mPB $CD34^+$-selected cells (AllCells) were thawed as instructed and seeded at 100,000 cells/mL in X-VIVO 20 containing 100 ng/mL Tpo (Genentech). On day 6, cells were treated with either resveratrol (6.25, 12.5, 25, 50 μM), nicotinamide (6.25, 12.5, 25, 50 mM), or DMSO as a control (for resveratrol). On days 3, 6, 8, 10 cells were assessed for growth, viability and CD41 expression. DNA content was measured by flow cytometry on day 11 in all conditions.

Results

High concentrations of both RES and NIC were found to be cytotoxic. RES significantly decreased cell growth and viability at concentrations greater than or equal to 25 μM (Fig 6.1A). NIC was cytotoxic at concentrations greater than or equal to 25 mM (Fig 6.1B). Cells continuously treated with 12.5 mM NIC began to appear unhealthy towards the end of the 11-day culture. Concentrations ≤ 6.25 mM NIC inhibited growth but the cells remained healthy. Non-toxic doses of NIC and RES had no effect on the percentage of $CD41^+$ cells (Fig 6.1A-B). Moreover, RES did not alter Mk ploidy; (Fig 6.1C) and no further studies were conducted with RES. However, NIC had profound effects on Mk maturation. This observation led to many additional studies to extensively characterize and understand the effects of NIC on Mk maturation as discussed in Chapters 2-3.

Figure 6.1. Effect of resveratrol on primary Mk differentiation.

Primary human $CD34^+$-selected cells were cultured with 100 ng/mL Tpo. Varying concentrations of reveratrol or nicotinamide was added to cultures on day 5. Tpo only (red) cultures were used as a control. (A) Kinetics of total-cell fold-expansion and percentage of $CD41^+$ cells in Mk cultures with RES [6.25 μM (blue), 12.5 μM (green), 25 μM (black), 50 μM (gray)]. (B) Kinetics of total-cell fold-expansion and percentage of $CD41^+$ cells in Mk cultures with NIC [6.25 mM (blue), 12.5 mM (green), 25 mM (black), 50 mM (gray)]. (C) Percentage of high-ploidy Mks in cultures with non-cytotoxic concentrations of RES or NIC. All data shown is from a single biological experiment. No further studies were performed with RES.

A

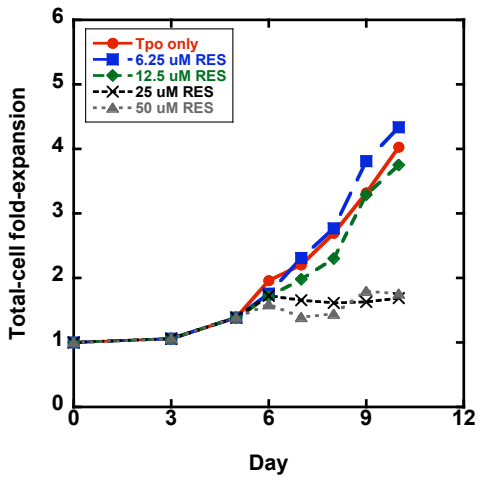
Tpo only
6.25 uM RES
12.5 uM RES
25 uM RES
50 uM RES
Total-cell fold-expansion
Day

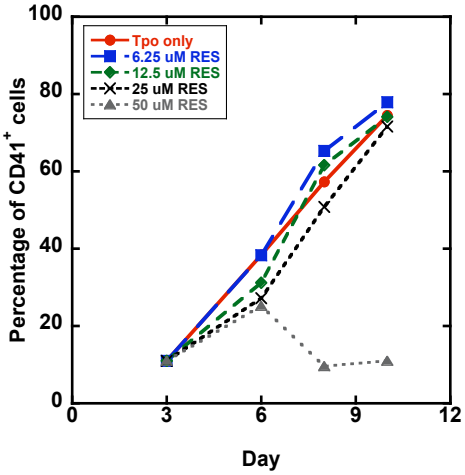
Tpo only
6.25 uM RES
12.5 uM RES
25 uM RES
50 uM RES
Percentage of CD41+ cells
Day

B

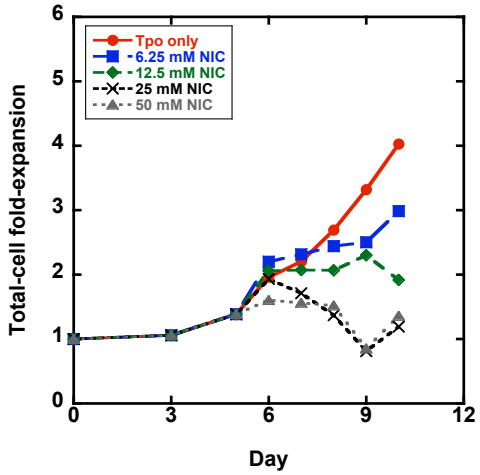
Tpo only
6.25 mM NIC
12.5 mM NIC
25 mM NIC
50 mM NIC
Total-cell fold-expansion
Day

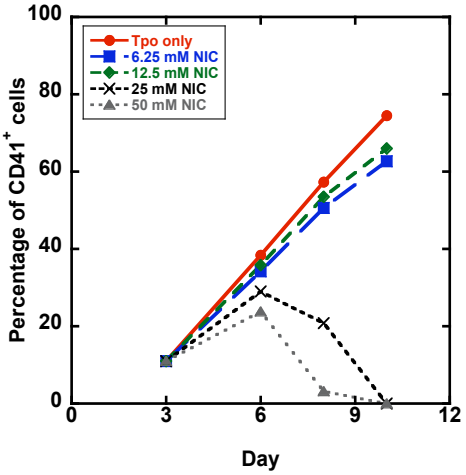
Tpo only
6.25 mM NIC
12.5 mM NIC
25 mM NIC
50 mM NIC
Percentage of CD41+ cells
Day

C

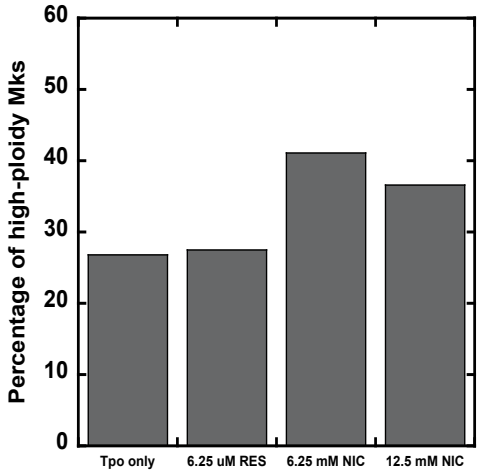
Percentage of high-ploidy Mks
Tpo only
6.25 uM RES
6.25 mM NIC
12.5 mM NIC

6.2. CHAPTER 3

6.2.1. Characterization of Mk cultures with SDF-1α, on fibronectin-coated surfaces, and with a cytokine cocktail

Aims

Studies were conducted to demonstrate that NIC is effective under a range of Mk-inducing culture conditions. We examined conditions that have previously been shown to promote increased Mk polyploidization and proplatelet formation. Stromal cell-derived factor 1α (SDF-1α) is a CXC chemokine that acts as a stimulator of pre-B lymphocyte cell growth and as a chemoattractant for T-cells, monocytes, and hematopoietic stem cells.[190,191] SDF-1α has also been shown to enhance Mk polyploidization and migration.[22,192,193] Additionally, culture of primary Mks on fibronectin (FN) coated surfaces has been shown by others to increase total-cell numbers, the percentage of $CD41^+$ cells, cell size and the extent of cell adhesion.[26] In murine Mks, Fox *et al*. found that the FN fragment H296, which engages the α4β1 integrin, enhanced Mk growth.[27] Therefore, we examined the effects of NIC under these potentially more optimal conditions for Mk growth. We also looked at the effects of NIC in a culture containing a cocktail of cytokines (SCF, IL-3, IL-6, Tpo), which better promotes Mk expansion compared to culture with Tpo only.

Methods

SDF-1α cultures

Frozen $CD34^+$ cells were cultured in X-VIVO 20 with 100 ng/mL of Tpo (Peprotech). SDF-1α (R&D Systems) was added at a concentration of 0.15 μg/mL on day 0. 6.25 mM NIC

was added to cells on day 2 and half-media exchanges were performed every other day. On days 5, 7, 9, & 11 cultures were analyzed for the percentage of $CD41^+$ cells and the percentage of high ploidy Mks. Expansion was monitored over the duration of culture.

FN cultures

Frozen primary human mPB $CD34^+$-selected cells were cultured with 100 ng/mL Tpo (Peprotech) on FN-coated surfaces beginning on day 0. 6.25 mM NIC was added on day 5 and half-media exchanges were performed every other day. FN-coated well-plates (BDBiocoat, BD Biosciences) rather than coated flasks were used in the anticipation of strong cell adherence. This allowed a well from each condition (Tpo only, Tpo + NIC) to be sacrificed at each time point for assessment of ploidy and to perform cell counts. When necessary, cells were trypsinized to analyze adherent cells. FN cultures were analyzed in a manner similar to the SDF-1α cultures described above.

Cocktail cultures

We aimed to demonstrate that NIC increases Mk ploidy in culture conditions that promote cell expansion to a greater extent than for Tpo only. For this, a cytokine cocktail of SCF, IL-3, IL-6 and Tpo was chosen.[194-196] Frozen mPB $CD34^+$-selected cells were thawed and seeded in X-VIVO 20 containing SCF (R&D; 10 ng/ml), IL-3 (Peprotech; 0.005 ng/ml), Tpo (Peprotech; 50 ng/ml), IL-6 (Peprotech; 10 ng/ml). Since we assumed that these cultures would mature more slowly than cells cultured with Tpo only, 6.25 mM NIC was added on day 5 as opposed to day 2

for SDF-1α cultures. Half-media exchanges were performed every other day in both conditions. Cocktail cultures were analyzed in a manner similar to the SDF-1α cultures described above.

Results

SDF-1α cultures

Cells cultured with Tpo only were characterized and compared to those cultured with Tpo + SDF and Tpo + SDF + NIC. SDF alone did not alter cell expansion, but growth was slowed in cultures containing SDF + NIC (Fig 6.2A). There was a significant decrease in the percentage of $CD41^+$ cells with this concentration of SDF compared to Tpo only cultures, but the decrease was less when NIC was added with SDF (Fig 6.2B). Polyploidization began earlier in cultures with SDF, which was expected based on the literature.[22] However, Tpo + SDF cultures produced the same percentage of high-ploidy Mks by day 11 as did cultures with Tpo only (Fig 6.2C). Tpo + NIC and Tpo + SDF + NIC cultures also yielded the same percentage of high-ploidy Mks by day 11. However, it should be restated that NIC was added on different days of culture – day 2 for SDF and day 5 for Tpo + NIC. Overall, these results demonstrate that the onset of polyploidization is earlier in cultures with SDF1-α, which leads to an increased percentage of high-ploidy Mks early in culture compared to cultures with Tpo only. NIC further increased the percentage of high ploidy Mks demonstrating the benefits of NIC still hold even when "more optimal" Mk culture conditions are used.

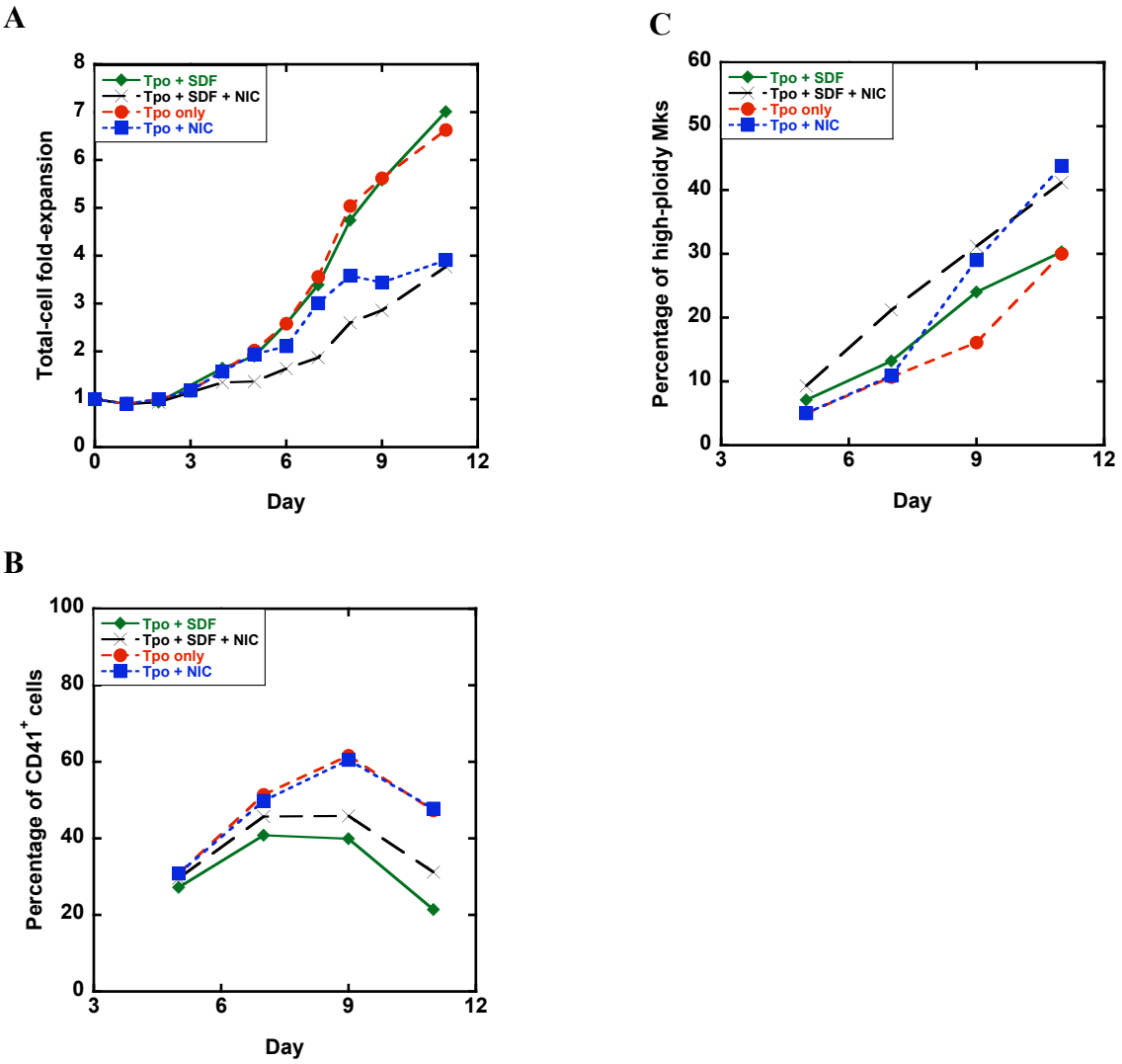

Figure 6.2. Effects of NIC in primary human Mk cultures containing SDF-1α.

Primary human mPB $CD34^+$-selected cells were cultured with 100 ng/mL Tpo. On day 0, SDF-1α was added to the cultures followed by NIC addition on day 2 [SDF-1α (green), SDF + NIC (black)]. Cultures with Tpo only (red) and Tpo + NIC (blue) were included as controls. (A) All cultures were monitored for total-cell fold-expansion. (B-C) Kinetics of the percentage of $CD41^+$ cells and high-ploidy Mks in each culture was determined using flow cytometry.

FN cultures

Mk differentiation of cells cultured with Tpo only and Tpo + NIC on FN-coated surfaces was compared with that of cells grown on standard tissue-culture-treated plasticware. As expected, FN increased Mk adhesion. In addition, the frequency of proplatelet-forming Mks was also greater with FN; however, this difference was not quantified. In contrast, the percentage of high-ploidy Mks was lower in cultures on FN surfaces compared to tissue culture plastic (Fig 6.3A). The addition of NIC increased polyploidization in FN cultures, but not to the extent observed with NIC addition in the absence of FN. Cultures on FN had a similar, perhaps slightly lower, percentage of $CD41^+$ cells (Fig 6.3B).

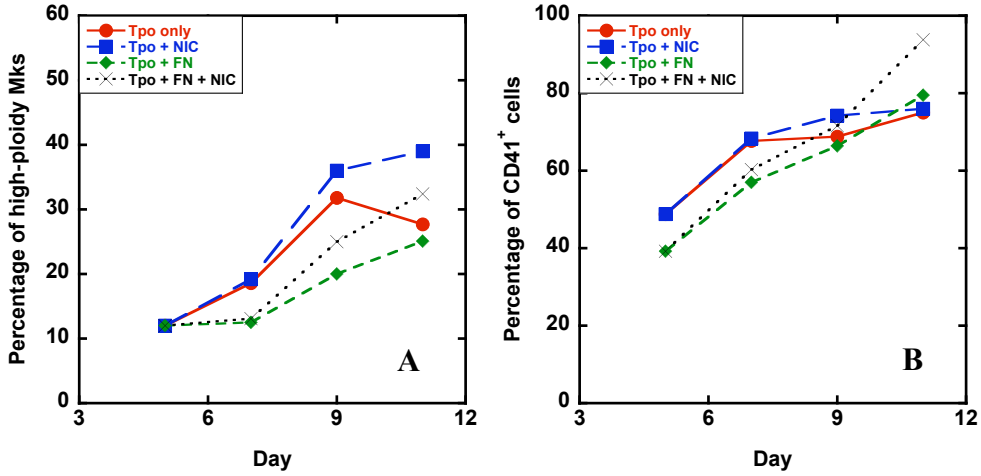

Figure 6.3. Effect of NIC on Mks cultured on fibronectin-coated surfaces.

Primary human mPB $CD34^+$-selected cells were cultured with 100 ng/mL Tpo. On day 0, cells were seeded into FN coated well plates (green). 6.25 mM NIC was added on day 5 (black). Tpo only (red) and Tpo + NIC (blue) cultures maintained in tissue culture treated flasks were included as controls. The percentage of (A) high-ploidy Mks and (B) $CD41^+$ cells in each culture was determined using flow cytometry.

Cocktail cultures

Under the culture conditions chosen, expansion was greater than that typically observed with Tpo only, which was to be expected. Twelve-fold expansion was obtained by day 11 (Fig 6.4A). This cytokine combination was also previously reported to give a high yield of Mks (80–90% $CD41^+$).[194-196] However, in our hands, a maximum percentage of only 25% $CD41^+$ cells was reached in the cocktail culture (28% in the cocktail + NIC culture) (Fig 6.4B). These percentages are similar to what is observed in cocktail cultures using IL-3, FLT-3, and Tpo.[197] Interestingly, despite the low fraction of $CD41^+$ cells, the kinetics of polyploidization for the cocktail and cocktail + NIC cultures closely resembled the historical averages for Tpo only and Tpo + NIC cultures (Fig 6.4C). However, cells appeared smaller in the cocktail + NIC culture, perhaps due to a suboptimal NIC concentration. No proplatelet-forming cells were observed in either culture. In summary, we demonstrate another Mk culture condition besides Tpo only where NIC enhances Mk polyploidization.

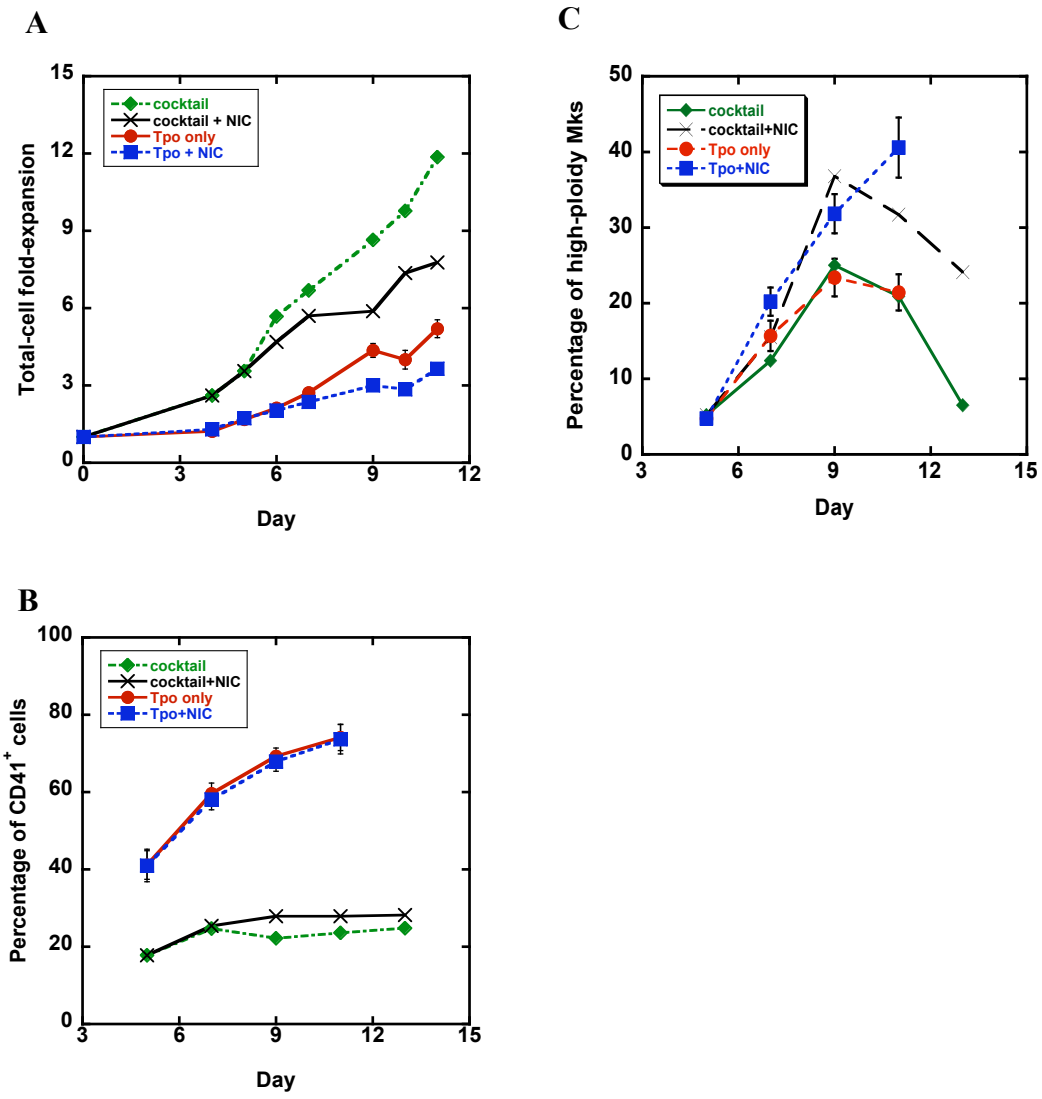

Figure 6.4. Effect of NIC on Mk differentiation in cocktail cultures.

Primary human mPB $CD34^+$-selected cells were cultured with IL-3, IL-6, SCF, and Tpo (green). On day 5, 6.25 mM NIC was added to a portion of the cells (black). (A) Kinetics of total-cell fold-expansion. (B) Kinetics of number of CD41+ cells as a percentage of viable cells. (C) Percentage of high-ploidy Mks in cocktail and cocktail + NIC cultures. The historical averages and SEM of Tpo only (red), Tpo + NIC (blue) cultures are also shown for comparison (n = 16). Data for cocktail cultures is from one biological experiment. Replicate experiments were not performed.

6.2.2. p53 activity in primary Mks

Aims

Levels of intracellular NAD have been shown to alter p53 binding to DNA as discussed in Section 3.5.2.2. Therefore, we examined the level of p53 activity in cell extracts prepared from Tpo only and Tpo + NIC cultures.

Methods

DNA binding of p53 was assessed using the TransBinding p53 ELISA kit (Panomics; Fremont, CA) following the manufacturer's instructions. Briefly, nuclear extracts were prepared using the Nuclear Extraction kit (Panomics) on cells sampled from Tpo only and Tpo + NIC cultures on days 7, 9, and 11. For each sample, 6 μg of nuclear extract was incubated with biotinylated p53-consensus-binding-sequence oligonucleotides. After immobilization on streptavidin-coated 96 well plates, complexes were detected using a primary anti-p53 antibody and a secondary antibody conjugated to horseradish peroxidase. Samples were measured in duplicate and assay specificity was assessed by incubation of lysates with nonbiotinylated consensus sequence oligonucleotides, which resulted in a 92% reduction of the signals. The assay was performed for only one biological experiment.

Results

p53 activity was similar in Tpo only and Tpo + NIC cells on day 7 (Fig 6.5). However, by day 11, NIC cells exhibited greater p53 binding. Based on previous studies by others,[52] the increased NAD levels resulting from NIC addition would have been expected to decrease p53

activity. Furthermore, an increase in p53 activity is not observed with maturation in the Tpo only cells as would be expected based on p53 activity data in CHRF cells induced to undergo megakaryocytic differentiation using PMA.[137] However, measurement of p53 activity in a replicate biological experiment has yet to performed. Therefore, no definitive conclusions can be made at this point. However, additional assays to examine the role of p53 in Mk ploidy should be investigated (Section 5.2.2.3).

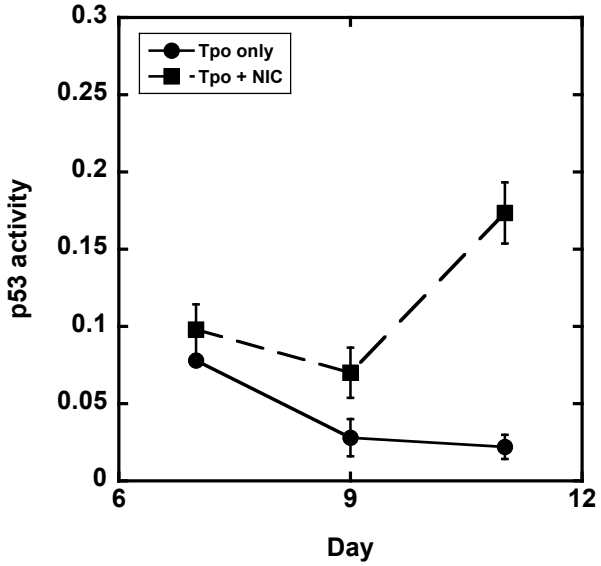

Figure 6.5. p53 activity in primary Mk cultures.

Nuclear extracts of cells from Tpo only and Tpo + 6.25 mM NIC cultures were analyzed for binding to the p53 consensus sequence in an ELISA assay. Error bars represent SD from replicate samples from the same biological experiment.

6.2.3. G1ME cell culture with NIC

Aims

We wanted to examine the role of GATA1 in the effects of NIC on Mk ploidy. G1ME cells are Tpo-dependent primary murine cells that lack GATA-1 and do not become polyploid when cultured with Tpo.[198] We wanted to determine whether NIC would increase polyploidization in G1ME cells.

Methods

G1ME cells were obtained from John Crispino at University of Chicago and were cultured in α-MEM containing 20% FBS, 1% pen/strep, 1% L-glutamine, and 20 ng/mL human Tpo (Genentech). Cells were seeded at 150,000 cells/mL in T-25 flasks with or without NIC. The concentration of NIC ranged from 6.25–50 mM. Cells were monitored for cell growth and DNA content was assessed by PI staining of DNA. High-ploidy cells are those with DNA content $\geq$ 8N.

Results

NIC was able to increase the ploidy G1ME cells. On day 3 after NIC addition, untreated cultures contained 7.4% high-ploidy cells compared to 24.5% with 6.25 mM NIC. Concentrations of NIC $\geq$ 12.5 mM were cytotoxic. DNA histograms also show that the highest ploidy class reached was increased with NIC (Fig 6.6). Untreated G1ME cultures contained a small percentage of 8N cells compared to 32N with NIC. Therefore, this suggests that GATA-1 may not be essential for the ability of NIC to increase Mk ploidy.

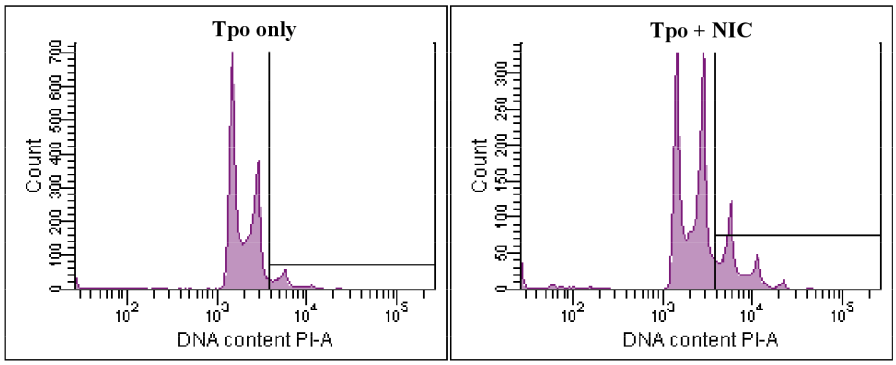

Figure 6.6. DNA histograms of G1ME cells.

DNA histograms of G1ME cells cultured with and without 6.25 mM NIC for 3 days.

6.2.4. Gene silencing by short interfering RNA (siRNA) in hematopoietic cell lines

6.2.4.1. RNAi for influencing Mk apoptosis

My original proposed thesis research involved using siRNA-mediated gene silencing as a tool for influencing megakaryocyte differentiation. The initial goals were to (1) demonstrate efficient transfection and (2) construct an effective siRNA expression vector to target the apoptosis effector protease, caspase-3. The following summary describes the studies carried out towards these objectives.

Plasmid construction

To generate a caspase-3 knockdown vector, oligonucleotides encoding a short hairpin transcript corresponding to nt 417–435 of caspase-3 mRNA (GenBank accession no. NM004346) were annealed and cloned into pRNAT-U6.1 Neo siRNA expression vector (Genscript). This is a published caspase-3 siRNA sequence which has demonstrated knockdown

of caspase-3.[199] pRNAT-U6.1 Neo co-expresses cGFP along with the siRNA of interest for the purpose of assessing transfection efficiency and for analyzing protein levels in the transfected cell population via flow cytometry. Bacterial colonies were used for plasmid preparation and positive clones were confirmed by sequencing. The resulting plasmid was designated as cas3-1. Plasmid was purified using a Qiagen Maxiprep Endo-free kit (Qiagen, Hilden, Germany). For simplicity of method development, only one siRNA construct was prepared. Future siRNA studies would involve construction of 3–5 siRNA sequences for each target gene.

Cell transfection

Initial studies focused on two megakaryocytic cell lines to serve as models for megakaryopoiesis, CHRF-288 and MEG-01. Optimal transfection efficiency of MEG-01 cells was obtained using electroporation (BioRad gene pulser). Briefly, 10 million cells were washed with cold PBS, and resuspended in electroporation buffer (30.8 mM NaCl, 120.7 mM KCl, 8.1 mM Na_2HPO_4, 1.5 mM KH_2PO_4, 5 mM $MgCl_2$) with 20 μg plasmid DNA. Cells were incubated for 15 minutes on ice before pulsing at 975 μF, 20V. Following electroporation, cells were allowed to recover for 10 minutes on ice followed by 15 minutes at room temperature before being put into culture with fresh media. Transfection efficiency determined by GFP expression was ~50% 48 hours post-electroporation.

The transfection efficiency of the CHRF-288 cell line was also explored using several transfection methods: lipofection, electroporation and nucleoporation. In all cases, transfection efficiency was less than 10%. Cells electroporated (no DNA) would remain relatively healthy, whereas, cells pulsed in the presence of DNA progressively became non-viable within a few

days after electroporation. Despite precautions taken to ensure high quality DNA and minimize DNA quantity used, toxicity still occurred. This particular cell type appeared to be sensitive to the uptake and expression of foreign DNA and alternative methods of transfection such as the use of retroviral or lentiviral vectors may be required to achieve higher transfection efficiency. Subsequent efforts from others in our group have now demonstrated lentiviral transduction of CHRF cells.[137] Overall, these studies confirmed that the success of siRNA-mediated gene silencing is limited by the ability to achieve sufficient cell transfection, which is often challenging in hematopoietic cells.

Assessment of caspase-3 knockdown

Following transfection of MEG-01 cells with cas3-1 siRNA, analysis of the level of caspase-3 protein in the GFP^+ population was performed using flow cytometry. While an efficiency of ~50% via electroporation was achieved with the MEG-01 line, the spontaneous differentiation of these cells in culture and subsequent release of platelet-like particles combined with electroporation debris resulted in difficulty assessing intracellular target protein levels by flow cytometry. Cell sorting to remove debris prior to antibody staining was necessary to achieve consistent protein expression results. Since this would have been required at each time point, caspase-3 knockdown with the cas3-1 construct was assessed in an alternative cell line, K562 cells. A decrease of ~40–50% in caspase-3 expression (flow cytometry) was observed in K562 cells transfected with the cas3-1 construct in comparison to control cells receiving the empty vector (Fig 6.7). While K562 cells can undergo megakaryocyte differentiation, they

unfortunately do not show a high degree of apoptosis, which made it difficult to determine if caspase-3 knockdown affected the percentage of apoptotic cells.

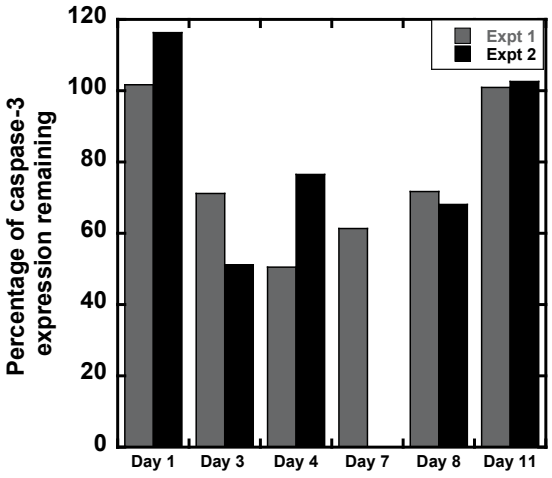

Figure 6.7. Knockdown of caspase-3 in K562 cells receiving cas3-1 siRNA expression vector. K562 cells were transfected with cas3-1 and the transfected cell population was subsequently analyzed for caspase-3 expression using intracellular flow cytometry. The data shown represents the percentage of caspase-3 remaining following transfection for two time-course experiments (Expt 1 and Expt 2).

6.2.4.2. RNAi for influencing hematopoietic cell differentiation

Studies were also performed with the goal of using RNAi for examining hematopoietic cell lineage commitment. For this, a defined lineage commitment decision was used. The decision point at which commitment to either the megakaryocytic or erythroid lineage is made by a bipotent progenitor cell was chosen. p38 MAP kinase served as the target gene due to its reported importance in erythroid differentiation and absence of involvement in megakaryocyte differentiation.[112] Therefore, p38 MAP kinase was used for preliminary experiments to demonstrate the feasibility of working with siRNA as a method to gain a better understanding of hematopoietic differentiation.

Plasmid construction

To generate a p38 knockdown vector, oligonucleotides encoding a short hairpin transcript corresponding to nt 576-596 of p38 mRNA (GenBank accession no. NM-001315) were annealed and cloned into pRNAT-U6.1 Neo siRNA expression vector which co-expresses cGFP (Genscript). A BLAST search was performed to ensure minimum off target specificity.

Cell Transfection

The multipotential K562 cell line was used as a model for examining lineage commitment due to its ability to undergo erythroid and megakaryocyte differentiation in response to butyrate and PMA treatment, respectively. Cell transfections were performed as described above. Transfection efficiency determined by GFP expression was ~80% 48 hours post-electroporation (Fig 6.8).

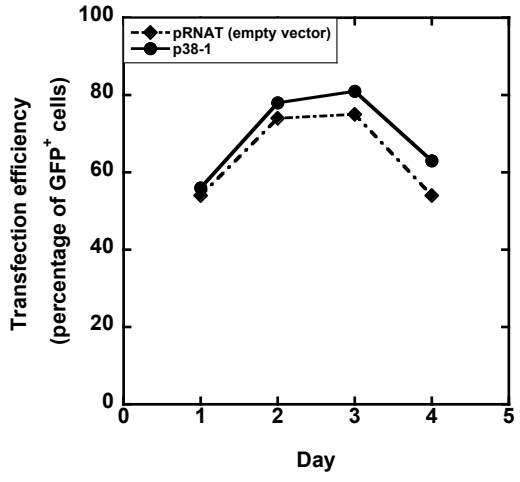

Figure 6.8. Transfection efficiency of K562 cells. Efficiency was determined by flow cytometric analysis of GFP expression. The data shows efficiencies for transfection with either empty vector (diamonds) or the siRNA-expression vector (circles).

Assessment of p38 MAPK knockdown

Following transfection of K562 cells with p38-1 siRNA, analysis of p38 MAPK expression was determined. Since transfection efficiency was high in this cell line, western blotting was utilized to assess p38 proteins levels in whole cell lysates. In general, the maximum decrease in target protein levels mediated by siRNA is typically observed 48-96 hours post transfection. Therefore, cell lysates were prepared every 24 hours for 4 days following electroporation and total p38 protein levels in control cells (received empty vector) were compared to those of siRNA treated K562 cells. Analysis of band intensity was performed with ImageQuant software. A 35-40% decrease in p38 expression was observed after 3-4 days in cells transfected with the p38-1 construct in comparison to control cells receiving the empty vector (Fig 6.9).

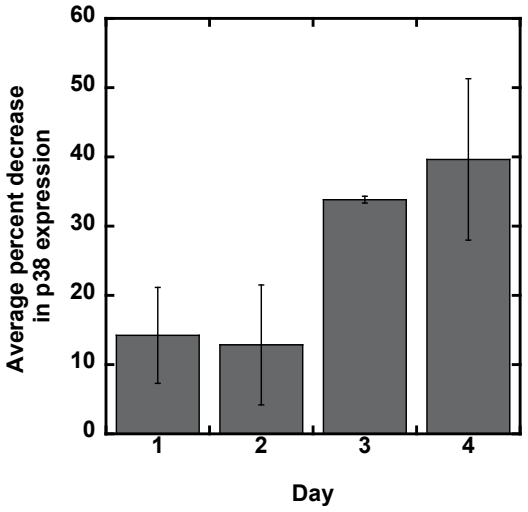

Figure 6.9. **Knockdown of p38 in K562 cells receiving p38-1 siRNA expression vector.**

K562 cells were transfected with p38-1 and subsequently analyzed for p38 expression using western blotting. Protein levels were quantified using Image Quant 5.2 analysis software. The data shown represents the average percentage decrease in p38 expression following transfection (n = 2).

Characterization of erythroid and megakaryocyte differentiation of K562 cells

Both erythroid and megakaryocyte differentiation of K562 cells were characterized prior to assessing the effect of p38 siRNA on differentiation.

Phorbol 12-myristate 13-acetate (PMA)-induced megakaryocyte differentiation of K562 cells

Surface marker expression in response to PMA and butyrate treatment was characterized using flow cytometry (Fig 6.10). Expression is reported as the ratio of geometric means: stained to isotype control. As expected, unstimulated K562 cells were negative for the megakaryocytic markers CD41, CD42, and CD61, but did express glycophorin A (GlyA). Treatment of cells with 10 ng/ml PMA resulted in decreased expression of GlyA and a gradual increase in CD41 and CD61 expression. Cells remained negative for CD42 expression. The effect of PMA on cell growth and morphology was also examined. Unstimulated K562 cells grow in suspension and typically double ~ every 24 hours. However, upon PMA addition, cell proliferation ceased and the majority of cells became adherent. An increase in cell size was also observed with PMA treatment (Fig 6.11).

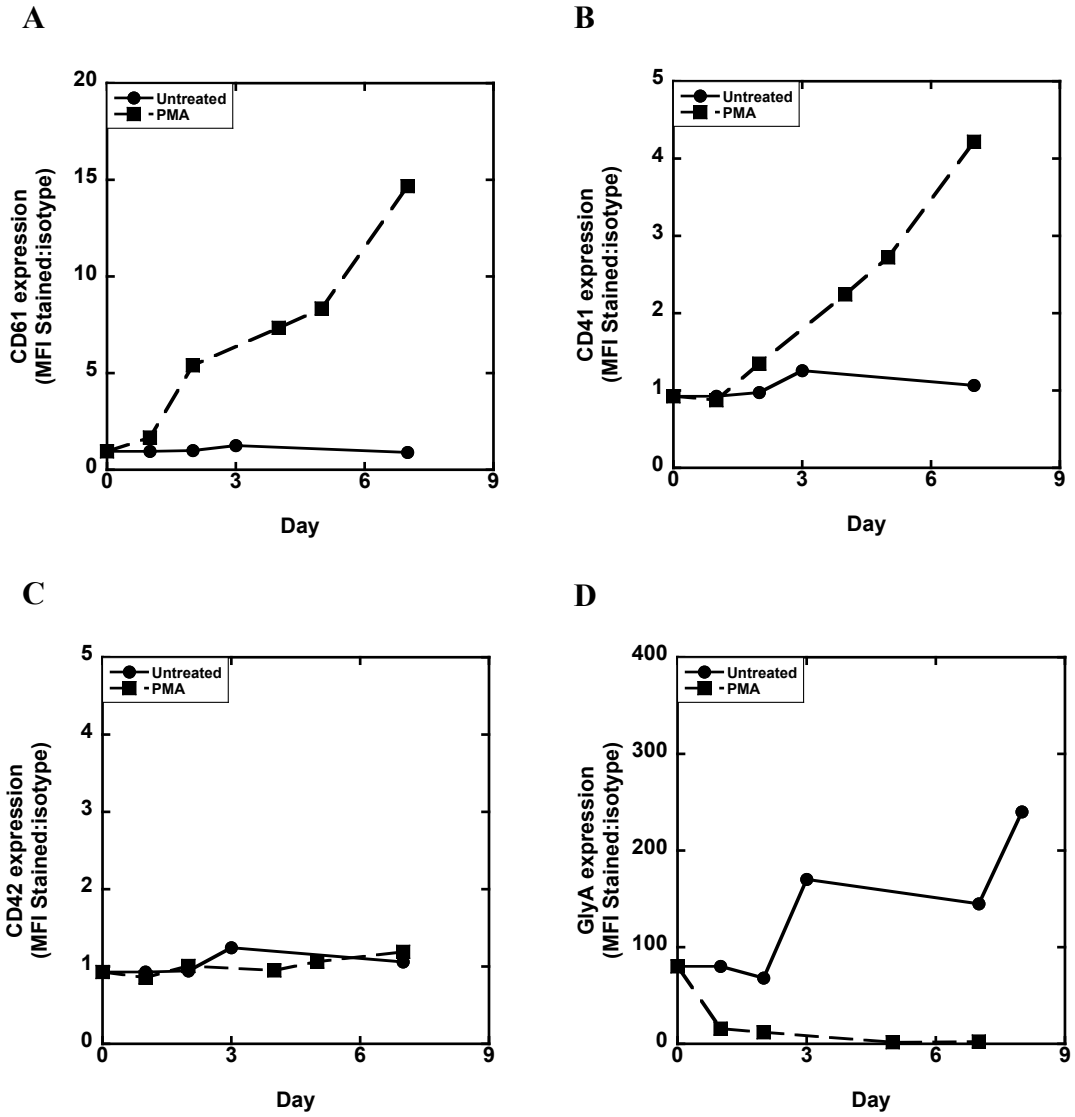

Figure 6.10. **PMA induced megakaryocytic differentiation of K562 cells.**

K562 cells were treated with 10 ng/ml PMA (squares) or an equal volume of DMSO (circles) on Day 0. The data shows surface marker expression of (A) CD61, (B) CD41, (C) CD42, and (D) glycophorin A over time relative to the fluorescence intensity of an isotype control.

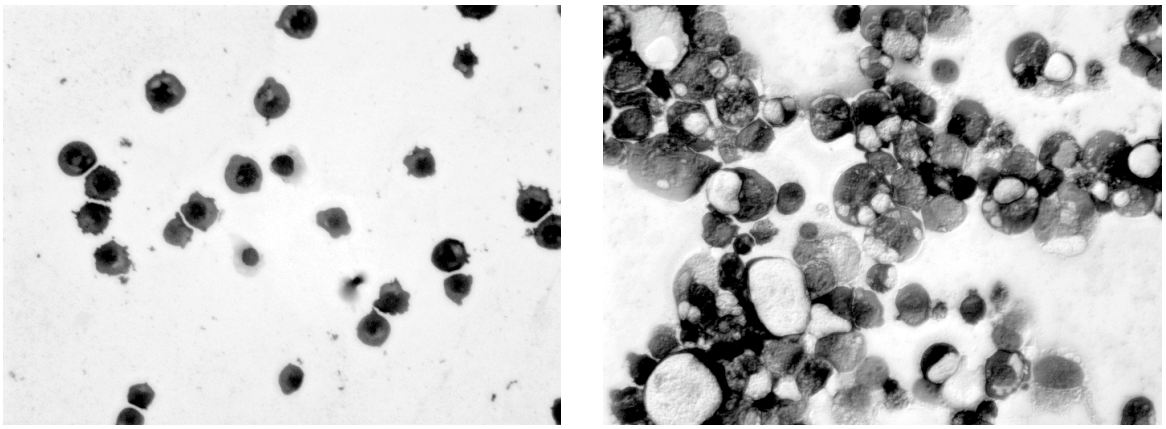

Figure 6.11. Morphology of PMA treated K562 cells.

Images show giemsa staining of K562 cells after 4 days of treatment with either 10 ng/ml PMA (right) or an equal volume of DMSO (left).

Butyrate-induced erythroid differentiation of K562 cells

Erythroid differentiation of K562 cells was induced by treatment with 0.6 mM butyrate. K562 cell growth and GlyA expression were assessed. Butyrate had a slightly negative effect on cell proliferation (Fig 6.12A) and treatment resulted in increased GlyA expression (Fig 6.12B). Others report that use of a p38 inhibitor (SB203580) prevents butyrate-induced erythroid differentiation as assessed by benzidine staining of hemoglobin. Therefore, we examined whether SB203580 treatment also prevents induced GlyA expression. SB203580 was added to cultures 1 hour before stimulation with 0.6 mM butyrate and cells were subsequently stained for GlyA. Treatment with SB203580 prevented any increase in GlyA expression with butyrate (Fig 6.12B).

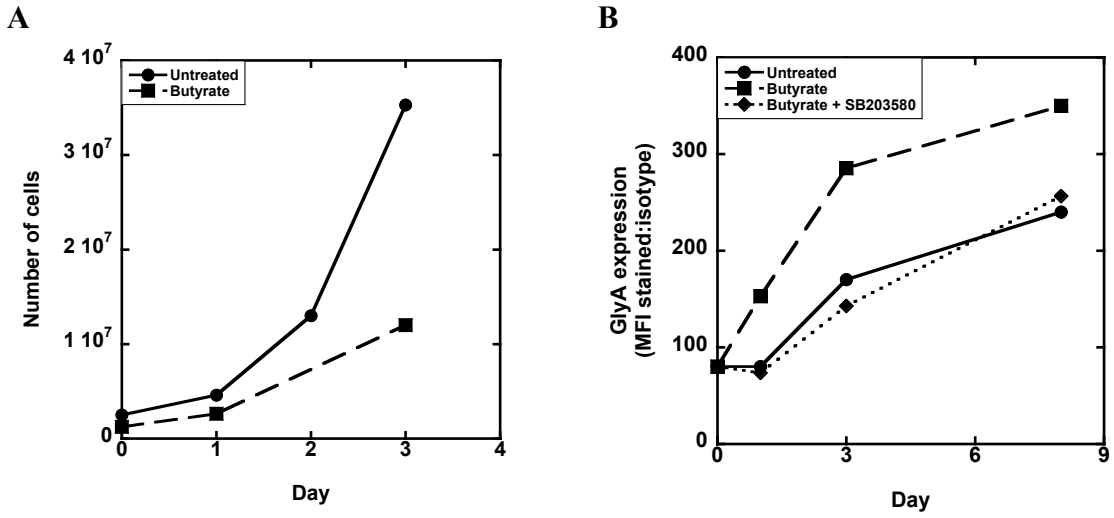

Figure 6.12. Butyrate-induced differentiation of K562 cells.

(A) Butyrate inhibits expansion of K562 cells. (B) GlyA expression was assessed using flow cytometry in untreated K562 cells (circles) and cells treated with either 0.6 mM butyrate (squares) or butyrate + SB203580 (diamonds).

Effect of p38 MAPK knockdown on erythroid differentiation

On Days 3 and 4 post transfection – presumably at the point of highest p38 knock down – cells were treated with 0.6 mM sodium butyrate to induce erythroid differentiation. Following induction, cells were assessed for erythroid differentiation as determined by GlyA expression. K562 cells treated with a p38 chemical inhibitor (SB203580) prior to butyrate addition were included as a control. While SB203580 treatment prevented induced GlyA expression on cells, the p38 siRNA expression vector was not effective (Fig 6.13). This suggests that greater knockdown of p38 expression than that obtained with the p38-1 sequence is necessary to reduce butyrate-induced erythroid differentiation. It is recognized that different siRNA sequences designed to target a single gene may differ in their efficacy in silencing; therefore, continuation

of this work would have required the comparison of 3-5 siRNA sequences specific to the target. Additionally, pools of several siRNA sequences could have been explored to more effectively silence gene expression rather than relying on a single siRNA sequence. A recent publication which uses a commercially available pool of siRNAs to silence p38 and reduce erythroid differentiation of K562 cells show that p38 remaining from incomplete gene silencing may be sufficient to allow erythroid differentiation.[200] This confirms that the level of gene knockdown is of critical importance in determining whether gene silencing produces an observable effect on cell phenotype. Had a substantial effect on erythroid differentiation been observed, studies would have been conducted to confirm that PMA-induced differentiation of K562 cells was unaltered, as it is expected that p38 plays no role in megakaryocyte differentiation.

In summary, molecular cloning methods for generating siRNA expression vectors were developed along with optimal conditions for DNA delivery to two megakaryocytic cell lines, K562 and MEG-01 cells. Future extensions of this work would have focused on delivery of siRNA to primary hematopoietic stem cells with the anticipation that primary cell transfection would be challenging and may require the use of viral vectors to obtain sufficient efficiency. Also, several siRNA sequences for each target gene would be tested for obtaining optimal knockdown.

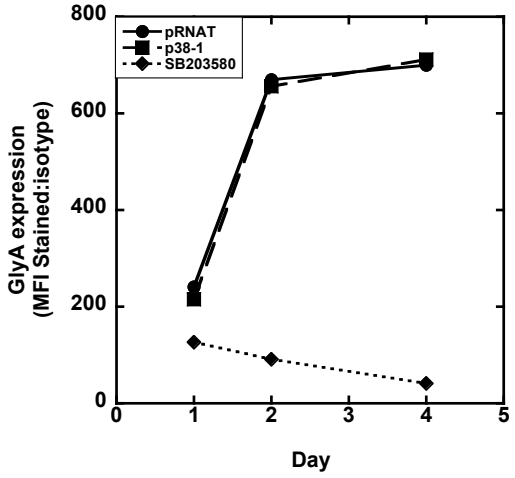

Figure 6.13. Effect of p38 knockdown on GlyA expression in butyrate-treated K562 cells.

K562 cells were transfected with either the empty vector pRNAT (circles) or a p38 siRNA expression vector (squares). On day 3 post-transfection, cells were treated with 0.6 mM butyrate to induce erythroid differentiation. Following induction, cells were assessed for GlyA expression. Cells treated with the p38 inhibitor SB203580 prior to butyrate addition were included as a control.

7. References

1. Rongvaux A, Andris F, Van Gool F, Leo O. Reconstructing eukaryotic NAD metabolism. Bioessays. 2003;25:683-690.

2. Debili N, Coulombel L, Croisille L, et al. Characterization of a bipotent erythro-megakaryocytic progenitor in human bone marrow. Blood. 1996;88:1284-1296.

3. Vannucchi AM, Paoletti F, Linari S, et al. Identification and characterization of a bipotent (erythroid and megakaryocytic) cell precursor from the spleen of phenylhydrazine-treated mice. Blood. 2000;95:2559-2568.

4. Kuroda J, Kimura S, Kobayashi Y, Wada K, Uoshima N, Yoshikawa T. Unusual myelodysplastic syndrome with the initial presentation mimicking idiopathic thrombocytopenic purpura. Acta Haematol. 2002;108:139-143.

5. Nurden AT. Qualitative disorders of platelets and megakaryocytes. J Thromb Haemost. 2005;3:1773-1782.

6. Balduini CL, Savoia A. Inherited thrombocytopenias: molecular mechanisms. Semin Thromb Hemost. 2004;30:513-523.

7. Elting LS, Rubenstein EB, Martin CG, et al. Incidence, cost, and outcomes of bleeding and chemotherapy dose modification among solid tumor patients with chemotherapy-induced thrombocytopenia. J Clin Oncol. 2001;19:1137-1146.

8. Vadhan-Raj S, Patel S, Bueso-Ramos C, et al. Importance of Predosing of Recombinant Human Thrombopoietin to Reduce Chemotherapy-Induced Early Thrombocytopenia. J Clin Oncol. 2003;21:3158-3167.

9. de Sauvage FJ, Hass PE, Spencer SD, et al. Stimulation of megakaryocytopoiesis and thrombopoiesis by the c-Mpl ligand. Nature. 1994;369:533-538.

10. LaIuppa JA, Papoutsakis ET, Miller WM. Evaluation of cytokines for expansion of the megakaryocyte and granulocyte lineages. Stem Cells. 1997;15:198-206.

11. Ryu KH, Chun S, Carbonierre S, et al. Apoptosis and megakaryocytic differentiation during ex vivo expansion of human cord blood CD34+ cells using thrombopoietin. Br J Haematol. 2001;113:470-478.

12. Falcieri E, Bassini A, Pierpaoli S, et al. Ultrastructural characterization of maturation, platelet release, and senescence of human cultured megakaryocytes. Anat Rec. 2000;258:90-99.

13. Li J, Kuter DJ. The end is just the beginning: megakaryocyte apoptosis and platelet release. Int J Hematol. 2001;74:365-374.

14. Mattia G, Vulcano F, Milazzo L, et al. Different ploidy levels of megakaryocytes generated from peripheral or cord blood CD34+ cells are correlated with different levels of platelet release. Blood. 2002;99:888-897.

15. Clarke MC, Savill J, Jones DB, Noble BS, Brown SB. Compartmentalized megakaryocyte death generates functional platelets committed to caspase-independent death. J Cell Biol. 2003;160:577-587.

16. Ryu KH, Chun S, Carbonierre S, et al. Apoptosis and megakaryocytic differentiation during ex vivo expansion of human cord blood CD34+ cells using thrombopoietin. Br J Haematol. 2001;113:470-478.

17. Li J, Kuter DJ. The end is just the beginning: megakaryocyte apoptosis and platelet release. Int J Hematol. 2001;74:365-374.

18. Mostafa SS, Miller WM, Papoutsakis ET. Oxygen tension influences the differentiation, maturation and apoptosis of human megakaryocytes. Br J Haematol. 2000;111:879-889.

19. Williams JL, Pipia GG, Datta NS, Long MW. Thrombopoietin requires additional megakaryocyte-active cytokines for optimal ex vivo expansion of megakaryocyte precursor cells. Blood. 1998;91:4118-4126.

20. Proulx C, Boyer L, Hurnanen DR, Lemieux R. Preferential Ex Vivo Expansion of Megakaryocytes from Human Cord Blood CD34(+)-Enriched Cells in the Presence of Thrombopoietin and Limiting Amounts of Stem Cell Factor and Flt-3 Ligand. J Hematother Stem Cell Res. 2003;12:179-188.

21. Kie JH, Yang WI, Lee MK, et al. Decrease in apoptosis and increase in polyploidization of megakaryocytes by stem cell factor during ex vivo expansion of human cord blood CD34+ cells using thrombopoietin. Stem Cells. 2002;20:73-79.

22. Guerriero R, Mattia G, Testa U, et al. Stromal cell-derived factor 1alpha increases polyploidization of megakaryocytes generated by human hematopoietic progenitor cells. Blood. 2001;97:2587-2595.

23. Yang H, Miller WM, Papoutsakis ET. Higher pH promotes megakaryocytic maturation and apoptosis. Stem Cells. 2002;20:320-328.

24. Proulx C, Dupuis N, St-Amour I, Boyer L, Lemieux R. Increased megakaryopoiesis in cultures of CD34-enriched cord blood cells maintained at 39°C. Biotechnology and Bioengineering. 2004;88:675-680.

25. Lannutti BJ, Blake N, Gandhi MJ, Reems JA, Drachman JG. Induction of polyploidization in leukemic cell lines and primary bone marrow by Src kinase inhibitor SU6656. Blood. 2005;105:3875-3878.

26. Han P, Guo XH, Story CJ. Enhanced expansion and maturation of megakaryocytic progenitors by fibronectin. Cytotherapy. 2002;4:277-283.

27. Fox NE, Kaushansky K. Engagement of integrin alpha4beta1 enhances thrombopoietin-induced megakaryopoiesis. Exp Hematol. 2005;33:94-99.

28. Schick PK, Wojenski CM, He X, Walker J, Marcinkiewicz C, Niewiarowski S. Integrins involved in the adhesion of megakaryocytes to fibronectin and fibrinogen. Blood. 1998;92:2650-2656.

29. Zauli G, Bassini A, Vitale M, et al. Thrombopoietin enhances the alpha IIb beta 3-dependent adhesion of megakaryocytic cells to fibrinogen or fibronectin through PI 3 kinase. Blood. 1997;89:883-895.

30. Sato T, Ono M, Fujita H, et al. Development of a liquid culture system for megakaryocyte terminal differentiation: fibrinogen promotes megakaryocytopoiesis but not thrombopoiesis. Br J Haematol. 2003;121:315-323.

31. Knip M, Douek IF, Moore WP, et al. Safety of high-dose nicotinamide: a review. Diabetologia. 2000;43:1337-1345.

32. Capuzzi DM, Morgan JM, Brusco OA, Jr., Intenzo CM. Niacin dosing: relationship to benefits and adverse effects. Curr Atheroscler Rep. 2000;2:64-71.

33. D'Amours D, Desnoyers S, D'Silva I, Poirier GG. Poly(ADP-ribosyl)ation reactions in the regulation of nuclear functions. Biochem J. 1999;342 (Pt 2):249-268.

34. Frouin I, Maga G, Denegri M, et al. Human proliferating cell nuclear antigen, poly(ADP-ribose) polymerase-1, and p21waf1/cip1. A dynamic exchange of partners. J Biol Chem. 2003;278:39265-39268.

35. Kumari SR, Mendoza-Alvarez H, Alvarez-Gonzalez R. Functional interactions of p53 with poly(ADP-ribose) polymerase (PARP) during apoptosis following DNA damage: covalent poly(ADP-ribosyl)ation of p53 by exogenous PARP and noncovalent binding of p53 to the M(r) 85,000 proteolytic fragment. Cancer Res. 1998;58:5075-5078.

36. Kanai M, Tong WM, Sugihara E, Wang ZQ, Fukasawa K, Miwa M. Involvement of poly(ADP-Ribose) polymerase 1 and poly(ADP-Ribosyl)ation in regulation of centrosome function. Mol Cell Biol. 2003;23:2451-2462.

37. Grubisha O, Smith BC, Denu JM. Small molecule regulation of Sir2 protein deacetylases. Febs J. 2005;272:4607-4616.

38. Blander G, Guarente L. The Sir2 family of protein deacetylases. Annual Review of Biochemistry. 2004;73:417-435.

39. Bitterman KJ, Anderson RM, Cohen HY, Latorre-Esteves M, Sinclair DA. Inhibition of silencing and accelerated aging by nicotinamide, a putative negative regulator of yeast sir2 and human SIRT1. J Biol Chem. 2002;277:45099-45107.

40. Ito A, Kawaguchi Y, Lai CH, et al. MDM2-HDAC1-mediated deacetylation of p53 is required for its degradation. Embo J. 2002;21:6236-6245.

41. North BJ, Marshall BL, Borra MT, Denu JM, Verdin E. The human Sir2 ortholog, SIRT2, is an NAD+-dependent tubulin deacetylase. Mol Cell. 2003;11:437-444.

42. Takemura R, Okabe S, Umeyama T, Kanai Y, Cowan NJ, Hirokawa N. Increased microtubule stability and alpha tubulin acetylation in cells transfected with microtubule-associated proteins MAP1B, MAP2 or tau. J Cell Sci. 1992;103 (Pt 4):953-964.

43. Patel SR, Richardson JL, Schulze H, et al. Differential roles of microtubule assembly and sliding in proplatelet formation by megakaryocytes. Blood. 2005;106:4076-4085.

44. Nagata Y, Muro Y, Todokoro K. Thrombopoietin-induced polyploidization of bone marrow megakaryocytes is due to a unique regulatory mechanism in late mitosis. J Cell Biol. 1997;139:449-457.

45. Chong ZZ, Lin SH, Maiese K. The NAD+ precursor nicotinamide governs neuronal survival during oxidative stress through protein kinase B coupled to FOXO3a and mitochondrial membrane potential. J Cereb Blood Flow Metab. 2004;24:728-743.

46. Chong ZZ, Lin SH, Li F, Maiese K. The sirtuin inhibitor nicotinamide enhances neuronal cell survival during acute anoxic injury through AKT, BAD, PARP, and mitochondrial associated "anti-apoptotic" pathways. Curr Neurovasc Res. 2005;2:271-285.

47. Barry FA, Graham GJ, Fry MJ, Gibbins JM. Regulation of glycogen synthase kinase 3 in human platelets: a possible role in platelet function? FEBS Lett. 2003;553:173-178.

48. Harms C, Albrecht K, Harms U, et al. Phosphatidylinositol 3-Akt-kinase-dependent phosphorylation of p21(Waf1/Cip1) as a novel mechanism of neuroprotection by glucocorticoids. J Neurosci. 2007;27:4562-4571.

49. Fatrai S, Elghazi L, Balcazar N, et al. Akt induces beta-cell proliferation by regulating cyclin D1, cyclin D2, and p21 levels and cyclin-dependent kinase-4 activity. Diabetes. 2006;55:318-325.

50. Gera JF, Mellinghoff IK, Shi Y, et al. AKT activity determines sensitivity to mammalian target of rapamycin (mTOR) inhibitors by regulating cyclin D1 and c-myc expression. J Biol Chem. 2004;279:2737-2746.

51. Guerriero R, Parolini I, Testa U, et al. Inhibition of TPO-induced MEK or mTOR activity induces opposite effects on the ploidy of human differentiating megakaryocytes. J Cell Sci. 2006;119:744-752.

52. McLure KG, Takagi M, Kastan MB. NAD+ modulates p53 DNA binding specificity and function. Mol Cell Biol. 2004;24:9958-9967.

53. Evans J, Wang TC, Heyes MP, Markey SP. LC/MS analysis of NAD biosynthesis using stable isotope pyridine precursors. Anal Biochem. 2002;306:197-203.

54. Micheli V, Simmonds HA, Sestini S, Ricci C. Importance of nicotinamide as an NAD precursor in the human erythrocyte. Arch Biochem Biophys. 1990;283:40-45.

55. Jackson TM, Rawling JM, Roebuck BD, Kirkland JB. Large supplements of nicotinic acid and nicotinamide increase tissue NAD+ and poly(ADP-ribose) levels but do not affect diethylnitrosamine-induced altered hepatic foci in Fischer-344 rats. J Nutr. 1995;125:1455-1461.

56. Klaidman L, Morales M, Kem S, Yang J, Chang ML, Adams JD, Jr. Nicotinamide offers multiple protective mechanisms in stroke as a precursor for NAD+, as a PARP inhibitor and by partial restoration of mitochondrial function. Pharmacology. 2003;69:150-157.

57. Grant RS, Kapoor V. Murine glial cells regenerate NAD, after peroxide-induced depletion, using either nicotinic acid, nicotinamide, or quinolinic acid as substrates. J Neurochem. 1998;70:1759-1763.

58. O'Dorisio MS, Barker KL. Effects of estradiol on the biosynthesis of pyridine nucleotide coenzymes in the rat uterus. Biol Reprod. 1976;15:504-510.

59. Vaziri C, Saxena S, Jeon Y, et al. A p53-dependent checkpoint pathway prevents rereplication. Mol Cell. 2003;11:997-1008.

60. Elliott RB, Pilcher CC, Fergusson DM, Stewart AW. A population based strategy to prevent insulin-dependent diabetes using nicotinamide. J Pediatr Endocrinol Metab. 1996;9:501-509.

61. Gale EA, Bingley PJ, Emmett CL, Collier T. European Nicotinamide Diabetes Intervention Trial (ENDIT): a randomised controlled trial of intervention before the onset of type 1 diabetes. Lancet. 2004;363:925-931.

62. Lampeter EF, Klinghammer A, Scherbaum WA, et al. The Deutsche Nicotinamide Intervention Study: an attempt to prevent type 1 diabetes. DENIS Group. Diabetes. 1998;47:980-984.

63. Kim JY, Chi JK, Kim EJ, Park SY, Kim YW, Lee SK. Inhibition of diabetes in non-obese diabetic mice by nicotinamide treatment for 5 weeks at the early age. J Korean Med Sci. 1997;12:293-297.

64. O'Brien BA, Harmon BV, Cameron DP, Allan DJ. Nicotinamide prevents the development of diabetes in the cyclophosphamide-induced NOD mouse model by reducing beta-cell apoptosis. J Pathol. 2000;191:86-92.

65. Yamada K, Nonaka K, Hanafusa T, Miyazaki A, Toyoshima H, Tarui S. Preventive and therapeutic effects of large-dose nicotinamide injections on diabetes associated with insulitis. An observation in nonobese diabetic (NOD) mice. Diabetes. 1982;31:749-753.

66. Winter SL, Boyer JL. Hepatic toxicity from large doses of vitamin B3 (nicotinamide). N Engl J Med. 1973;289:1180-1182.

67. Dragovic J, Kim SH, Brown SL, Kim JH. Nicotinamide pharmacokinetics in patients. Radiother Oncol. 1995;36:225-228.

68. Bernier J, Denekamp J, Rojas A, et al. ARCON: accelerated radiotherapy with carbogen and nicotinamide in head and neck squamous cell carcinomas. The experience of the Co-operative group of radiotherapy of the european organization for research and treatment of cancer (EORTC). Radiother Oncol. 2000;55:111-119.

69. Hoskin PJ, Stratford MR, Saunders MI, Hall DW, Dennis MF, Rojas A. Administration of nicotinamide during chart: pharmacokinetics, dose escalation, and clinical toxicity. Int J Radiat Oncol Biol Phys. 1995;32:1111-1119.

70. Kaanders JH, Stratford MR, Liefers J, et al. Administration of nicotinamide during a five- to seven-week course of radiotherapy: pharmacokinetics, tolerance, and compliance. Radiother Oncol. 1997;43:67-73.

71. Horsman MR. Nicotinamide and other benzamide analogs as agents for overcoming hypoxic cell radiation resistance in tumours. A review. Acta Oncol. 1995;34:571-587.

72. Horsman MR, Hoyer M, Honess DJ, Dennis IF, Overgaard J. Nicotinamide pharmacokinetics in humans and mice: a comparative assessment and the implications for radiotherapy. Radiother Oncol. 1993;27:131-139.

73. Zimmet J, Ravid K. Polyploidy: occurrence in nature, mechanisms, and significance for the megakaryocyte-platelet system. Exp Hematol. 2000;28:3-16.

74. Vitrat N, Cohen-Solal K, Pique C, et al. Endomitosis of human megakaryocytes are due to abortive mitosis. Blood. 1998;91:3711-3723.

75. Italiano JE, Jr., Lecine P, Shivdasani RA, Hartwig JH. Blood platelets are assembled principally at the ends of proplatelet processes produced by differentiated megakaryocytes. J Cell Biol. 1999;147:1299-1312.

76. Zauli G, Vitale M, Falcieri E, et al. In vitro senescence and apoptotic cell death of human megakaryocytes. Blood. 1997;90:2234-2243.

77. Kaushansky K. Thrombopoietin: the primary regulator of platelet production. Blood. 1995;86:419-431.

78. Banu N, Wang JF, Deng B, Groopman JE, Avraham H. Modulation of megakaryocytopoiesis by thrombopoietin: the c-Mpl ligand. Blood. 1995;86:1331-1338.

79. Debili N, Wendling F, Cosman D, et al. The Mpl receptor is expressed in the megakaryocytic lineage from late progenitors to platelets. Blood. 1995;85:391-401.

80. Maurer AM, Liu Y, Caen JP, Han ZC. Ex vivo expansion of megakaryocytic cells. Int J Hematol. 2000;71:203-210.

81. Tomer A. Human marrow megakaryocyte differentiation: multiparameter correlative analysis identifies von Willebrand factor as a sensitive and distinctive marker for early (2N and 4N) megakaryocytes. Blood. 2004;104:2722-2727.

82. Raslova H, Baccini V, Loussaief L, et al. Mammalian target of rapamycin (mTOR) regulates both proliferation of megakaryocyte progenitors and late stages of megakaryocyte differentiation. Blood. 2006;107:2303-2310.

83. Ma D, Sun Y, Lin D, et al. CD226 is expressed on the megakaryocytic lineage from hematopoietic stem cells/progenitor cells and involved in its polyploidization. Eur J Haematol. 2005;74:228-240.

84. De Bruyn C, Delforge A, Martiat P, Bron D. Ex vivo expansion of megakaryocyte progenitor cells: cord blood versus mobilized peripheral blood. Stem Cells Dev. 2005;14:415-424.

85. Fugman DA, Witte DP, Jones CL, Aronow BJ, Lieberman MA. In vitro establishment and characterization of a human megakaryoblastic cell line. Blood. 1990;75:1252-1261.

86. Witte DP, Harris RE, Jenski LJ, Lampkin BC. Megakaryoblastic leukemia in an infant. Establishment of a megakaryocytic tumor cell line in athymic nude mice. Cancer. 1986;58:238-244.

87. Iancu-Rubin C, Nasrallah CA, Atweh GF. Stathmin prevents the transition from a normal to an endomitotic cell cycle during megakaryocytic differentiation. Cell Cycle. 2005;4:1774-1782.

88. Hevehan DL, Miller WM, Papoutsakis ET. Differential expression and phosphorylation of distinct STAT3 proteins during granulocytic differentiation. Blood. 2002;99:1627-1637.

89. Yang H, Haddad H, Tomas C, Alsaker K, Papoutsakis ET. A segmental nearest neighbor normalization and gene identification method gives superior results for DNA-array analysis. Proc Natl Acad Sci U S A. 2003;100:1122-1127.

90. Saeed AI, Sharov V, White J, et al. TM4: a free, open-source system for microarray data management and analysis. Biotechniques. 2003;34:374-378.

91. Balduini A, d'Apolito M, Arcelli D, et al. Cord blood in vitro expanded CD41 cells: identification of novel components of megakaryocytopoiesis. J Thromb Haemost. 2006;4:848-860.

92. Cramer EM, Norol F, Guichard J, et al. Ultrastructure of platelet formation by human megakaryocytes cultured with the Mpl ligand. Blood. 1997;89:2336-2346.

93. Jagtap P, Szabo C. Poly(ADP-ribose) polymerase and the therapeutic effects of its inhibitors. Nat Rev Drug Discov. 2005;4:421-440.

94. Grozinger CM, Chao ED, Blackwell HE, Moazed D, Schreiber SL. Identification of a class of small molecule inhibitors of the sirtuin family of NAD-dependent deacetylases by phenotypic screening. J Biol Chem. 2001;276:38837-38843.

95. Bedalov A, Gatbonton T, Irvine WP, Gottschling DE, Simon JA. Identification of a small molecule inhibitor of Sir2p. Proc Natl Acad Sci U S A. 2001;98:15113-15118.

96. Szabo C. Nicotinamide: a jack of all trades (but master of none?). Intensive Care Med. 2003;29:863-866.

97. Scott GS, Szabo C, Hooper DC. Poly(ADP-ribose) polymerase activity contributes to peroxynitrite-induced spinal cord neuronal cell death in vitro. J Neurotrauma. 2004;21:1255-1263.

98. Shino Y, Itoh Y, Kubota T, Yano T, Sendo T, Oishi R. Role of poly(ADP-ribose)polymerase in cisplatin-induced injury in LLC-PK1 cells. Free Radic Biol Med. 2003;35:966-977.

99. Du L, Zhang X, Han YY, et al. Intra-mitochondrial poly(ADP-ribosylation) contributes to NAD+ depletion and cell death induced by oxidative stress. J Biol Chem. 2003;278:18426-18433.

100. Endres M, Scott GS, Salzman AL, Kun E, Moskowitz MA, Szabo C. Protective effects of 5-iodo-6-amino-1,2-benzopyrone, an inhibitor of poly(ADP-ribose) synthetase against peroxynitrite-induced glial damage and stroke development. Eur J Pharmacol. 1998;351:377-382.

101. Metcalf D, Carpinelli MR, Hyland C, et al. Anomalous megakaryocytopoiesis in mice with mutations in the c-Myb gene. Blood. 2005;105:3480-3487.

102. Sakamoto H, Dai G, Tsujino K, et al. Proper levels of c-Myb are discretely defined at distinct steps of hematopoietic cell development. Blood. 2006;108:896-903.

103. Hayano T, Kikuchi M. Molecular cloning of the cDNA encoding a novel protein disulfide isomerase-related protein (PDIR). FEBS Lett. 1995;372:210-214.

104. Jessop CE, Chakravarthi S, Watkins RH, Bulleid NJ. Oxidative protein folding in the mammalian endoplasmic reticulum. Biochem Soc Trans. 2004;32:655-658.

105. Dryden SC, Nahhas FA, Nowak JE, Goustin AS, Tainsky MA. Role for human SIRT2 NAD-dependent deacetylase activity in control of mitotic exit in the cell cycle. Mol Cell Biol. 2003;23:3173-3185.

106. Michishita E, Park JY, Burneskis JM, Barrett JC, Horikawa I. Evolutionarily conserved and nonconserved cellular localizations and functions of human SIRT proteins. Mol Biol Cell. 2005;16:4623-4635.

107. Ford E, Voit R, Liszt G, Magin C, Grummt I, Guarente L. Mammalian Sir2 homolog SIRT7 is an activator of RNA polymerase I transcription. Genes Dev. 2006;20:1075-1080.

108. van den Oudenrijn S, von dem Borne AE, de Haas M. Differences in megakaryocyte expansion potential between CD34(+) stem cells derived from cord blood, peripheral blood, and bone marrow from adults and children. Exp Hematol. 2000;28:1054-1061.

109. Giammona LM, Fuhrken PG, Papoutsakis ET, Miller WM. Nicotinamide (vitamin B3) increases the polyploidisation and proplatelet formation of cultured primary human megakaryocytes. Br J Haematol. 2006;135:554-566.

110. Olsson A, Olofsson T, Pero RW. Specific binding and uptake of extracellular nicotinamide in human leukemic K-562 cells. Biochem Pharmacol. 1993;45:1191-1200.

111. Devin A, Nogueira V, Leverve X, Guerin B, Rigoulet M. Allosteric activation of pyruvate kinase via NAD+ in rat liver cells. Eur J Biochem. 2001;268:3943-3949.

112. Miyazaki R, Ogata H, Kobayashi Y. Requirement of thrombopoietin-induced activation of ERK for megakaryocyte differentiation and of p38 for erythroid differentiation. Ann Hematol. 2001;80:284-291.

113. Wagner TC, Scott MD. Single Extraction Method for the Spectrophotometric Quantification of Oxidized and Reduced Pyridine Nucleotides in Erythrocytes. Analytical Biochemistry. 1994;222:417-426.

114. Shah GM, Poirier D, Duchaine C, et al. Methods for Biochemical-Study of Poly(Adp-Ribose) Metabolism in-Vitro and in-Vivo. Analytical Biochemistry. 1995;227:1-13.

115. Fingar DC, Salama S, Tsou C, Harlow E, Blenis J. Mammalian cell size is controlled by mTOR and its downstream targets S6K1 and 4EBP1/eIF4E. Genes Dev. 2002;16:1472-1487.

116. Yonezawa K, Tokunaga C, Oshiro N, Yoshino K. Raptor, a binding partner of target of rapamycin. Biochem Biophys Res Commun. 2004;313:437-441.

117. Tee AR, Manning BD, Roux PP, Cantley LC, Blenis J. Tuberous sclerosis complex gene products, Tuberin and Hamartin, control mTOR signaling by acting as a GTPase-activating protein complex toward Rheb. Curr Biol. 2003;13:1259-1268.

118. Tee AR, Fingar DC, Manning BD, Kwiatkowski DJ, Cantley LC, Blenis J. Tuberous sclerosis complex-1 and -2 gene products function together to inhibit mammalian target of rapamycin (mTOR)-mediated downstream signaling. Proc Natl Acad Sci U S A. 2002;99:13571-13576.

119. Drayer AL, Olthof SG, Vellenga E. Mammalian target of rapamycin is required for thrombopoietin-induced proliferation of megakaryocyte progenitors. Stem Cells. 2006;24:105-114.

120. Lindsley JE, Rutter J. Nutrient sensing and metabolic decisions. Comp Biochem Physiol B Biochem Mol Biol. 2004;139:543-559.

121. Sarbassov DD, Ali SM, Sabatini DM. Growing roles for the mTOR pathway. Curr Opin Cell Biol. 2005;17:596-603.

122. Sekulic A, Hudson CC, Homme JL, et al. A direct linkage between the phosphoinositide 3-kinase-AKT signaling pathway and the mammalian target of rapamycin in mitogen-stimulated and transformed cells. Cancer Res. 2000;60:3504-3513.

123. Nave BT, Ouwens M, Withers DJ, Alessi DR, Shepherd PR. Mammalian target of rapamycin is a direct target for protein kinase B: identification of a convergence point for opposing effects of insulin and amino-acid deficiency on protein translation. Biochem J. 1999;344 Pt 2:427-431.

124. Rolfe M, McLeod LE, Pratt PF, Proud CG. Activation of protein synthesis in cardiomyocytes by the hypertrophic agent phenylephrine requires the activation of ERK and involves phosphorylation of tuberous sclerosis complex 2 (TSC2). Biochem J. 2005;388:973-984.

125. Roux PP, Ballif BA, Anjum R, Gygi SP, Blenis J. Tumor-promoting phorbol esters and activated Ras inactivate the tuberous sclerosis tumor suppressor complex via p90 ribosomal S6 kinase. Proc Natl Acad Sci U S A. 2004;101:13489-13494.

126. Ma L, Chen Z, Erdjument-Bromage H, Tempst P, Pandolfi PP. Phosphorylation and functional inactivation of TSC2 by Erk implications for tuberous sclerosis and cancer pathogenesis. Cell. 2005;121:179-193.

127. Minamiguchi H, Kimura T, Urata Y, et al. Simultaneous signalling through c-mpl, c-kit and CXCR4 enhances the proliferation and differentiation of human megakaryocyte progenitors: possible roles of the PI3-K, PKC and MAPK pathways. Br J Haematol. 2001;115:175-185.

128. Fichelson S, Freyssinier JM, Picard F, et al. Megakaryocyte growth and development factor-induced proliferation and differentiation are regulated by the mitogen-activated protein kinase pathway in primitive cord blood hematopoietic progenitors. Blood. 1999;94:1601-1613.

129. Majka M, Ratajczak J, Villaire G, et al. Thrombopoietin, but not cytokines binding to gp130 protein-coupled receptors, activates MAPKp42/44, AKT, and STAT proteins in normal human CD34+ cells, megakaryocytes, and platelets. Exp Hematol. 2002;30:751-760.

130. Hasmann M, Schemainda I. FK866, a highly specific noncompetitive inhibitor of nicotinamide phosphoribosyltransferase, represents a novel mechanism for induction of tumor cell apoptosis. Cancer Res. 2003;63:7436-7442.

131. Matsumura I, Kanakura Y. Molecular control of megakaryopoiesis and thrombopoiesis. Int J Hematol. 2002;75:473-483.

132. Chang F, Lee JT, Navolanic PM, et al. Involvement of PI3K/Akt pathway in cell cycle progression, apoptosis, and neoplastic transformation: a target for cancer chemotherapy. Leukemia. 2003;17:590-603.

133. Datta SR, Brunet A, Greenberg ME. Cellular survival: a play in three Akts. Genes Dev. 1999;13:2905-2927.

134. SA A. A Study to Assess APO866 for the Treatment for Advanced Melanoma. ClinicalTrials.gov Identifier: NCT00432107; Feb 2007.

135. Burkle A. Poly(ADP-ribose). The most elaborate metabolite of NAD+. Febs J. 2005;272:4576-4589.

136. Smith JS, Brachmann CB, Celic I, et al. A phylogenetically conserved NAD+-dependent protein deacetylase activity in the Sir2 protein family. Proc Natl Acad Sci U S A. 2000;97:6658-6663.

137. Fuhrken PG. Genome-Scale Transcriptional Analysis of Megakaryocytic Cell Cultures Reveals Insights into Lineage-Specific Differentiation. Chemical and Biological Engineering. Ph.D. Evanston: Northwestern University; 2007.

138. Voulgarelis M, Giannouli S, Ritis K, Tzioufas AG. Myelodysplasia-associated autoimmunity: clinical and pathophysiologic concepts. Eur J Clin Invest. 2004;34:690-700.

139. Van Etten RA, Shannon KM. Focus on myeloproliferative diseases and myelodysplastic syndromes. Cancer Cell. 2004;6:547-552.

140. Heaney ML, Golde DW. Myelodysplasia. N Engl J Med. 1999;340:1649-1660.

141. Hofmann WK, Kalina U, Koschmieder S, Seipelt G, Hoelzer D, Ottmann OG. Defective megakaryocytic development in myelodysplastic syndromes. Leuk Lymphoma. 2000;38:13-19.

142. Kobayashi Y, Ozawa M, Maruo N, Kondo M. Megakaryocytic ploidy in myelodysplastic syndromes. Leuk Lymphoma. 1993;9:55-61.

143. Geissler D, Zwierzina H, Pechlaner C, et al. Abnormal megakaryopoiesis in patients with myelodysplastic syndromes: analysis of cellular and humoral defects. Br J Haematol. 1989;73:29-35.

144. Li X, Pu Q. Megakaryocytopoiesis and apoptosis in patients with myelodysplastic syndromes. Leuk Lymphoma. 2005;46:387-391.

145. Raman BK, Van Slyck EJ, Riddle J, Sawdyk MA, Abraham JP, Saeed SM. Platelet function and structure in myeloproliferative disease, myelodysplastic syndrome, and secondary thrombocytosis. Am J Clin Pathol. 1989;91:647-655.

146. Sandstrom CE, Bender JG, Papoutsakis ET, Miller WM. Effects of CD34+ cell selection and perfusion on ex vivo expansion of peripheral blood mononuclear cells. Blood. 1995;86:958-970.

147. McAdams TA, Miller WM, Papoutsakis ET. pH is a potent modulator of erythroid differentiation. Br J Haematol. 1998;103:317-325.

148. Lam LT, Ronchini C, Norton J, Capobianco AJ, Bresnick EH. Suppression of erythroid but not megakaryocytic differentiation of human K562 erythroleukemic cells by notch-1. J Biol Chem. 2000;275:19676-19684.

149. Huang L. Transcriptional Analysis of Ex Vivo Granulocyte (Neutrophil) Development. Chemical and Biological Engineering. Ph.D. Evanston: Northwestern University; 2006.

150. Broudy VC, Kaushansky K. Biology of thrombopoietin. Curr Opin Pediatr. 1998;10:60-64.

151. Park H, Park SS, Jin EH, et al. Identification of functionally important residues of human thrombopoietin. J Biol Chem. 1998;273:256-261.

152. Terada M, Fujiki H, Marks PA, Sugimura T. Induction of erythroid differentiation of murine erythroleukemia cells by nicotinamide and related compounds. Proc Natl Acad Sci U S A. 1979;76:6411-6414.

153. Wang Z, Zhang Y, Kamen D, Lees E, Ravid K. Cyclin D3 is essential for megakaryocytopoiesis. Blood. 1995;86:3783-3788.

154. Datta NS, Williams JL, Long MW. Differential modulation of G1-S-phase cyclin-dependent kinase 2/cyclin complexes occurs during the acquisition of a polyploid DNA content. Cell Growth Differ. 1998;9:639-650.

155. Zimmet JM, Ladd D, Jackson CW, Stenberg PE, Ravid K. A role for cyclin D3 in the endomitotic cell cycle. Mol Cell Biol. 1997;17:7248-7259.

156. Geng Y, Yu Q, Sicinska E, et al. Cyclin E ablation in the mouse. Cell. 2003;114:431-443.

157. Garcia P, Frampton J, Ballester A, Cales C. Ectopic expression of cyclin E allows non-endomitotic megakaryoblastic K562 cells to establish re-replication cycles. Oncogene. 2000;19:1820-1833.

158. Kawasaki A, Matsumura I, Miyagawa J, et al. Downregulation of an AIM-1 kinase couples with megakaryocytic polyploidization of human hematopoietic cells. J Cell Biol. 2001;152:275-287.

159. Geddis AE, Kaushansky K. Megakaryocytes express functional Aurora-B kinase in endomitosis. Blood. 2004;104:1017-1024.

160. Geddis AE, Kaushansky K. Endomitotic megakaryocytes form a midzone in anaphase but have a deficiency in cleavage furrow formation. Cell Cycle. 2006;5:538-545.

161. Gaben AM, Saucier C, Bedin M, Redeuilh G, Mester J. Mitogenic activity of estrogens in human breast cancer cells does not rely on direct induction of mitogen-activated protein kinase/extracellularly regulated kinase or phosphatidylinositol 3-kinase. Mol Endocrinol. 2004;18:2700-2713.

162. Ciccarelli C, Marampon F, Scoglio A, et al. p21WAF1 expression induced by MEK/ERK pathway activation or inhibition correlates with growth arrest, myogenic differentiation and onco-phenotype reversal in rhabdomyosarcoma cells. Mol Cancer. 2005;4:41.

163. Luther-Wyrsch A, Costello E, Thali M, et al. Stable transduction with lentiviral vectors and amplification of immature hematopoietic progenitors from cord blood of preterm human fetuses. Hum Gene Ther. 2001;12:377-389.

164. Schomber T, Kalberer CP, Wodnar-Filipowicz A, Skoda RC. Gene silencing by lentivirus-mediated delivery of siRNA in human CD34+ cells. Blood. 2004;103:4511-4513.

165. Pohl M, Sprenger GA, Muller M. A new perspective on thiamine catalysis. Curr Opin Biotechnol. 2004;15:335-342.

166. Haupt Y, Maya R, Kazaz A, Oren M. Mdm2 promotes the rapid degradation of p53. Nature. 1997;387:296-299.

167. Sphyris N, Harrison DJ. p53 deficiency exacerbates pleiotropic mitotic defects, changes in nuclearity and polyploidy in transdifferentiating pancreatic acinar cells. Oncogene. 2005;24:2184-2194.

168. Baek KH, Shin HJ, Yoo JK, et al. p53 deficiency and defective mitotic checkpoint in proliferating T lymphocytes increase chromosomal instability through aberrant exit from mitotic arrest. J Leukoc Biol. 2003;73:850-861.

169. Bernofsky C, Swan M. An improved cycling assay for nicotinamide adenine dinucleotide. Analytical Biochemistry. 1973;53:452-458.

170. Umemura K, Kimura H. Determination of oxidized and reduced nicotinamide adenine dinucleotide in cell monolayers using a single extraction procedure and a spectrophotometric assay. Analytical Biochemistry. 2005;338:131-135.

171. Micheli V, Sestini S. Determining NAD synthesis in erythrocytes. Methods Enzymol. 1997;280:211-221.

172. Rafaeloff-Phail R, Ding LY, Conner L, et al. Biochemical regulation of mammalian AMP-activated protein kinase activity by NAD and NADH. Journal of Biological Chemistry. 2004;279:52934-52939.

173. Jing M, Ismail-Beigi F. Role of 5 '-AMP-activated protein kinase in stimulation of glucose transport in response to inhibition of oxidative phosphorylation. American Journal of Physiology-Cell Physiology. 2006;290:C484-C491.

174. Hwang YYC, Shaw S, Kaneko M, Redd H, Marrero MB, Ramasamy R. Aldose reductase pathway mediates JAK-STAT signaling: a novel axis in myocardial ischemic injury. Faseb Journal. 2005;19:795-+.

175. Tretter L, Adam-Vizi V. Generation of reactive oxygen species in the reaction catalyzed by alpha-ketoglutarate dehydrogenase. J Neurosci. 2004;24:7771-7778.

176. Ferrero E, Belloni D, Contini P, et al. Transendothelial migration leads to protection from starvation-induced apoptosis in CD34(+)CD14(+) circulating precursors: evidence for PECAM-1 involvement through Akt/PKB activation. Blood. 2003;101:186-193.

177. Lin SJ, Guarente L. Nicotinamide adenine dinucleotide, a metabolic regulator of transcription, longevity and disease. Curr Opin Cell Biol. 2003;15:241-246.

178. Devadas S, Zaritskaya L, Rhee SG, Oberley L, Williams MS. Discrete generation of superoxide and hydrogen peroxide by T cell receptor stimulation: selective regulation of mitogen-activated protein kinase activation and fas ligand expression. J Exp Med. 2002;195:59-70.

179. Jackson SH, Devadas S, Kwon J, Pinto LA, Williams MS. T cells express a phagocyte-type NADPH oxidase that is activated after T cell receptor stimulation. Nat Immunol. 2004;5:818-827.

180. Chatterjee PK, Cuzzocrea S, Thiemermann C. Inhibitors of poly (ADP-ribose) synthetase protect rat proximal tubular cells against oxidant stress. Kidney Int. 1999;56:973-984.

181. Kamat JP, Devasagayam TP. Nicotinamide (vitamin B3) as an effective antioxidant against oxidative damage in rat brain mitochondria. Redox Rep. 1999;4:179-184.

182. Shen CC, Huang HM, Ou HC, Chen HL, Chen WC, Jeng KC. Protective effect of nicotinamide on neuronal cells under oxygen and glucose deprivation and hypoxia/reoxygenation. J Biomed Sci. 2004;11:472-481.

183. Kang HT, Lee HI, Hwang ES. Nicotinamide extends replicative lifespan of human cells. Aging Cell. 2006;5:423-436.

184. Brozik A, Casey NP, Hegedus C, et al. Reduction of Bcr-Abl function leads to erythroid differentiation of K562 cells via downregulation of ERK. Ann N Y Acad Sci. 2006;1090:344-354.

185. Woessmann W, Zwanzger D, Borkhardt A. ERK signaling pathway is differentially involved in erythroid differentiation of K562 cells depending on time and the inducing agent. Cell Biol Int. 2004;28:403-410.

186. Witt O, Sand K, Pekrun A. Butyrate-induced erythroid differentiation of human K562 leukemia cells involves inhibition of ERK and activation of p38 MAP kinase pathways. Blood. 2000;95:2391-2396.

187. Kaeberlein M, McDonagh T, Heltweg B, et al. Substrate-specific activation of sirtuins by resveratrol. J Biol Chem. 2005;280:17038-17045.

188. Avalos JL, Bever KM, Wolberger C. Mechanism of sirtuin inhibition by nicotinamide: altering the NAD(+) cosubstrate specificity of a Sir2 enzyme. Mol Cell. 2005;17:855-868.

189. Denu JM. Vitamin B3 and sirtuin function. Trends Biochem Sci. 2005;30:479-483.

190. Bleul CC, Fuhlbrigge RC, Casasnovas JM, Aiuti A, Springer TA. A highly efficacious lymphocyte chemoattractant, stromal cell-derived factor 1 (SDF-1). J Exp Med. 1996;184:1101-1109.

191. Mohle R, Bautz F, Rafii S, Moore MA, Brugger W, Kanz L. The chemokine receptor CXCR-4 is expressed on CD34+ hematopoietic progenitors and leukemic cells and mediates transendothelial migration induced by stromal cell-derived factor-1. Blood. 1998;91:4523-4530.

192. Hamada T, Mohle R, Hesselgesser J, et al. Transendothelial migration of megakaryocytes in response to stromal cell-derived factor 1 (SDF-1) enhances platelet formation. J Exp Med. 1998;188:539-548.

193. Hodohara K, Fujii N, Yamamoto N, Kaushansky K. Stromal cell-derived factor-1 (SDF-1) acts together with thrombopoietin to enhance the development of megakaryocytic progenitor cells (CFU-MK). Blood. 2000;95:769-775.

194. Shim MH, Hoover A, Blake N, Drachman JG, Reems JA. Gene expression profile of primary human CD34+CD38lo cells differentiating along the megakaryocyte lineage. Exp Hematol. 2004;32:638-648.

195. Guerriero R, Testa U, Gabbianelli M, et al. Unilineage megakaryocytic proliferation and differentiation of purified hematopoietic progenitors in serum-free liquid culture. Blood. 1995;86:3725-3736.

196. Lannutti BJ, Shim MH, Blake N, Reems JA, Drachman JG. Identification and activation of Src family kinases in primary megakaryocytes. Exp Hematol. 2003;31:1268-1274.

197. Chen C. Megakaryocytic Transcriptional Program and Developmental Plasticity. Interdepartmental Biological Sciences Program. Ph.D. Evanston: Northwestern University; 2006.

198. Stachura DL, Chou ST, Weiss MJ. Early block to erythromegakaryocytic development conferred by loss of transcription factor GATA-1. Blood. 2006;107:87-97.

199. Wurzer WJ, Planz O, Ehrhardt C, et al. Caspase 3 activation is essential for efficient influenza virus propagation. Embo J. 2003;22:2717-2728.

200. Huang M, Wang Y, Collins M, Graves LM. CPEC induces erythroid differentiation of human myeloid leukemia K562 cells through CTP depletion and p38 MAP kinase. Leukemia. 2004;18:1857-1863.